Title
Action selection and coordination: Perspectives from movement speed learning

Author
Hillenbrand, Sarah Frances

Publication Date
2015

Peer reviewed|Thesis/dissertation

Action selection and coordination:
Perspectives from movement speed learning

by

Sarah Frances Hillenbrand

A dissertation submitted in partial satisfaction of the

requirements for the degree of

Doctor of Philosophy

in

Neuroscience

in the

Graduate Division

of the

University of California, Berkeley

Committee in Charge:

Professor Richard B. Ivry, Ph.D. (Chair)
Professor Michael A. Silver, Ph.D.
Professor David Whitney, Ph.D.
Professor Steve L. Lehman, Ph.D.

Summer 2015

Abstract

Action selection and coordination:
Perspectives from movement speed learning

By

Sarah Frances Hillenbrand

Doctor of Philosophy in Neuroscience

University of California, Berkeley

Professor Richard B. Ivry, Chair

In his 1945 book *The Phenomenology of Perception*, French philosopher Maurice Merleau-Ponty wrote, “The body is our general medium for having a world.” When learning to move, our bodies implicitly know what to do, letting experiences tweak our neural circuits to etch in precise models of the world. These experiences wire up complex capabilities in bodies that were born ready to move, but did not yet know what a pen, a cartwheel, or a hug was.

What is arguably more difficult is using our minds to gain explicit understanding of the processes governing learning and movement. For this, we have science. Merleau-Ponty later wrote, “Science manipulates things and gives up living in them. It makes its own limited models of things; operating upon these indices or variables to effect whatever transformations are permitted by their definition, it comes face to face with the real world only at rare intervals.” In this dissertation, I present the outcomes of my own manipulations, my own limited models which, at rare intervals, come face to face with the ways in which our bodies construct our world.

In Chapter 2, I investigated a potential problem for the use of functional magnetic resonance imaging (fMRI) to study human motor behavior. Task-related changes in heart rate can cause changes in the blood oxygen level dependent (BOLD) signal, potentially masking effects of interest. Correcting for heart rate fluctuations did not fundamentally change the brain's responses to arm movements. However, because these corrections did improve the explanatory power of fMRI analyses, my work stands as an illustration of the efficacy of this correction.

In Chapter 3, I had people learn to produce movements of certain speeds in a virtual shuffleboard game. When learning movement directions, delayed feedback impairs performance due to processing limitations in a brain structure called the cerebellum. Because feedback is naturally delayed in shuffleboard, I asked whether delays affect learning of speeds, as well. They did not, suggesting that the cerebellum is not involved in learning movement speeds from errors.

In Chapter 4, I sought to confirm this speculation using fMRI. I scanned the brains of people as they played shuffleboard. I found no evidence that the cerebellum was involved in the processing of errors of movement speed. However, successful task performance robustly activated the dorsal striatum, a structure involved in learning from rewards and forming habits. These results suggest that, when people learn to move at certain speeds, they depend more on memories of times they got it right than on feedback telling them to speed up or slow down.

Acknowledgments

I am first and foremost deeply grateful to my advisor, Richard Ivry, who is a fearsome experimentalist, an inspirational leader, and a kind and caring mentor. These traits are rare in isolation and unheard of in a single individual. I consider myself lucky to have learned from him.

This work has also benefited greatly from the efforts of the following individuals. Thanks to:

Chapter 2:

John Schlerf, my co-author, for foundational training in understanding, selecting, and implementing fMRI analyses, all delivered with superhuman patience.

Rick Redfern, for frequent miscellaneous repairs made with minimal judgment.

Chapter 3:

Kristin Calsada, a summer student whose assistance and patience in getting experiments up and running were invaluable.

Trisha Vaidyanathan, Ashok Krishna, and Janice Chua, trusted research assistants, who contributed heroic data collection efforts.

Chapter 4:

Katherine Okpara and Tina Tu, two intelligent, reliable, and fun research assistants who have been of tremendous help through countless pilot studies, scan sessions, and programming challenges.

Ben Inglis, for counsel on scan sequences and artifacts, and for general wit and wisdom.

Financial support:

This work was supported by the National Science Foundation Graduate Research Fellowship Program and the National Institutes of Health (NS074917, HD060306).

Data presented in Chapters 2-4 were collected at the Henry J. Wheeler, Jr. Brain Imaging Center at the University of California, Berkeley, which receives support from the National Science Foundation through their Major Research Instrumentation Program, award number BCS-0821855.

Table of Contents

List of Figures

Chapter 2

Chapter 3

Chapter 4

Appendix: Supplementary material for Chapter 4

List of Tables

Chapter 2

Chapter 4

Chapter 1: Introduction

Humans and other organisms are capable of skillfully executing a stunningly diverse repertoire of motor behaviors. Given that very few of these behaviors are possible at birth, lifelong learning is required to build up this repertoire. People must learn to select the correct actions, and to coordinate those actions, using feedback about what they did right and what they did wrong. This feedback is used to issue corrections both as the movement unfolds in real time and on subsequent attempts at executing the same movement.

Often thought of as an implicit process, a form of knowing *how* to do something, folk wisdom holds that motor learning is the process of sculpting a poorly understood "muscle memory." However, motor learning also requires explicit knowledge of facts about the world: for instance, information about a surface's friction, an object's weight, and proper movement technique can all influence both the selection and coordination of actions (cf. Stanley & Krakauer, 2013). Motor learning is likely to rely upon some combination of explicit and implicit processing. However, the division of labor between neural circuits that encode models of ourselves and of the world is not clear. At present, there is one point of agreement in the motor learning community, and that is simply that there must exist more than just one neural system for motor learning (Karni et al., 1998; Smith et al., 2006; Taylor et al., 2014; and for review, see Shadmehr et al., 2010 and Krakauer & Mazzoni, 2011).

In order to become motorically competent adults, it is thought that people form internal representations, or models, of the consequences of their actions. These consequences may be sensory: for instance, in reaching for a cup of coffee, I see and feel my arm traveling across my desk. I compare the actual and intended consequences of my movement to form what is termed a *sensory prediction error*, adjusting subsequent movements to bring the actual and intended consequences into better alignment. People are also thought to form models of the likely outcomes of actions: whether a reward will be received for a given action or not. When an expected reward is not received, this creates a negative *reward prediction error*; when an unexpected reward is received, this creates a positive reward prediction error. Prediction errors, sensory or reward-based, require experience to build accurate predictions. Motor learning, then, is perhaps better described as the acquisition of internal models that have predictive power for the control of movements.

In a task which required participants to compensate for a rotation imposed on their cursor by reaching in the opposite direction, it has been demonstrated that people can learn from either rewards and from errors (Izawa & Shadmehr, 2011). However, only errors induce sensory recalibration, indicating that the selection of actions is likely to be driven by rewards, while the coordination of actions is likely to be driven by errors. Despite this neat division of labor, real-world behaviors are not so neat: At any given moment, any body in motion is simultaneously selecting and coordinating actions. Nevertheless, in studying human motor learning, key differences exist between task used to model reward-based and error-based learning.

From rewards or lack thereof, people learn which behaviors to repeat and which to avoid (Sutton & Barto 1998; Schultz 1998; O'Doherty et al., 2004; Daw et al., 2006; Niv 2009; Glascher et al., 2010). Although selecting appropriate actions is in a way a prerequisite for the appropriate coordination of those actions by the motor system, action selection is often thought of as a cognitive process, with little consideration of the motor system. Behavioral studies of

reward learning draw heavily upon the ways in which instrumental conditioning and decision-making have been modeled. Participants often learn from binary feedback to learn associations between actions and positive or negative outcomes—that is, the success or failure of their decisions in producing a reward (O'Doherty et al., 2004; Daw et al., 2006; Niv 2009; Glascher et al., 2010).

From errors, people learn precise patterns of coordinated muscle activations to achieve their goals with increasing skill and accuracy (Shadmehr & Mussa-Ivaldi 1994; Thoroughman & Shadmehr 2000; Fine & Thoroughman 2006, 2007; Thoroughman & Taylor 2007; Tanaka et al., 2009). Behavioral studies of human motor learning often alter the mapping between actions and the physical consequences of those actions. This has been achieved by rotating cursor feedback in a paradigm known as visuomotor rotation learning (Redding & Wallace, 1988; Martin et al., 1996; Krakauer et al., 2000; Mazzoni & Krakauer, 2006), jumping the target to another location mid-movement (Diedrichsen et al., 2005), introducing a force field into the workspace (Shadmehr & Mussa-Ivaldi, 1994; Donchin et al., 2003), or altering the gain of movements (Turner et al., 2003; Krakauer et al., 2004). People must then achieve their goal of reaching the target by learning from sensory feedback and adjusting their movements on a trial-by-trial basis (Desmurget & Grafton, 2000). Many types of movements have been studied this way in laboratory settings, including saccades (for review, see Iwamoto & Kaku, 2010), locomotion (for review, see Torres-Oviedo et al., 2011), and reaching movements (for review, see Krakauer & Mazzoni, 2011). In case after case, people learn to compensate for a range of feedback perturbations.

The divisions between reward- and error-based learning run deeper than their behavioral signatures: indeed, these processes appear to occur in different brain structures entirely. Reward-based learning is thought to occur in the striatum, while error-based learning is thought to occur in the cerebellum (for review, see Houk & Wise, 1995; Doya 2000; Shadmehr & Krakauer, 2008). Patient studies and neuroimaging studies have shed new light on the neural underpinnings of motor learning. Patients with damage to brain regions known as the striatum and the cerebellum (among them, patients with Parkinson's Disease and cerebellar ataxia, respectively) have been critically important in identifying roles for these structures human motor learning, and these roles have frequently been confirmed through the use of neuroimaging (Pascuale-Leone et al., 1993; Martin et al., 1996; Gabrieli et al., 1997; Doyon et al., 1997; Imamizu et al., 2000; Desmurget et al., 2003; Desmurget et al., 2004; Krakauer et al., 2004; Maschke et al., 2004; Seidler et al., 2004; Diedrichsen et al., 2005; Seidler et al., 2006; Grafton et al., 2008; Tunik et al., 2009; Viviani et al., 2009; Schlerf et al., 2012; for review, see Doyon et al., 2003 & Seidler 2010).

A neuroimager by training, I began my graduate research with the goal of using functional magnetic resonance imaging (fMRI) to disentangle the processes driving reward- and error-based learning. The analysis of fMRI data often relies upon regression to identify brain regions where activity matches one or more predictions (see Friston et al., 1995, but see Poline & Brett, 2012). However, the “brain activity” measured is not neural but, in fact, hemodynamic in origin. The blood oxygen level dependent (BOLD) signal measured by fMRI is thought to reflect underlying neural activity (for review, see Logothetis & Wandell, 2004).

The relationship between neural activity and the BOLD signal is complicated by sources of physiological noise like heart rate and respiration. In an earlier study from our laboratory,

error-related activations in the cerebellum nearly escaped detection because heart rate was relatively depressed following errors compared to correct trials (Schlerf et al., 2012). The relative decrease in blood flow to the head gave the appearance that the cerebellum was more responsive not to errors, but to correct trials. Similarly, increases in heart rate may result in the delivery more blood to the brain. If these increases or decreases are correlated with aspects of the task, we reasoned, estimating true neural responses may in fact be impossible.

In a first experiment, I investigated whether changes in heart rate caused by a simple movement task could be estimated and removed from the fMRI timeseries data (Chapter 2). Simple movements elicited an increase in heart rate but no change in another measure, respiratory variation. Correcting for heart rate, but not respiratory variation, resulted in subtle changes to the shape of plotted BOLD responses. Furthermore, correcting for heart rate significantly improved model fit for a majority of participants in the primary motor cortex and for a minority of participants in the cerebellum. The magnitude of this improvement, on average, was similar for heart rate and respiratory variation corrections. As testament to the importance of considering task-related changes in the rate of physiological processes, both corrections resulted in larger improvements than a rate-insensitive correction that is commonly used by fMRI researchers. These results highlight the need to include records of the rate of change in possible sources of physiological noise in fMRI analyses, with the caveat that all corrections may not be equally effective for all individuals and all regions of the brain.

Turning from the study of how to improve imaging methodology, I next set out to study actual human motor learning in the brain. For this, I designed a novel behavioral task based on the real-world game of shuffleboard. However, as ever, it was necessary to truly understand behavior before identifying its basis in the brain. Chapter 3, I present the results of a behavioral study designed to pinpoint the effects of naturally-occurring delays and other forms of delay in the shuffleboard task. In real-world shuffleboard, people learn despite a delay of up to several seconds between movement and feedback about that movement. In studies of visuomotor rotation learning, by contrast, delaying feedback by as little as several hundreds of milliseconds diminishes learning dramatically (Kitazawa et al., 1995). The putative reason for this cost of delay is that learning will only occur when motor representations and error signals in the cerebellum co-occur (cf. Ito, 2002). The cerebellum contains a gridlike map of movement- and feedback-transmitting fibers which run perpendicular to each other, and learning is thought to proceed through modifications to the strength of synapses at the junctions between the two fiber types. If a delay is injected, the movement representation is already gone by the time an error signal passes through this junction, and no learning can occur. Using a virtual shuffleboard task, I asked whether this cost of delayed feedback applied to learning movement speeds, as it does to learning movement directions.

Performing movements accurately requires specifying the appropriate direction and speed (or force, or amplitude, depending on the circumstances). These two movement variables, thought to be specified independently in the brain, play by very different sets of rules when it comes to how quickly learning occurs and how broadly it generalizes to new contexts (Bock 1992; Pine et al., 1996; Krakauer et al., 2000; Vindras & Viviani, 2002; Turner et al., 2003; Krakauer et al., 2004). Assuming at least some degree of separation in the neural encoding of speed and direction, the shuffleboard task offers an opportunity to examine temporal constraints on learning in a different domain. A range of temporal manipulations were used to investigate the

effects of feedback delay, predictability, and ecological validity (i.e. similarity to the physics of real-world shuffleboard). In three experiments, we found limited evidence that delays impact the learning of movement speeds. There was a slight advantage of predictably timed feedback, but this advantage was limited to situations where predictability was created through the use of a range of temporal intervals thought to extend beyond the limits of cerebellar error processing. These results indicate that the temporal constraints imposed on learning by the circuitry of the cerebellum do not apply when movements are adjusted in terms of speed, rather than direction.

Given that temporal constraints on learning were minimal in the shuffleboard task, it would be reasonable to assume that the cerebellum might not be a critical component in the neural network required for learning this task. To address this hypothesis, I turned to fMRI in Chapter 4. We adapted the shuffleboard task to include frequent changes in target location and perturbations on participants' visual feedback. By ensuring the persistence of errors throughout the scan session, we were able to image the brains of people as they made trial-by-trial adjustments to movement speed.

We identified the primary motor cortex and right anterior lobe of the cerebellum as involved in movement. However, the remainder of our effects of interest were found outside of the cerebellum. The dorsal striatum was found to be involved in feedback processing, and responded more strongly to correct trials than to errors. This region, thought to be involved in habit formation, reward learning, and the regulation of movement vigor and variability, may be driving learning in the shuffleboard task by reinforcing the formation of memories of desired movement speeds. While we cannot definitively rule out a role for the cerebellum in such a task, our results suggest that, when movement speeds must be updated from one trial to the next, performance relies less upon error processing than upon reward processing. Future work will use computational model-based predictions to identify regions involved in the implementation of updated motor plans on subsequent trials.

The work presented in this dissertation began with the goal of better understanding how people process feedback to learn from errors and rewards. To get at this, it was first necessary to be sure the effects measured using fMRI were truly neural in origin and not the result of confounding factors Chapter 2). Next, in approaching the study of motor learning itself, it was important to account for behavioral differences in multiple forms of motor learning (Chapter 3). Finally, it was time to peek inside the skull in order to determine where in the brain errors and rewards are processed to govern intentional adjustments to movement speed (Chapter 4). Motor learning, despite its centrality to our existence as organisms who navigate and manipulate the world, remains a complex and poorly understood phenomenon. It is my hope that the work presented here in some small way provides guidance on how to approach the study of motor learning and insight into its some of its numerous determinants.

Chapter 2: Impact of task-related changes in heart rate on estimation of hemodynamic response and model fit of BOLD responses

Modified from manuscript submitted as Hillenbrand, S.F., Ivry, R.B., and Schlerf, J.E., Impact of task-related changes in heart rate on estimation of hemodynamic response and model fit

2.1 Introduction

Functional magnetic resonance imaging (fMRI) is widely used to examine responses of the human brain to a variety of tasks and stimuli. One disadvantage of the method is that it provides an indirect measurement of neural activity by measuring changes in the blood oxygenation level dependent (or BOLD) signal, changes that occur on a much slower time scale than the corresponding changes in the activity of local neural populations (Ogawa & Lee, 1990; Logothetis, 2003). This issue is mitigated by block designs where stimuli or task conditions alternate between present and absent for tens of seconds at a time. Some psychological processes, however, are only appropriately studied in event-related designs in which the events of interest are brief.

In order to determine whether a particular brain area is active in a given task, most researchers employ a general linear model (GLM) and regression analysis to identify brain regions in which the BOLD response matches a set of predictions (see Friston et al., 1995, but see Poline & Brett, 2012). The relationship between neural activity and the changes in blood flow, volume, and oxygenation that form the basis of the BOLD signal is complex (Buxton & Frank, 1997; for review, see Logothetis & Wandell, 2004). Fortunately, the fMRI response is essentially linear and time-invariant (Boynton et al., 1996; Dale & Buckner, 1997; Friston et al., 1994), and the brain response can often be efficiently extracted using events separated by only a few seconds (Dale 1999). Since the coupling between the neural and BOLD responses has a similar shape across a wide variety of conditions, a canonical hemodynamic response function (HRF) is frequently employed in fMRI analyses (Friston et al., 1998).

However, the HRF has been shown to differ across individuals, brain regions, and events (Handwerker et al., 2004). Generating a predicted BOLD response using the canonical HRF can therefore result in a poorer fit in comparison to individualized HRFs, potentially leading to mischaracterizations of neural activity (Hernandez et al., 2002; Handwerker et al., 2004).

The fit of any GLM can be diminished by failing to account for factors that are correlated with each other, a problem that is especially pronounced in event-related studies of BOLD signal that are more susceptible to noise. Two important and measurable but often ignored physiological covariates are heartbeats and respiration (Glover et al., 2000). The beating of the heart causes pulsations in blood vessels and cerebrospinal fluid (CSF), creating artifacts near large blood vessels, around ventricles, and even in deep sulci (Dagli et al., 1999). Additional artifacts are introduced by respiration, as the rise and fall of the chest cavity during breathing causes both brain motion and inhomogeneities in the magnetic field (Glover et al., 2000; Raj et al., 2001). It is therefore desirable to measure heartbeats and breathing to account for their influence on the BOLD response. The RETROICOR method developed by Glover and colleagues (2000) provides one such approach, charting the phase of cardiac and respiration processes relative to the time of image acquisition. Variance attributable to the phase of these processes may be removed in preprocessing of fMRI time series or accounted for by adding

nuisance regressors to the GLM.

One limitation of the RETROICOR correction is that it does not consider how changes in the rate of physiological processes may affect the BOLD signal. Changes in both heart and respiration rate can cause fluctuations in the BOLD signal (Birn et al., 2006, 2008; Shmueli et al., 2007; Chang et al., 2009; Chang & Glover, 2009). Importantly, these changes can be task-related, associated with variations in arousal (Tursky et al., 1969), movement preparation (Damen & Brunia, 1987), response inhibition (Jennings et al., 1991, 1992; for review see Jennings & van der Molen, 2002), and feedback processing (Crone et al., 2003, 2005).

We previously demonstrated the importance of considering task-related changes in non-neural, physiological processes in a study designed to identify neural regions responsive to movement errors (Schlerf et al., 2012). When physiological regressors were not included in the GLM analysis, movement errors led to a broadly distributed decrease in the BOLD response in the cerebellum. However, there was also a reliable reduction in heart rate following movement errors. Since there was sufficient heart rate fluctuation beyond that associated with the movement errors, the effect of heart rate on the BOLD response could be accurately and independently modeled (Schlerf et al., 2012). When this correction was applied, the cerebellar deactivations were no longer evident. Instead, an increase in the BOLD signal was observed on error trials that was restricted to the arm area of the anterior cerebellum. Thus, the error signal in the cerebellum was only evident after task-dependent changes in heart rate were included in the modeling of BOLD responses.

In the current study, we systematically investigated the potential consequences of task-related fluctuations in heart rate and respiration on the HRF using a progressive series of analyses. Rather than focusing on movement errors, we measured simpler behavioral variable: arm movement. We first demonstrate that heart rate is affected by arm movement, but respiration is not. Given these relationships, we examined how the inclusion of physiological regressors in the GLM influenced the shape of the estimated arm movement-related HRF. Finally, we quantified the added explanatory power of different sets of physiological regressors, individually and in combination.

2.2 Material and methods

2.2.1 Participants

Eleven healthy right-handed participants were tested (7 female, mean age 24.1 years). The participants provided written, informed consent under a protocol approved by the University of California, Berkeley Institutional Review Board.

2.2.2 Task

Prior to scanning, participants were fitted with a custom bite bar. During the scanning session, the bite bar was mounted to the head coil to minimize head movement. Stimuli were backprojected onto a screen mounted inside the bore of the magnet and viewed via a mirror mounted to the head coil. From a supine position, the participants held a robotic manipulandum (www.fmrirobot.org) in their right hand. The manipulandum was positioned over the participant’s abdomen and could be freely moved in a plane parallel to the scanner bed.

Participants were trained to make short (8 cm) out-and-back reaching movements along the axis of the body toward their head, chiefly by flexion about the elbow. They were instructed to terminate each return movement such that in between trials, the hand rested comfortably near the navel. Participants were instructed to move when a central fixation crosshair changed color from red to green. For all runs, the green crosshair was presented for 500 ms, regardless of inter-trial interval. Participants were told to initiate the movement as soon as they saw the color change, generating a rapid out and back movement. To minimize corrective movements, there was no visual feedback of hand position during scanning. At the termination of each return movement (when the hand coordinates were no more than 1 cm apart for a minimum of 500 ms), the start position of the hand for the next trial was automatically adjusted to correspond to the central fixation crosshair.

All participants completed a training session in a mock scanner 1-7 days prior to the scanning session. This served to familiarize the participants with the scanning environment and trained them in the movement task. The training session consisted of four runs and was designed to train the participants to make movements with relatively uniform amplitude in the scanner without relying on feedback. The training runs provided feedback that became progressively less informative as the training continued. In the first run, the participants received online feedback of the cursor position, as well as knowledge of results (KR) about reach amplitude at the end of each movement. KR was given in numeric form, shown above the fixation crosshair as a percentage of the desired 8 cm amplitude for 500 ms immediately following completion of the return movement. For the next run, they were only given KR (no online cursor feedback), and for the final two runs, no feedback was provided. At various points in the training session, the experimenter provided verbal coaching concerning movement initiation, speed, and amplitude.

The scanning session consisted of an anatomical scan and three functional scans (one localizer run and two task runs). The localizer run lasted 6 minutes and 40 seconds and consisted of 12 12-second blocks, with rest periods of 21.3 seconds in between each block. There were two types of blocks during the localizer run: reach and auditory (6 of each block type). Reach blocks were indicated by presentation of the word “Reach” on the screen. Participants then produced eight out-and-back movements, initiating each movement when they saw the fixation crosshair turn green. Over the 12-second block, the crosshair turned green every 1500 ms. Auditory blocks were indicated by the appearance of the word "Listen" on the screen, and participants heard eight balloon popping sounds, one every 1500 ms. These trials were part of a separate study and will not be discussed further here. The reach and auditory blocks alternated in a pseudorandom manner, with the order counterbalanced across participants.

The two task runs (as well as a practice reaching task run completed during the anatomical scan) consisted of 30 randomly timed reaches, with inter-movement intervals (IMIs) ranging between 4 and 22 seconds (run duration of 5 min). An optimization procedure was used to create the order of the IMIs: 1000 random sequences of IMIs were generated, and the six most efficient were selected, based on the contrast Move vs. Rest. From these six, sequences were selected at random for each participant's training, practice, and task runs.

Efficiency was calculated following the guidelines of Dale (1999), according to the equation:

$$Efficiency = 1/\ trace((X^TX)^{-1}) \qquad \text{(Equation 1)}$$

where the design matrix $X = [X_1X_2 \ldots X_{12}]$ is a horizontal concatenation of delta (stick) functions that represent the stimulus timing at each lag and *trace* refers to the sum of the eigenvalues of a given matrix. While efficiency is typically computed for a particular contrast, in the case of HRF extraction that contrast is simply the identity matrix, so we disregarded it here.

2.2.3 Imaging parameters

Data were collected on a 3 T MAGNETOM Trio scanner (Siemens Healthcare, Erlangen, Germany) at the University of California, Berkeley Brain Imaging Center. A 12-channel transverse electromagnetic send-and-receive radiofrequency head coil was used. One high-resolution T1-weighted MPRAGE anatomical scan (TR = 1900 ms; TE = 2.52 ms; 1 × 1 × 1 mm voxels; acquisition matrix 256 x 256; field of view 25 x 25 cm) was acquired for each participant. Multi-slice echo-planar imaging (EPI) was used to collect functional imaging data (gradient-echo EPI sequence; TR = 2000 ms; TE = 26 ms; 36 ascending sagittal slices; 3.3 x 3.13 x 3.13 mm voxels; flip angle, 90°; acquisition matrix 64 x 64; field of view 20 x 20 cm; 150 volumes per task run, 200 volumes per localizer run) using parallel imaging reconstruction (GRAPPA) with an acceleration factor of 2.

2.2.4 Physiological monitoring and analysis

During scanning, physiological signals were recorded using a BIOPAC physiological monitoring system (www.biopac.com). Heartbeat was measured using a photoplethysmograph placed on the participant's left index finger. Respiration was measured with a pneumatic pressure sensor placed several centimeters below the sternum and held in place with an elastic strap. Analog TTL signals generated by the scanner were recorded to temporally align these physiological measurements with the EPI time series. All data were recorded at 125 Hz, with separate recordings initiated for each functional run.

Physiological regressors were created using the Physiological Log Extraction for Modeling (PhLEM) v1.0 toolbox for SPM5 (Verstynen & Deshpande, 2011). The PhLEM package marks respiration and heartbeat events using an automatic peak detection algorithm. On a few occasions, the spacing between the detected peaks indicated that a peak had been missed by the algorithm. In these cases (0.03% of all events), the data were visually inspected and peaks were manually added at the appropriate deflection in the waveform.

The heart rate time series was computed following the methods described in Chang et al. (2009). For each 6 s window centered on a given 2 s TR in the fMRI time series, the mean inter-beat interval was computed and expressed in units of beats per minute. This time series was then shifted by 0-11 TRs to produce 12 time series lags of 0-22 seconds (HR regressors). This agnostic approach imposes no constraint on the shape of the transfer function between heart rate and the BOLD signal.

The respiration time series was computed using a measure of respiratory variation (RV) (Chang et al., 2009), which is a simpler and more robust alternative to RVT (respiration volume per unit time) (Birn et al., 2008). Similar to the procedure for HR, RV was obtained by computing the standard deviation of the respiration waveform within a 6 s sliding window centered on each 2 s TR. This time series was then shifted by 0-11 TRs to produce 12 respiration volume (RV) regressors.

Regressors to estimate the effects of respiratory and cardiac phase were made using the RETROICOR method (Glover et al., 2000) as implemented in PhLEM (Verstynen & Deshpande, 2011). Using a Fourier expansion, the first two harmonics of the heartbeat and respiration events were computed. Both sine and cosine waveforms were included, yielding a total of eight phase regressors.

The effect of reaching movements on our two physiological variables of interest, heart rate (HR) and respiratory variation (RV), was assessed. HR and RV regressors served as dependent variables to identify task-related changes by time-locking the estimate of each variable to the onset of each movement cue. These values were calculated separately for each run, with the data normalized by subtracting out the mean heart rate for that run.

We opted to examine task-related changes in RV rather than in the respiration signal itself, following previous work in which the former has been used as a nuisance regressor (Chang et al., 2009). The RV regressor captures changes in depth and/or frequency of breaths, yielding a measurement that is associated with respiratory tidal volume. Changes in tidal volume are hypothesized to trigger a feedback loop involving vasodilation, blood flow changes, and ultimately, compensatory changes in the rate and depth of the breaths themselves (Birn et al., 2006, Chang & Glover, 2009).

2.2.5 fMRI data preprocessing

Functional imaging data were preprocessed and analyzed using SPM5 (www.fil.ion.ucl.ac.uk/spm) and Matlab (www.mathworks.com/products/matlab). The first five volumes of each run were discarded to remove T1 equilibration effects. Images were slice-time corrected using sinc interpolation and then realigned to the mean image of each run to correct for head movement. All functional images were then coregistered to an anatomical scan and smoothed with a Gaussian kernel (FWHM = 8 mm).

2.2.6 ROI localization

We focused on two *a priori* anatomical regions of interest (ROIs) to examine activations during reaching movements. The precentral gyrus ROI was selected to include contralateral primary motor cortex, and the right anterior lobe of the cerebellum (lobules I-V) ROI was selected to include the ipsilateral cerebellar representation of the hand (Table 2.1).

A GLM analysis was performed on the localizer data from each participant. Movement blocks and the irrelevant sound blocks were modeled by convolving their onset timing with the canonical hemodynamic response function (HRF) in SPM. No physiological regressors were included in the ROI definition procedure. Selecting ROIs based on their fit to a canonical HRF may introduce a bias in the estimates of the deconvolved hemodynamic responses, as this will preferentially identify voxels in which the response already resembles the canonical HRF. However, the block design of the localizer task reduces this bias, as the model fit in such a design is only weakly affected by the choice of response function (Handwerker et al., 2004; Handwerker et al., 2012).

Whole-brain t-statistic maps for the contrast Move vs. Rest were created. Local maxima in the *a priori* regions of interest were selected as peaks to center the individually specified ROIs. From these peaks, the ROIs were expanded outward to include all of the contiguous

voxels within the t-statistic map that exceeded a threshold of $p < .05$ (family-wise error corrected).

The number of voxels meeting this statistical criterion was computed for each ROI in each individual. Across participants, the smallest number of voxels meeting this criterion was 83. To keep the size of the ROIs constant, ROIs were limited to the 83 closest contiguous voxels in all participants. While M1 ROIs were centered on local maxima in the left (contralateral) precentral gyrus, the ROI could extend beyond the precentral gyrus. No local maximum was identified within the precentral gyrus for one participant. However, we were able to identify a peak in the postcentral gyrus, based on visual inspection of the anatomical scan to which functional images were coregistered, with the surrounding set of 83 contiguous voxels extending into the precentral gyrus. For two additional participants, a small number (< 10) of voxels in the ROI extended into the postcentral gyrus.

Cerebellar ROIs were centered on local maxima in the right ipsilateral anterior lobe (lobules I-V). To make the cerebellar ROIs, the t-statistic map was first masked by the cerebellar segmentation produced by the Spatially Unbiased Infra-tentorial (SUIT) toolbox in SPM5 (www.icn.ucl.ac.uk/motorcontrol/imaging/suit.htm, Diedrichsen et al., 2009). These masks were hand-edited by overlaying them on the anatomical scan for each participant and removing voxels outside the cerebellum (e.g., from parts of occipital cortex that lie just dorsal to the anterior lobe of the cerebellum).

For visualization purposes only (Figure 2.2), ROIs were warped to the MNI (M1) or SUIT (cerebellum) templates and overlaid on a group-averaged anatomical scan in MNI space to create an overlap map. This visualization was created using AFNI (afni.nimh.nih.gov). Note, however, that all analyses were conducted in participants' native space.

2.2.7 HRF estimation

A separate GLM was calculated for each of the two task runs for each participant. The basic, uncorrected GLM modeled movements as delta (stick) functions at movement cue onset and at 11 lags of 2 seconds each, using a Finite Impulse Response (FIR) expansion model. Within the M1 and cerebellar ROIs, parameter estimates were obtained and averaged across voxels. The mean parameter estimates for the contrast Move vs. Rest within each ROI, when plotted over the 11 lags, provide an estimate of the hemodynamic response to movement within the ROI. Additional GLMs included combinations of physiological regressors. The basic physiological regressors were 12 lags of heart rate (HR), 12 lags of respiratory variation (RV), or 8 phase regressors. The set of phase regressors always included both cardiac and respiratory phase, as commonly implemented using the RETROICOR method (Glover et al., 2000). We tested models including HR alone, RV alone, phase alone, all pairwise combination of the regressors (HR + RV, HR + phase, and RV + phase), and a model that included all three.

In summary, the HRF was estimated using eight separate GLM analyses: the Uncorrected model (not including physiological covariates) and seven Corrected models (Table 2.2). The parameter estimates comprising the deconvolved HRF for each of the Corrected models were compared to those of the Uncorrected model using a 2-way repeated-measures ANOVA, with factors Time (12 lags, beginning with movement cue onset) and Model (2 models: Uncorrected vs. Corrected).

2.2.8 Percent variance explained and model comparisons

The percent variance explained by each of the eight models was calculated and compared to that of the other models using three tiers of nested model pairs (Figure 2.4). The first level involved a comparison of each of the models containing a single set of regressors (HR at 12 lags, RV at 12 lags, or the 8 phase regressors) to the Uncorrected model. The second level compared models with two sets of regressors to the models containing single sets of regressors (e.g., HR plus phase was compared to HR only and, in a separate comparison, to phase only). The third level compared the model that included all three regressors to each of the three paired-regressor models.

Analyzing nested models allowed us to determine what effect each additional regressor or set of regressors had on the overall percent variance explained. It also allowed an assessment of whether the variance explained by a given set of regressors could be redundantly explained by another set of regressors. This is particularly important, as it was previously unknown whether RV and HR have redundant effects on the BOLD response, especially in a task-dependent context. It is possible that both variables would provide a comparable improvement in fit over the uncorrected model. However, Schlerf et al. (2012) found that only HR provided a useful correction, perhaps related to the observation that there was a significant change in HR following movement errors, but not in RV.

To quantify variance explained, pairwise F-tests were used, taking into account differences in degrees of freedom based on the different numbers of free parameters in the models, according to the equation:

$$F = [(RSS_{reduced} - RSS_{full}) / (\#\text{ of additional parameters})] / RSS_{full} / (\#\text{ of time points} - \#\text{ of parameters in full model} - \#\text{ of runs}) \quad \text{(Equation 2)}$$

with *RSS* standing for Residual Sum of Squares, and where the reduced model is the model that includes fewer physiological parameters than the full model, at each level of comparison.

2.3 Results

2.3.1 Head motion

Head motion during the task was minimal, likely because the participants were restrained by a bite bar and had previously completed a training session within a simulated scanner environment. The maximum excursion of the head in any direction was calculated for each of the localizer and task runs. The median maximum excursion from the initial head position was 0.3 mm (mean = 0.4 mm, sd = 0.2 mm) for the localizer run and 0.2 mm (mean = 0.2 mm, sd = 0.8 mm) for the task runs. Head position drifted more than 1 mm in only two individuals, both during the initial localizer run (1.3 mm and 1.4 mm).

2.3.2 Evoked change in heart rate and respiration

Across participants, each reach induced an increase in heart rate of about 1%, peaking at 4 s after the movement cue onset and returning to baseline at approximately 8 s (Figure 2.1A).

Figure 2.1 Change in physiological measures evoked by reaches
Mean evoked change in heart rate (HR, panel A) and respiratory variation (RV, panel B) regressors, normalized by subtracting out the mean values across each run. Shaded area represents standard error of the mean across participants. Vertical line indicates movement cue onset, time = 0 s.

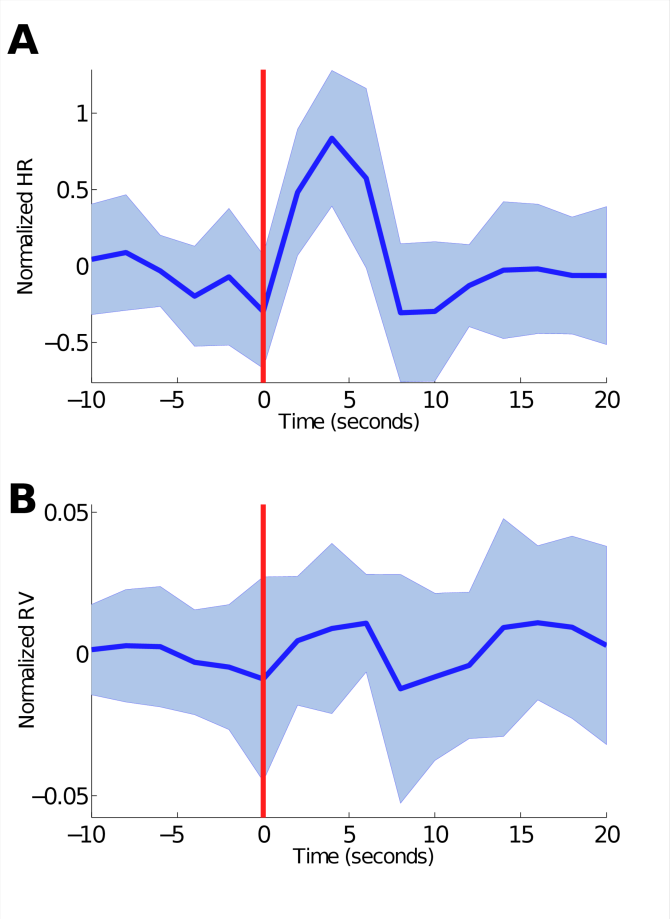

This result is in agreement with previous reports of the influence of movement on HR (Damen & Brunia, 1987, Jennings & van der Molen, 1991, 1992, Schlerf et al., 2012). A negligible increase of about 0.0015% was observed for RV, with two broader peaks, one around 6 s after the movement cue and the other at around 16 s (Figure 2.1B).

To statistically evaluate these changes, one-way repeated-measures ANOVAs were conducted on the two dependent variables (HR, RV). Four time windows were used in separate ANOVAs to identify long- and short-term changes due to movements as well as changes leading up to the movement and longer-scale fluctuations. The first was limited to the five samples after movement, spanning 0 – 10 s. The second and third each included eleven samples: one window extended from 20 s prior to movement cue onset and included the sample taken coincident with the movement cue onset (time = 0 s), while the other extended from the movement cue onset to 20 s following the movement cue onset. The fourth window included 21 samples, starting 20 s prior to movement cue onset and extending to 20 s after the movement cue onset, for a total

window size of 42 seconds. The 5-sample window was selected to focus on movement-triggered changes, whereas the 21-sample window was used to include effects of readiness or anticipation preceding movements, as well as longer-latency movement-triggered changes.

The effect of time on HR was significant for all four time windows, although the effect was considerably weaker in the window preceding the movement cue onset (5 sample: $F(4,10) = 17.12$, $p < .00001$; 11 sample preceding: $F(10,10) = 2.05$, $p = .04$; 11 sample following: $F(10,10) = 12.06$, $p < .0001$; 21 sample: $F(20,10) = 7.85$, $p < .00001$). The effect of time was not significant for RV over any time window (5 sample: $F(4,10) = 1.68$, $p = .17$, 11 sample preceding: $F(10,10) = 0.88$, $p = .56$; 11 sample following: $F(10,10) = 1.22$; $p = .29$, 21 sample: $F(20,10) = 1.24$; $p = .23$).

2.3.3 HRF estimation

The localizer run was used to identify functional ROIs. Table 2.1 lists the coordinates of the centers of the ROIs for each participant, along with the t-statistic thresholds used to restrict the ROIs to the most reliably active voxels. Figure 2.2 shows location and overlap of ROIs.

The HRF within each M1 and cerebellar ROI was estimated using eight separate GLM analyses: the uncorrected model and the seven corrected models (GLMs that included HR, RV, and phase alone, all pairwise combinations, and the Fully Corrected model that includes all three variables). The mean parameter estimates at each lag in the Move vs. Rest contrast are plotted for each ROI in Figure 2.3. These plots represent the hemodynamic response to reaching movements in each ROI. Because differences among the models were minimal, we only show the results from the Uncorrected and Fully Corrected models, although all models were included in the statistical tests.

The HRFs for each of the Corrected models were compared to the Uncorrected model using seven 2-way repeated-measures ANOVAs, with factors Time (12 TRs, beginning with movement cue onset and extending for 22 s) and Model (Corrected vs. Uncorrected model).

All ANOVAs revealed a significant main effect of Time. While the effect of Model was not significant for any of the ANOVAs, all comparisons in which the Corrected model included HR as a regressor yielded a significant interaction between Time and Model for both the M1 and cerebellar ROIs ($p < .0001$ in all cases where HR was included, 4 of 7 models), indicating that the Corrected models yielded shapes of the HRF time courses that were different from those generated by the Uncorrected model. Table 2.2 summarizes these interaction effects.

To identify differences between time points in the group HRF, *post hoc* paired t-tests were conducted using Bonferroni adjusted alpha levels of $p < .004$ per test (.05/12). No time point reached significance at this threshold. Including physiological regressors in the model resulted in a slightly lower peak in the cerebellar HRF (Figure 2.3). A similar pattern was observed for M1, with the addition of a more pronounced reduction in the post-stimulus undershoot compared to the cerebellar HRF, although differences between the HR models and the uncorrected model failed to reach significance at all time points.

Table 2.1 Regions of interest
Maximum T-statistic at ROI center in M1 and cerebellum (T-peak), along with center coordinates of each ROI. ROIs were generated by including the 83 nearest contiguous voxels above the threshold ($p < .05$, family-wise error corrected).

Subject	M1 T-peak	M1 coordinate	Ce T-peak	Ce coordinate
1	10.49	-30 -28 68	11.68	7 -56 -13
2	14.54	-21 -45 58	10.54	16 -43 -27
3	13.7	-23 -32 68	8.39	25 -61 -19
4	10.38	-22 -30 69	9.16	28 -42 -28
5	17.13	-18 -34 64	15.45	16 -32 -26
6	9.76	-12 -19 68	11.94	19 -25 -28
7	12.85	-27 -29 69	16.09	2 -42 -10
8	12.76	-28 -9 57	20.76	27 -20 -26
9	14.42	-45 -20 58	16.15	4 -30 -11
10	8.69	-12 -19 68	9.86	28 -13 -19
11	9.28	-28 -28 59	9.78	22 -27 -28

Figure 2.2 Regions of interest
Overlap map of individual 83-voxel ROIs in M1 (A) and cerebellum (B), spatially normalized for visualization only and overlaid on group-averaged anatomical slices in MNI space. Color bar at right indicates proportion of overlap of the ROIs of individual participants. Midsaggital view of slices in shown on the right for each panel.

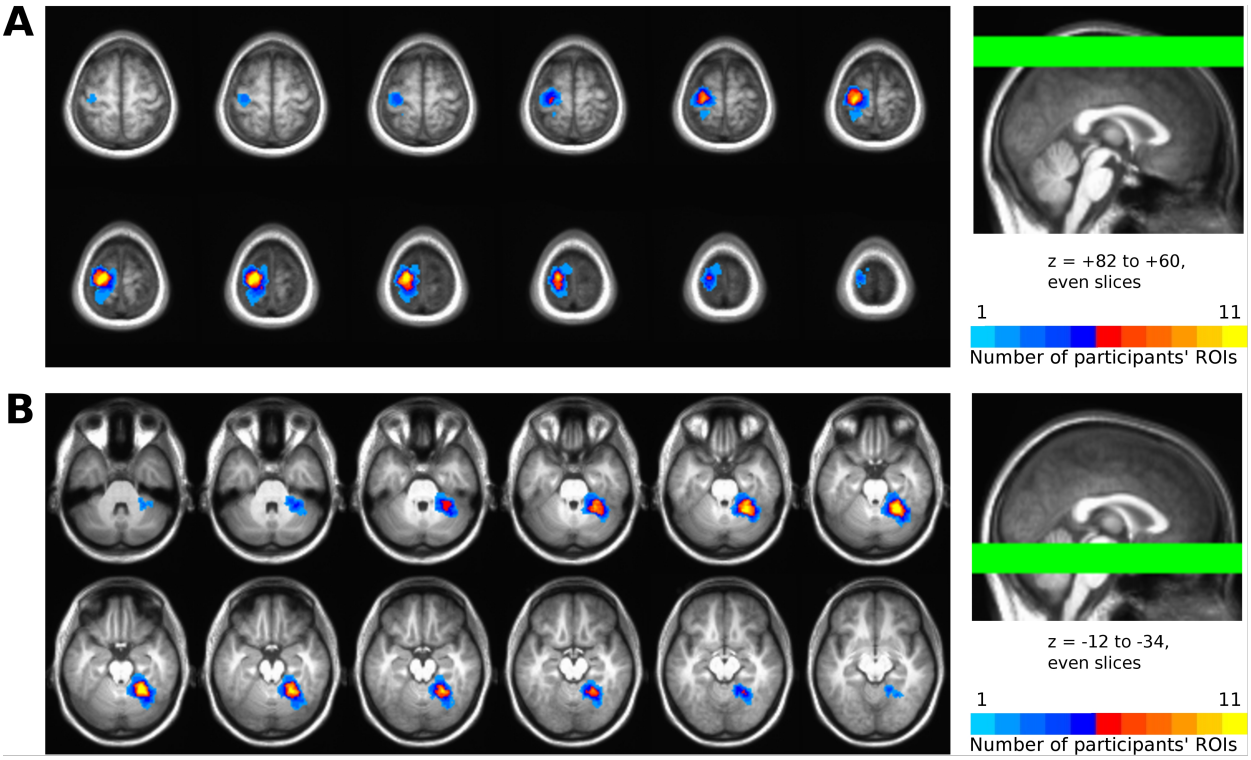

Figure 2.3 Deconvolved HRFs
HRFs deconvolved from each participant's ROI for the Uncorrected (gray) and Fully Corrected (black) models in M1 (A) and Cerebellum (B). Bottom row of each panel shows the mean HRF across all participants. Axes and legends for individual plots are as labeled in group plots. In individual plots, error bars represent the standard error of the mean across voxels; in group plot, error bars are within-participant (Loftus) error bars, given that our statistical tests of interest (i.e., uncorrected vs. corrected) are conducted within-participant.

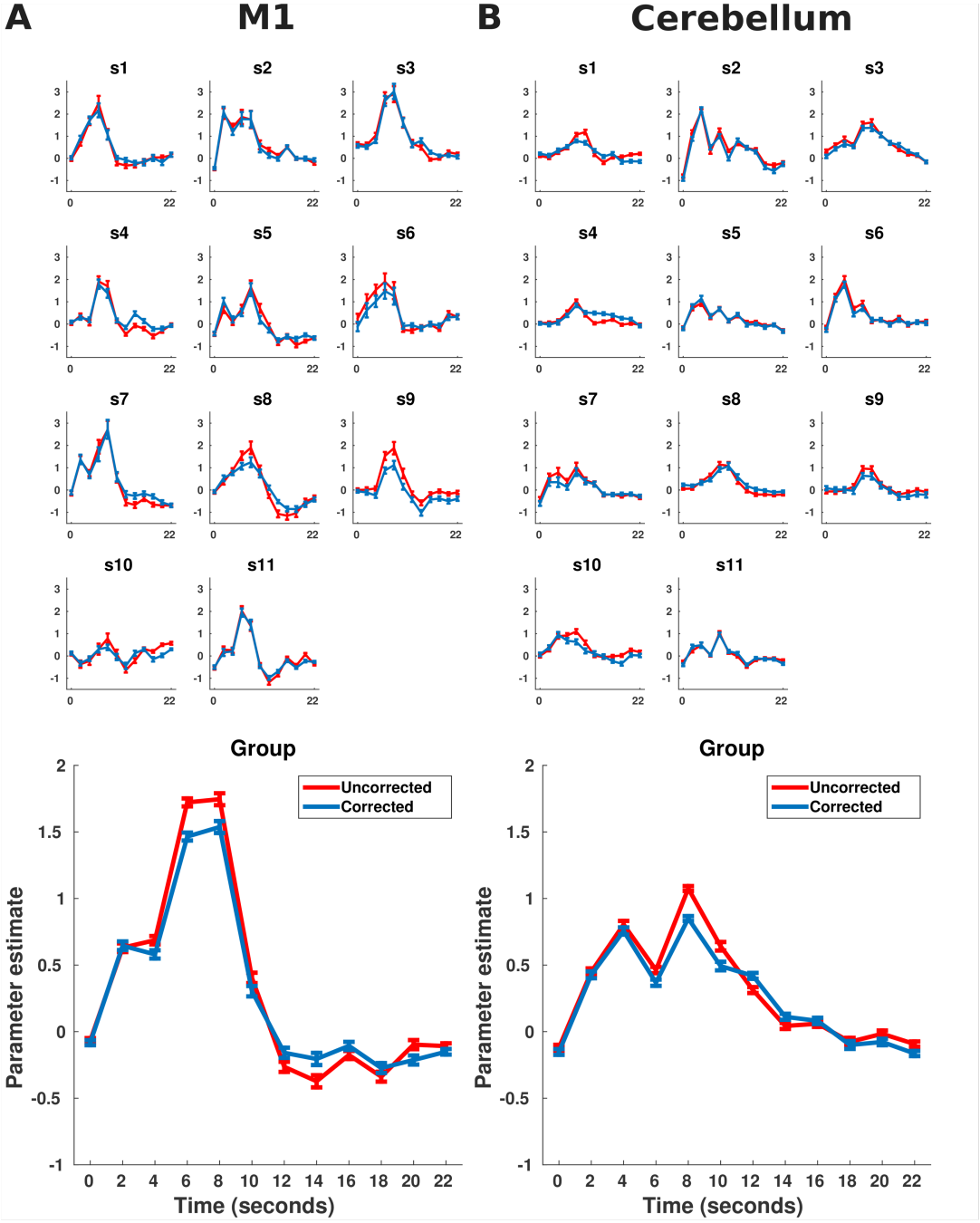

Table 2.2 Comparison of deconvolved HRFs from the Uncorrected model with each of seven Corrected models
Interaction term quantifies time-dependent differences in HRF between models.

	M1		Cerebellum	
Model	**Interaction F**	**Interaction P**	**Interaction F**	**Interaction P**
RV + HR + phase	4.6	**0.0001**	4	**0.0001**
HR + phase	5.7	**0.0001**	6.4	**0.0001**
RV + phase	0.9	0.51	0.7	0.71
HR + RV	4	**0.0001**	4.1	**0.0001**
HR only	5	**0.0001**	7	**0.0001**
RV only	0.7	0.73	0.4	0.95
Phase only	1.9	0.053	1.2	0.33

2.3.4 Percent Variance Explained and Model Comparisons

We next asked whether including task-dependent effects on the physiological variables improved the fit of our eight GLMs. Table 2.3 reports percent variance explained by each of the models. For all models, percent variance explained was greater in M1 compared to the cerebellum. Given that the responses in M1 tended to have higher peaks, be more consistent across participants, and bear a stronger resemblance to the canonical HRF, this result is perhaps unsurprising. However, it is possible that our ROI selection procedure resulted in greater heterogeneity of responses among voxels in the cerebellar ROI due to the ROIs extending beyond the anterior lobe.

For each region, including a new set of regressors (individually or in combination) yielded a mean increase of variance explained between 6.9 and 12.3% (Figure 2.4). The addition of HR and RV regressors tended to improve model fits more than phase regressors. Overall, for M1, the increase for the Fully Corrected model compared to the Uncorrected model ranged from 23.9% to 37.5% across participants. The comparable range for the cerebellum was 22.8% to 31.1%. Figure 2.4 illustrates, in the percentages adjacent to each arrow, the mean additional percent variance explained by the addition of each set of regressors.

A nested series of pairwise F-tests were used to test the impact of adding each set of physiological regressors. For each F-test, a given model was compared to a subordinate, reduced model from which one set of regressors had been removed (see Equation 2). This allowed quantification of the improvement in model fit due to the addition of a given variable as defined by a set of regressors. In M1, adding HR and RV regressors significantly improved the fit for a majority of participants, while adding phase did not (Figure 2.4). In the cerebellum, the number of participants with significantly improved fit was lower, and there were no substantial differences when adding HR, RV, or phase regressors.

Given the similarity of the mean additional percent variance explained in M1 and the cerebellum following the addition of physiological regressors, the disparity in number of participants with significantly improved fit is somewhat surprising. Paired t-tests on additional percent variance explained for each correction were used to directly compare the relative efficacy of these corrections in M1 and the cerebellum. No significant differences were found for any of the nine corrections ($p > 0.15$ for all). Thus, while the effects tended to reach statistical

Table 2.3 Percent variance explained
Values represent mean percent variance explained, standard error of the mean, and minima and maxima across participants, within all participants' M1 and Cerebellar (Ce) ROIs, for each model.

Model	M1 mean	M1 sem	M1 min	M1 max
Uncorrected	24.6	1.8	12.6	34.7
RV	36.9	1.4	31.5	47.1
HR	36.1	1.8	27.6	45.0
Phase	32.5	1.9	19.4	41.4
RV + HR	46.6	1.4	40.2	54.8
RV + Phase	43.7	1.3	36.1	51.1
HR + Phase	43.3	1.7	34.2	50.9
RV + HR + Phase	52.6	1.2	45.7	58.6

Model	Ce mean	Ce sem	Ce min	Ce max
Uncorrected	15.8	1.3	10.2	23.4
RV	26.3	1.8	20.3	38.3
HR	26.2	1.8	19.9	36.0
Phase	23.1	1.3	16.3	31.3
RV + HR	26.2	1.9	29.2	45.9
RV + Phase	33.3	1.7	26.7	43.3
HR + Phase	33.2	1.8	25.8	42.5
RV + HR + Phase	41.7	1.9	35.2	51.3

significance for individual participants only in M1, the overall magnitude and pattern of improvements was quite similar for both M1 and the cerebellum.

2.4 Discussion

The current study examined how task-related changes in heart rate and respiration influence the BOLD response and therefore might impact the interpretation of neural activity. Specifically, we assessed how including physiological nuisance regressors, some of which contained task-related fluctuations, altered the shape of the computed hemodynamic response function. The inclusion of these regressors allowed us to account for additional variance, even as the overall shape of the HRF remained relatively unchanged.

2.4.1 Improvements in model fit obtained using nuisance variable regression

fMRI studies that seek to account for physiological fluctuations typically include heart rate and respiration as nuisance regressors in the GLM. Indeed, in analyses of functional connectivity, these physiological corrections are increasingly common (e.g., Birn et al., 2008,

Figure 2.4 Model comparisons: Increase in percent variance explained and nested F-tests Percentage values represent the mean additional percent variance explained by each correction (percent variance explained in the full model minus that of the reduced model, as in Eq. 2) for M1 (A) and Cerebellum (B) ROIs. Values in parentheses are the number of the 11 participants for whom each correction resulted in a significant improvement in model fit ($p < 0.05$), accounting for the reduction in the degrees of freedom due to additional regressors.

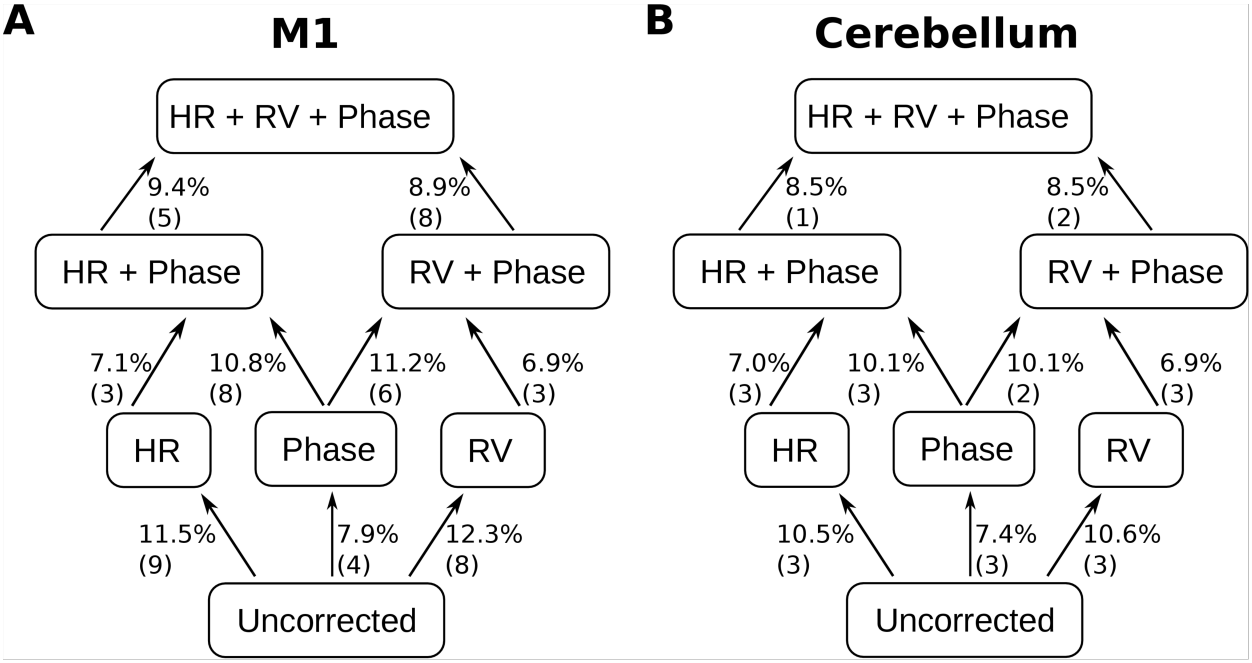

2009; Chang et al., 2012). The benefits of this type of nuisance variable regression for task-related fMRI, however, have not been widely considered. Schlerf et al. (2012) provide an extreme example in which the failure to account for the effects of task-related changes in heart rate on fMRI responses led to a radically different interpretation than that obtained when heart rate changes were included in a GLM. The current study used a nested analysis of a set of physiological variables, either modeled individually or in combination within the GLMs.

In our set of GLMs, those that included heart rate or respiratory variation as a nuisance regressor tended to produce greater improvements in variance explained than those that included phase. With the fully corrected model, the mean percent variance explained increased from 24.6% to 52.6% in M1 and from 15.8% to 41.7% in the cerebellum (Table 2.3). In both regions, inclusion of RV, HR, and phase regressors in isolation resulted in mean improvements of around 10% (Figure 2.4). These increases are considerably higher than those reported in a previous resting state fMRI study in which the inclusion of cardiac rate regressors only explained an additional 1% of the variance (Shmueli et al., 2007). This difference is likely due to the increased sensitivity of our task- and ROI-based approach. Indeed, the magnitude of our correction effect is similar to that of Chang et al. (2009), who used a whole-brain analysis of resting state data but only in voxels where a significant proportion of the variance was explained by physiological regressors.

Overall, the inclusion of physiological regressors at the individual level improved the fit

more reliably in M1 than in the cerebellum. Adding HR to the GLM produced a significant improvement in fit in the cerebellar ROI for only three participants (compared to nine for M1), a result that was unexpected given the cerebellar findings of Schlerf et al. (2012), which study did not directly compare the two regions but found that a similar set of lagged heart rate regressors explained about 3% of the variance in the BOLD signal across the cerebellar cortex. Furthermore, the shapes of the responses to changes in heart rate were similar to those deconvolved by Schlerf et al., 2012. There are, however, a number of noteworthy differences between the studies. First, our movement-related ROIs were comprised predominantly by voxels in lobules I-V, whereas the heart rate-modulated activity in Schlerf et al. was predominantly located in lobule VI. Second, the movement task used in the current study did not employ visual targets or involve visual feedback. Third, the movement vs. rest contrast in the current study typically produces more reliable activations in the cerebellum (and M1) than the errors vs. correct trials contrast examined by Schlerf et al. Accounting for a confounding factor such as heart rate may be more important for statistical contrasts that produce less reliable results.

Including cardiac and respiratory phase, as implemented using RETROICOR and other methods, has been shown to provide a significant improvement over uncorrected models (Hu et al., 1995; Glover et al., 2000). However, adding the rate of cardiac and respiratory events to models may account for non-overlapping portions of variance, given that only heart rate shows task-related changes. By using a set of nested GLM analyses, we were able to determine whether additional sets of regressors redundantly account for variance that could equally well be attributed to different sets of regressors. For instance, both alone and in combination with other sets of regressors, phase regressors accounted for a smaller proportion of additional variance than either set of rate-based regressors. Tracking the influence across the levels of the M1 tree in Figure 2.4, the inclusion of HR accounts for about 10% additional variance when added to the uncorrected model, to a model that already includes phase, or to a model that already includes both RV and phase.

Prior studies of the redundancy of information in physiological regressors have led to the recommendation that the regressors be consolidated, either by averaging correlated regressors or by replacing sets of shifted time series with single regressors that have been convolved with an appropriate response function (respiratory, Birn et al., 2008, and cardiac, Chang et al., 2009). Our FIR approach, with 11 additional regressors probing the lagging influence of these processes, had two advantages over previous approaches. First, it allows for the deconvolution of the full HRF. Second, it allows the impact of physiological regressors to vary over time. However, our approach does entail a greater reduction in the degrees of freedom for statistical testing, and this may have increased the prevalence of null results at the individual level.

2.4.2 Task-related changes in physiological variables and their impact on the hemodynamic response

Using a simple movement task in a slow event-related paradigm, we observed a robust task-related increase in heart rate of about 1%. While the increase in heart rate occurred slightly faster (peaking around four seconds) than the canonical hemodynamic response (which peaks at around six seconds), the overlap in the time courses of these two responses is considerable and therefore of concern for interpretations of underlying neural activity. Since each beat of the heart delivers oxygenated hemoglobin to the brain, and the BOLD signal is a measurement of the ratio

of deoxygenated and oxygenated hemoglobin, changes in heart rate will modulate the BOLD signal and may therefore be misattributed to neural activity. That is, task-related changes in heart rate could, at least in some cases, be so closely linked to the task parameters as to be indistinguishable from neural changes.

Many fMRI analysis packages, by default, convolve task regressors with a canonical HRF to model event-related responses. For some participants, this may produce an poor fit of the data (reviewed in Handwerker et al., 2012). Handwerker et al. (2004) provided an example where a 1 s error in an individual-specific HRF reduced the explained variance by 10%, and at 2 s error the explained variance was reduced by 38%. Given that the HRF varies greatly across individuals, it has been recommended that a separate task run be included to obtain individual-specific HRFs (Aguirre et al., 1998; D'Esposito et al., 1999; Handwerker et al., 2004). While this approach can help account for relatively large inter-individual differences, smaller differences in the shape of the HRF may still remain across brain regions. Moreover, these regional differences may be differentially influenced by physiological factors, depending on their proximity to vasculature and sulci (Birn et al., 2006, 2008).

Our analyses of the deconvolved hemodynamic response revealed subtle effects of physiological corrections. The deconvolved HRFs in both the M1 and cerebellar ROIs were similar at the group level, but the inclusion of physiological regressors in the GLM yielded heterogeneous changes in the deconvolved HRFs of individual participants. Given the variation in the HRF across individuals, brain regions, and task parameters (Handwerker et al., 2004; Birn et al., 2008), as well as the spatial heterogeneity of susceptibility to physiological influences across the brain (Birn et al., 2008; Chang et al., 2009), differences in the shape of task responses caused by task-related physiological covariates are likely to be minor and irrelevant to the decision to use the canonical HRF to model task responses. However, the current results point to an important role for HR correction in accurately estimating the hemodynamic response, particularly when a task-related change in heart rate is present.

In the group data, the HR correction lowered the peak of the estimated HRF in both M1 and the cerebellum (Figure 2.3). The lower peaks indicate that some of the variance attributed to movement-related neural activity (via the Move vs. Rest contrast) was accounted for by the HR correction. This observation is in accord with the known impact of heart rate changes on the BOLD signal (Shmueli et al., 2007). This relationship has been described by a cardiac response function (CRF), deconvolved from fMRI data recorded while participants were lying at rest in the scanner. With a deconvolved CRF, heart rate is positively correlated with the BOLD signal at lags of around 4 s and negatively at lags around 12 s (Chang et al., 2009). The initial positive correlation, combined with the increase in heart rate induced by our movement task, offers an explanation for the reduced HRF peaks following addition of HR regressors. Specifically, variance that had previously been misattributed to neural responses was re-allocated to physiological variables, decreasing parameter estimates for the movement regressors at these lags.

Because of the involuntary nature of the autonomic process, heart rate is less controllable experimentally than respiration (Birn et al., 2006, 2008). However, the discrete nature of heartbeats has the advantage of reducing the number of possible sources of variance in the BOLD signal compared to changes in either the rate or depth of respiration. Importantly, a movement task such as that employed here can be a reliable modulator of heart rate. Indeed, a movement task might be used to drive a change in heart rate should an experimenter wish to

explore individual physiological response functions. Convolving physiological regressors with this function avoids the loss of degrees of freedom imposed by an exhaustive lagged approach. Furthermore, modeling individual-specific changes in heart rate due to movements as small as button presses could account for unwanted sources of variance across a range of tasks. Other cognitively or emotionally demanding tasks are known to influence heart rate, and, as such, the BOLD response would likely be influenced by the inclusion of heart rate regressors in a GLM.

Respiration, on the other hand, was not reliably modulated during our simple movement task. The lack of an effect of RV regressors on the shape of the hemodynamic response is consistent with our previous event-related study of movement errors (Schlerf et al., 2012). Naturally-occurring changes in respiration may result from depth, duration, and/or frequency of breaths, necessitating tighter experimental control through cued breathing tasks in order to independently assess these sources of variance (Birn et al., 2006, 2008, 2009). However, it is unclear to what extent cued changes in respiration mimic naturally-occurring changes in respiration (Birn et al., 2008). Further research on the impact of RV on fMRI signals is needed, given the lack of effect of RV on the HRF but comparable efficacy of HR and RV in nuisance variable regression in the current study (Table 2.3, Figure 2.4).

2.5 Conclusions

Sources of variance in fMRI studies that are unaccounted for may influence the shape of the hemodynamic response function (HRF) and/or model fit. These unmodeled variables may be particularly problematic when they are correlated with task factors. We modeled a set of physiological variables as nuisance regressors to examine their impact on the deconvolved hemodynamic response and on model fit. Regressing out task-related changes in heart rate (HR) resulted in subtle changes in the HRF in both cerebellum and M1, with or without the presence of respiratory variation (RV) and phase regressors. These results indicate that the BOLD response can be more accurately estimated by including HR in a GLM even when changes in HR are correlated with changes in the contrast of interest. As assessed by model fit at the group level, the inclusion of both RV and HR regressors resulted in significant improvements in model fit that exceeded those of phase regressors, further underscoring the need to account for both task-related and task-independent changes in the rate of physiological processes when inferring patterns of neural activity from fMRI time series.

Chapter 3: Limited effect of temporal constraints on feedback in learning to control movement speed

3.1 Introduction

Humans learn from their mistakes. Across a variety of tasks, sensory information about errors can be used to update subsequent movements on a trial-by-trial basis (Desmurget & Grafton, 2000). In laboratory settings, errors can be induced and studied by altering the mapping between a participant's movements and the outcomes of those movements. Such studies have shown that people can successfully use feedback about errors to adapt hand movements to a variety of perturbations, including visuomotor (prism) rotations (Redding & Wallace, 1988; Martin et al., 1996; Krakauer et al., 2000; Mazzoni & Krakauer, 2006), force fields (Shadmehr & Mussa-Ivaldi, 1994; Donchin et al., 2003), target jumps (Diedrichsen et al., 2005), and gain alterations (Turner et al., 2003; Krakauer et al., 2004). In these tasks, the spatial mismatch between expected and actual feedback provides a teaching signal that can be used to adjust subsequent movements.

Various lines of evidence suggest that error-based learning in motor control may be limited to situations in which the feedback about an error arrives within a small temporal window after the movement is completed. In a dramatic example involving visuomotor rotation learning, shuttered prism goggles were used to delay endpoint feedback by precise intervals ranging from 0 to 1000 ms, and learning was attenuated by about 50% when feedback was delayed by as little as 500 ms (Kitazawa et al., 1995).

More generally, temporal constraints in the subsecond range are ubiquitous in sensorimotor learning. Studies of eyeblink conditioning in rabbits, where the presentation of a tone is followed by a puff of air, have demonstrated that conditioning is less robust when the conditioned and unconditioned stimulus are more than 300 ms apart (Schneiderman & Gormezano, 1964; Smith 1968). Below this limit, animals are able to learn highly precise representations of the interval between the conditioned and unconditioned stimuli, timing their eyeblink appropriately in order to attenuate the aversive air puff (Millenson et al., 1977; McCormick & Thompson, 1984). Similar intervals are important for linking contextual cues to motor outputs in humans: When the gap between the two events exceeds 600 ms, people are unable to use contextual information to facilitate motor performance on subsequent trials (Howard et al., 2012; Howard et al., 2013).

The circuitry and physiology of the cerebellum have been proposed to provide a basis for these temporal constraints (Ito 2002; Ohyama et al., 2003). The cerebellum has been implicated not only in error-based learning (Martin et al., 1996; Diedrichsen et al., 2005; Donchin et al., 2012; Schlerf et al., 2012) but also as a structure that contains precise temporal representations within the subsecond range (for review, see Ivry & Spencer, 2004; Mauk & Buonamano, 2004). For example, in eyeblink conditioning, lesions to the cerebellar cortex degrade the fidelity of temporally specific stimulus-response associations. Following such lesions, the eyeblink may still occur, but it is inappropriately timed (McCormick & Thompson, 1984; Perrett et al. 1993; Koekkoek et al. 2003). At the cellular level, error-based learning is thought to be the result of long-term depression (LTD) occurring at Purkinje cell synapses (Marr, 1969; Albus, 1971; Ito, 1984). This form of LTD is critically dependent upon the temporal coincidence of motor commands carried by parallel fibers and error signals carried by climbing fibers (for review, see

Ito 2002). Disruption of this critical link between movement and feedback about that movement diminishes the brain's ability to form associations.

Despite these limitations, the results from a pair of recent studies challenge the idea of temporal specificity for feedback processing in sensorimotor adaptation. With online feedback, interference from a delay was mitigated if the participant was trained with delayed feedback during a baseline phase prior to the introduction of the perturbation (Honda et al., 2012a,b). Thus, it may be that the critical temporal factor is consistency, whether immediate or delayed.

The notion that motor skills may be learned with delayed feedback is also supported by an abundance of real-world tasks that involve delayed feedback. Players of bocce, golf, and archery routinely experience delayed outcome feedback. Moreover, shuffleboard players move and release a puck, watching as it slides along a surface to its final resting place. In this context, there is a relationship between movement velocity and feedback delay, such that greater applied forces will lead to longer delays between the hand movement and the puck coming to a complete stop. As the puck travels, it may come to a stop at the target location, travel further than anticipated and pass the target earlier than anticipated (an overshoot), or fail to reach the target altogether (an undershoot). Thus, only successful movements result in feedback about the outcome of the movement (binary success or failure) and the nature of the error (continuous size and direction) co-occurring; unsuccessful movements may result in feedback about the outcome occurring either before or after the size and direction of the error are apparent.

Although the player has access to both the felt sense of their arm movement and vision of the puck as it travels, precise information about the size and direction of the error produced by his/her movement is determined only when the puck has come to a stop. Proprioceptive feedback from early portions of a movement can provide a useful temporal cue for the timing of subsequent movements (Schmidt & Christina, 1969). As such, it is possible that these delays become predictable from the early proprioceptive information. However, during the early stages of learning, endpoint feedback is necessary for identifying the proprioceptive signals that lead to positive outcomes. How the brain binds delayed feedback to long-completed movements in order to update future motor plans remains unclear.

It has been hypothesized that the cerebellum is capable of issuing and updating separate spatial and temporal predictions about feedback, allowing learning to occur despite delays between these two sources of feedback (Miall et al., 1996). Compensation for delayed feedback has also been observed in manual tracking studies (Foulkes & Miall, 2000; Miall & Jackson, 2006), suggesting that the cost of delaying feedback can be overcome in certain situations. In compensating for a delay while tracking a moving target, intermittent corrective movements become more precise but not necessarily more frequent or smoother (Miall & Jackson, 2006). This suggests that delay adaptation occurs through direct modification of feedforward motor commands, rather than by simply delaying these commands using a separate temporal prediction error (Miall & Jackson, 2006, but see also Farshchiansadegh et al., 2015). However, a role for a separate temporal prediction in other tasks, particularly those which rely on endpoint feedback, cannot be ruled out. A recent study of manual tracking with delayed feedback demonstrated an important role for the predictability of the trajectory of a tracked stimulus in adapting to a delay (Rohde et al., 2013). Furthermore, the temporal specificity of stimulus-response associations formed in eyeblink conditioning suggests that temporal models of feedback may be as precise and important as visuospatial ones.

One common feature of visuomotor rotation learning, force field learning, and manual

tracking tasks is that participants maintain spatial accuracy by updating an internal model of how their movements will traverse the workspace (Shadmehr & Mussa-Ivaldi, 1994; Miall & Reckess, 2002; Tseng et al., 2007). These adjustments may occur via the cerebellar error signal updating the weights of connections between visually tuned neurons in the parietal cortex and directionally tuned neurons in the motor cortex (Tanaka et al. 2009). Gain adaptation, by contrast, is an example of a task where learning is based on errors of movement amplitude (and therefore, a correlate of amplitude, movement speed), rather than movement direction. Specifying an appropriate gain for a movement necessarily entails temporal prediction, as movements that are hypo- or hypermetric will terminate early or late.

Some behavioral studies have characterized roles of prior exposure, variability, and sensory feedback in learning to produce movements of particular speeds and amplitudes (Schmidt 1969; Zelaznik & Spring, 1976; Zelaznik et al., 1987). Studies of gain adaptation have primarily focused on the vestibulo-ocular reflex (Kawato & Gomi, 1992; Raymond & Lisberger, 1998). Computational models of vestibulo-ocular reflex adaptation have proposed a unified mechanism for control of gain and timing (Yamazaki & Nagao, 2012), building on previous neural network-based accounts of timed responses in eyeblink conditioning (Buonomano & Mauk, 1994; Medina et al., 2000). However, most studies of trial-by-trial error-based learning in reaching tasks have relied on visuomotor (prism) rotations, the application of force fields, and target jumps. In all of these cases, learning is guided by errors of movement direction. As a consequence of this focus, it remains unclear whether feedback delays similarly affect the learning of both movement speed and direction.

Constraints associated with tasks that involve using feedback to correct directional errors (e.g., visuomotor rotations) may not generalize to tasks requiring corrections in movement speed or amplitude. Behaviorally, motor adaptation to a change in cursor gain proceeds quickly and generalizes broadly across the workspace (Bock 1992; Pine et al., 1996; Krakauer et al., 2000; Vindras & Viviani, 2002). Adaptation to visuomotor rotations, on the other hand, proceeds more slowly and generalizes narrowly around trained targets (Pine et al., 1996; Krakauer et al., 2000; Brayanov et al., 2012). Neurally, movement direction and amplitude are thought to be specified in independent circuits, each subject to distinct computational constraints (Bock 1992; Krakauer et al., 2004; Vindras & Viviani, 2002).

It remains unknown whether gain and/or amplitude-based learning is subject to similar temporal constraints as those observed in studies of direction-based learning. In learning to specify movement direction, artificial delays in feedback timing do not convey additional information about the success or failure of the movement. In contrast, when learning the desired amplitude and speed of a movement, the timing of feedback can convey an additional error signal that is redundant with the spatial signal. In shuffleboard, for instance, a puck that undershoots the target stops short in both time and space; similarly, a puck that overshoots the target continues to travel past the desired time and location. This redundancy may enhance learning by rendering the temporal and spatial error congruent, potentially leading to supra-additive efficacy of the two cues (Ernst & Banks 2002; Ivry & Richardson 2002).

The effect of this congruence leads to the prediction that, in movement speed learning, delayed feedback may result in superior performance relative to immediate feedback. Specifically, it is possible that temporal predictions afforded by meaningful delays may play a facilitatory role in anticipating and learning from delayed feedback on a trial-by-trial basis. We hypothesized that predictably delayed feedback—that is, feedback presented at a delay that is

correlated with some movement parameter—may provide temporally predictive information that bolsters the accuracy of adjustments to future movements. Such an advantage could ultimately outweigh any cost of delayed feedback that may be present in movement speed learning. Temporal predictions may become more important when learning to compensate for errors of movement speed, as movements with differing speeds, amplitudes, or forces may have consequences that are differently extended in time. Given that there is a clear cost of delayed feedback in learning to adjust movement direction (Kitazawa et al., 1995), and that delays do not typically scale with error direction in ecological settings, an advantage of predictability may be unique to learning movement speeds.

A novel paradigm was devised to test the role of temporal constraints on learning to produce movements of certain speeds. This paradigm, a virtual shuffleboard task, relies on naturally committed errors rather than perturbations, as participants needed to learn to move a sensitive controller in order to hit a target that was presented at different distances from the start position. In each trial, the participant pushed a virtual puck across a "release line." Hand speed at the crossing of this line determined how far the puck "traveled" up the screen, with greater movement speeds reaching farther (higher) positions. Participants had access to both visual and proprioceptive cues while the puck was under their control. Once released, the visual feedback was removed, only reappearing at the final endpoint.

Groups of participants were provided with identical spatial feedback, but the timing of this feedback varied. We hypothesized that predictably delayed feedback—that is, feedback presented at a delay that is correlated with some movement parameter—may provide a temporal prediction that enhances the accuracy of adjustments to future movements. Experiment 1 searched for a cost of simple feedback delays on learning. Experiment 2 examined the impact of potentially informative delays in variable feedback timing schemes, examining the effects of predictability and of ecological validity on learning. In Experiment 3, these effects were re-examined with a shortened range of delays, selected to correspond to the range required for cerebellar-dependent learning (under 600 ms, cf. Howard et al., 2012).

3.2 Material and methods

3.2.1 Participants

140 participants were recruited for this study. Of these, six were excluded for poor performance as outlined in section 3.2.7, resulting in a total of 134 participants (77 female, mean age = 20.8, sd = 2.2).

All participants were right handed with normal or corrected-to-normal vision and completed an informal colorblindness test prior to the study. All participants were naive to the purpose of the study and received course credit for their participation, along with a bonus of two cents for every hit target. The participants provided written informed consent in accord with a protocol approved by the Institutional Review Board at the University of California, Berkeley.

3.2.2 Experimental Setup

Participants were seated comfortably at a table and instructed to hold the handle of the manipulandum (fmrirobot.org) with their knuckles pointing forward. Movements were made by

Figure 3.1 Experimental setup and task
A. Participants held the handle of a robotic manipulandum to move an onscreen cursor.
B. Presentation of a puck in the lower portion of the screen was the cue to move.
C. Example endpoint feedback shown in red for misses.
D. Example endpoint feedback shown in green for hits.

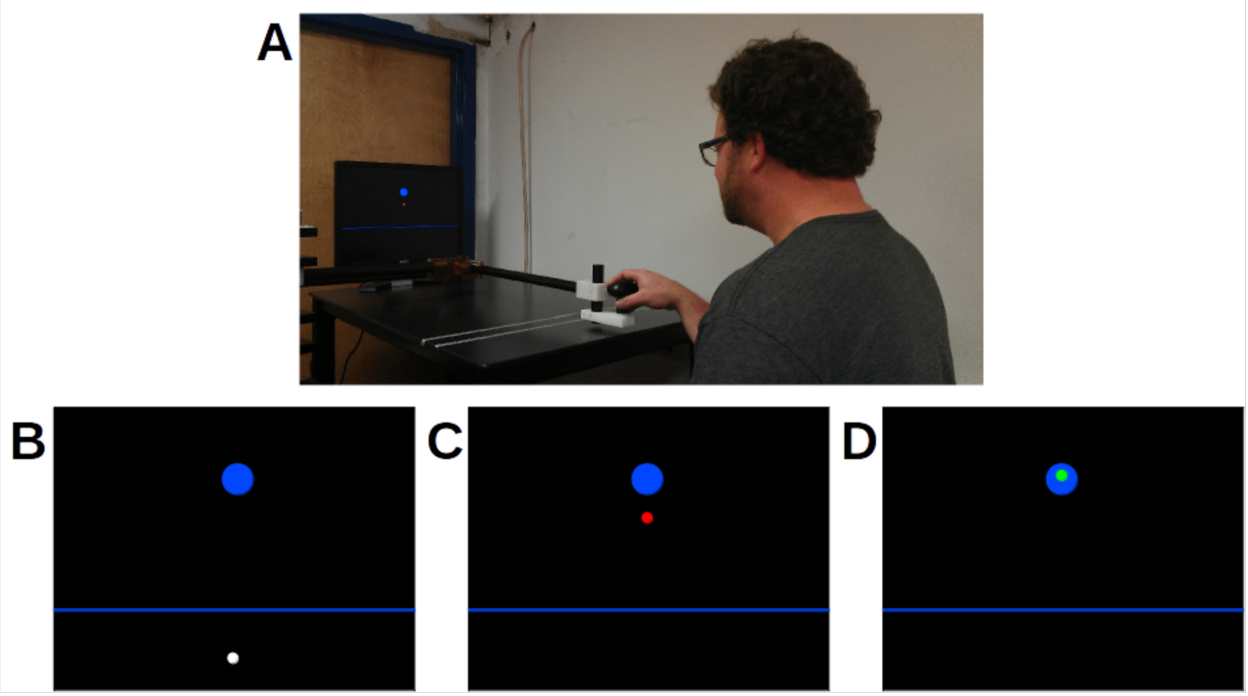

moving the handle away from the body in the z-plane. They were instructed not to rest their elbow on the table (to avoid curved reaching trajectories). The manipulandum recorded hand position at 1000 Hz.

Stimuli were displayed on an LCD monitor placed 1.1 meters from the edge of the table (Figure 3.1A). This allowed sufficient space for the arm of the manipulandum to move freely. Note that the horizontal plane of motion was perpendicular to the monitor. This setup also situated the participant at the edge of a much longer space than the height of the monitor, creating the impression of a long distance to be covered by their puck. When the puck was visible, it was constrained to move only along the y-axis (vertically on-screen), ignoring lateral deviations produced by participants in the x-direction (horizontally on-screen). Participants were informed of this constraint and instructed to minimize side-to-side movements.

3.2.3 Task Instructions

Participants were told they would be playing a virtual shuffleboard game. In real-world shuffleboard games played on a physical surface (usually the ground or a long, narrow table), the speed of the puck at the moment of release determines how far the puck will travel along a given surface. The experimenter demonstrated this concept by pushing and releasing a real puck on a smooth surface while emphasizing the importance of the translation from hand speed to distance for task success.

In the virtual simulation of this game, the on-screen puck was presented as a white circle with a radius of 0.5 cm (Figure 3.1B). The puck was automatically released when the participant's hand crossed the blue release line; participants were instructed not to simulate a releasing action. Hand speed at the moment the hand crossed the line determined how far the puck would travel. To reinforce this, the puck was visible only as their hand approached the release line. Once the participant's hand crossed the line, the puck disappeared, reappearing at a distance from the line as determined by their hand speed (endpoint-only feedback). The color of the puck at the time of its reappearance provided additional feedback: red if it landed outside of the target (Figure 3.1C) and green if it landed within the boundaries of the target (Figure 3.1D).

The participant's goal was to move his/her hand at a speed that caused the puck to land on one of four target locations. Targets were presented visually as blue circles with an on-screen radius of 1.5 cm. The target could be situated 2.0, 5.3, 8.8, or 12.0 cm from the center of the screen. The release line was located 5 cm below the center of the screen, with the puck's start position 15 cm below the center of the screen.

After initially demonstrating the speed-to-distance translation with a real object on a table, the experimenter demonstrated 10-30 trials of the task at varying speeds using the manipulandum, confirming verbally that the participant understood they would be required to adjust their hand speed to hit various targets. Participants were told to "follow through" on their movement in a manner that felt natural. They were reminded that movement speed, and not the distance covered by the movement, would determine the distance traveled by the puck. Participants moved the handle back to the start location immediately following each trial. They received two cents for each "hit," and the total amount accumulated was displayed on screen at the end of each block.

3.2.4 Task Structure

The experimental session was composed of five blocks. Within each block, there were eight miniblocks that consisted of 12 consecutive trials with a single target. Each of the four targets was presented twice during a block. The order of targets was pseudo-randomized, subject to the constraint that the target position changed for each miniblock.

At the beginning of each trial, a target and a puck appeared on the screen, signaling the participant to move. Once the participant's hand moved past the release line, the puck disappeared and reappeared some distance from the line. Feedback timing was defined relative to the time that the participant's hand crossed the line. The red or green puck feedback remained visible for 500 ms. A new target appeared after the participant moved back to the starting region and maintained a steady position for 500 ms (change in hand position below 1 cm). Participants could take a break at any time, although very few took breaks during a block.

3.2.5 Speed-to-Distance Mapping to Determine Puck Endpoint

Participants' hand speeds at the moment of puck "release" were determined by calculating the time it took to traverse a 5 cm window preceding the release line (Figure 3.2A). The distance traveled for a given hand speed was calculated as:

$$d = -v^2/a \qquad \text{(Equation 1)}$$

Figure 3.2 Schematic of distance and timing manipulations for Experiments 1-3
A. Schematic representation of the mapping of movement speed to feedback distance, which was identical for all experiments. Blue circles indicate the approximate speed required to hit each of four targets situated at different distances from the release line. This mapping is in fact slightly parabolic, as per Equation 1. However, in the space sampled here, the relationship is essentially linear.
B. Schematic representation of timing manipulations for Experiment 1.
C. Schematic representation of timing manipulations for Experiment 2. For simplicity, axes uniformly terminate at 1000 ms. The actual range of feedback times for hitting any target was 160-1058 ms (Physics) and 380-1142 ms (Reverse Physics). Maximum feedback times were 1440 ms (Physics, at far edge of screen) and 1300 ms (Reverse Physics, at release line). When randomized, feedback occurred between 0 and 1200 ms (Random Group).
D. Schematic representation of the timing manipulations for Experiment 3. For simplicity, axes uniformly terminate at 1000 ms. The actual range of feedback times for successfully hitting any target was 214-631 ms (Short Physics) and 169-586 ms (Short Reverse Physics). The maximum feedback times were 800 ms (Short Physics, at far edge of screen) and 800 ms (Short Reverse Physics, at release line). When randomized, feedback occurred between 0 and 800 ms (Short Random Group).

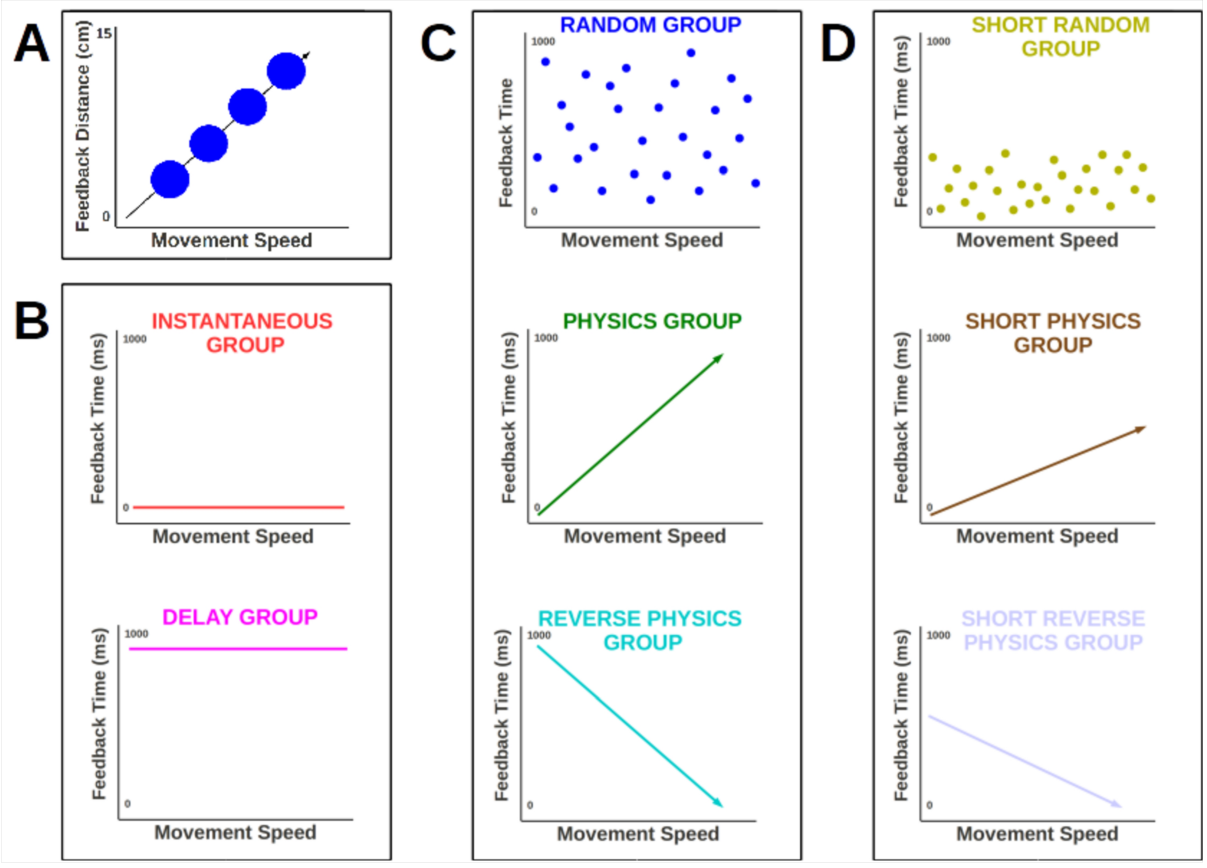

where *d* is the distance the puck will travel, *v* is the velocity at the moment of release, and *a* is a constant representing deceleration, given a fixed coefficient of friction for a surface. Across all experiments, the deceleration constant *a* was set to 30,000 s. This value was selected such that speeds of 5.0 cm/s and 87.2 cm/s caused the puck to land at the release line or far edge of the monitor, respectively. The range of speeds required to hit the four targets was 40.7-50, 51.5-58.8, 61.0-67.6, and 68.5-73.5 cm/s. Given that participants could see the cursor moving as it approached the line, the task was programmed such that the space above/beyond the release line had a greater coefficient of friction than the space below/preceding the line. However, the speed-to-distance mapping remained constant across all participants and all sessions. If a participant produced a speed that caused the puck to "land" beyond the edge of the monitor, a "Too fast" warning was displayed.

3.2.6.i Timing Manipulations, Experiment 1

Two groups were tested in Experiment 1 (Figure 2B). For the Instantaneous group (n = 16, 6 female, mean age 21.4), the feedback puck appeared as soon as the participant's hand crossed the release line. For the Delay group (n = 15, 10 female, mean age 20.5), the onset of the feedback puck was delayed for 1000 ms (Figure 3.2B).

3.2.6.ii Timing Manipulations, Experiment 2

Three groups were tested in Experiment 2 (Figure 2C). For the Physics group (n = 16, 9 female, mean age 20.9, one of 17 excluded), the time required for the puck to come to a complete stop (i.e., time at which feedback appeared) was calculated as:

$$t = -v/a \qquad \text{(Equation 2)}$$

where *t* is time elapsed between release and the puck stopping/reappearing, *v* and *a* are as in equation 1. Because the coefficient of friction (and, therefore, the deceleration constant) was arbitrary, as was the mapping between virtual space and the monitor, feedback times were transformed to fall within a range of times that fit the monitor's boundaries. To ensure a realistic task environment, a spatial and temporal discontinuity between locations before and after the release line was not ideal. However, allowing participants to view the puck as it traveled towards the release line while still using an unscaled feedback mapping beyond the release line would have required a monitor that approximated the length of a real-world shuffleboard table. To avoid this, the virtual shuffleboard table was truncated to omit the first portion of the puck's trajectory following the release line. As such, the puck was limited to land at any location between the release line and the edge of the monitor. The screen-adjusted feedback time was given as:

$$t\_adjusted = -k*v/a - s \qquad \text{(Equation 3)}$$

where *k* was 410,850 ms, *s* was 956 ms, and the total range of feedback times was 0 to 1440 ms. For successful movements, the ranges of feedback times for each of the four targets corresponded, from closest to farthest, to 160-413, 455-655, 714-895, and 920-1058 ms. Relative to the moment at which the hand crossed the release line, participants received endpoint

feedback at the screen-adjusted feedback time.

This mapping was flipped for participants in the Reverse Physics group (n = 17, 8 female, mean age 21.5) by subtracting the feedback time for the Physics timing group from a fixed value of *b*:

$$t\_reverse = b - (-k*v/a - s) \quad \text{(Equation 4)}$$

where *b* is 1300 ms. For the extreme cases, the feedback time was 0 ms (for fast movements that carried the puck off the monitor) and 1300 ms (for slow movements that resulted in the puck stopping just past the release line). For successful movements, the ranges of feedback times for each target, from closest to farthest, were 886-1142, 645-844, 405-586, and 242-380 ms. Note that this range differs slightly from the Physics timing, as a compromise was made between aligning the ranges of feedback times within each target and aligning the feedback times for pucks landing at the edges of the workspace.

As a control, the Physics and Reverse Physics groups' performance were compared to a third group that was tested with Random timing (16, 10 female, mean age 20.4, one of 17 excluded). For these participants, the feedback delay was a random value from the range of 100-1200 ms. Note again that this range differs from both the Physics and Reverse Physics ranges. Once again, priority was given to presenting feedback at times that aligned with the ranges corresponding to the four targets, rather than the complete range across the workspace. The Random timing scheme's range is slightly expanded outside of these limits to allow for occasional feedback times matching extreme trials for the Physics and Reverse Physics groups.

3.2.6.iii Timing Manipulations, Experiment 3

Three groups were tested in Experiment 3 (Figure 2D): Short Random, Short Physics, and Short Reverse Physics. For all groups tested in Experiment 3, the range of feedback delays was compressed relative to Experiment 2. After setting *k* to 190,000 ms and *s* to 300 ms (Equation 3), the resulting range of feedback times was 0 to 800 ms.

For the Short Physics group (n = 23, 15 female, mean age 20.2, one of 24 excluded), the ranges of feedback times given for hitting each of the four targets were 214-333, 353-445, 472-556, and 568-631 ms. In an attempt to obtain data wherein baseline performance was more similar to other groups, a second group of nine Short Physics participants was recruited after the group size reached 15. However, baseline performance for this second group was similarly poor. Analyzing the group of 15 and the group of 9 separately does not change the results of comparisons between Short Physics and other groups, nor does analyzing the first and last 12 participants as separate groups. As such, the results for the large merged group are reported here.

For the Short Reverse Physics group (n = 15, 10 female, mean age 21.6, two of 17 excluded), *b* was set to 800 ms (Equation 4), so that a puck landing at the edge of the monitor reappeared at 0 ms, while a puck reappearing just at the release line reappeared at 800 ms. The ranges of feedback times for hitting each of the four targets were 467-586, 355-447, 244-328, and 169-232 ms. Note that our goal of compressing feedback to below 600 ms (cf. Howard et al., 2012; Howard et al., 2013) applies approximately to the maximum feedback time for a successful movement (i.e., the farthest successful throw for the Short Physics group—feedback time 586 ms—and the closest successful throw for the Short Reverse Physics group—feedback

time 631 ms, a small expansion beyond the desired range).

For the Short Random group (n = 16, 9 female, mean age 20.9, one of 17 excluded), feedback was presented at randomly selected time within the range of 0-800 ms. As in Experiment 2, the Short Random timing scheme's range was slightly expanded outside of these limits to allow for occasional feedback times matching extreme trials for the Short Physics and Short Reverse Physics groups.

3.2.7 Exclusion criteria

Participants whose data suggested that they had not understood the task were excluded using three criteria. First, one participant was excluded for failing to traverse the release line in one smooth movement on more than 5% of the trials. Second, three participants were excluded because they were of low overall performance compared to the rest of their group. This was defined by calculating the mean error, on all trials across all blocks, for each of the 8 groups. Participants whose overall mean error was more than two standard deviations above their group's mean error were excluded. It should be noted that this approach failed to exclude participants with abnormally high error from the Short Physics group in Experiment 3, as the mean and variance of error for this group were exceptionally high. Finally, for each individual participant, the mean feedback distance was plotted as a function of target distance, averaging the data over all trials in all blocks. For a participant who is responding to changes in target location, this plot should have a positive slope, because far targets require faster movements to achieve an appropriate feedback distance. A too-shallow slope would indicate that the participant was not adjusting their movement speed in response to the change in target locations but rather simply moving at relatively the same speed for all targets. Therefore, if the slope of a given participant's function was more than two standard deviations below the group mean slope, he/she was excluded. Two participants were excluded for this reason (one each in Physics and Short Physics). A third participant (Short Reverse Physics) who was excluded for high mean error also met the criterion for exclusion by this metric.

3.3 Results

Across all experiments, all groups reduced their absolute error over the course of five task blocks, from an overall mean of 2.4 cm in block 1 to a mean of 1.7 cm in block 5. However, the task remained quite challenging throughout the session: mean percent hits (calculated as the mean of group means, weighting groups rather than individuals equally) increased from 47.6% in block 1 to 52.7% in block 5. Participants improved their accuracy by scaling their hand speed as a function of target distance, and as participants' performance improved over the course of the session, faster movements were associated with larger errors, a pattern that is consistent with known speed-accuracy tradeoffs (Fitts 1954; Schmidt 1969; Schmidt et al., 1979). All groups' absolute error varied as a function of target distance (Figures 3, 4, and 5, panels C and D). The negative correlation between movement speed, amplitude, or force and the accuracy of that movement is captured by Fitts' Law (Fitts 1954), and borne out across all three experiments.

Given the robust effects of target distance and task block, differences in the groups' learning functions across the five task blocks, as well as the groups' overall percent improvement, were assessed. Where the temporal manipulations created the potential for target-

specific effects of feedback latency, these effects were assessed as well.

3.3.1 Experiment 1

Experiment 1 examined the effect of feedback delay in the shuffleboard task, comparing the performance of participants who received feedback as soon as the hand crossed the release point (Instantaneous) or after a 1 s delay (Delay). Superior learning by the Instantaneous group would constitute a replication of Kitazawa et al. (1995), extending the reach of a known temporal constraint in visuomotor rotation learning to movement speed learning. Alternatively, equivalent performance would provide evidence for a mechanism for movement speed learning that is not subject to these constraints.

Both groups improved at the task over five task blocks. This reduction was evident both in the absolute error data (Figure 3.3A) and when the data were normalized with respect to performance in block 1 (Figure 3.3B), and was consistent across all targets (Figure 3.3C). To compare the two groups' learning functions, a two-way mixed effects ANOVA was conducted on the raw absolute error scores, with factors of group and block. There was no reliable difference between groups, $F(1,4) = 2.65$, $p = .102$, nor was there a significant group x block interaction, $F(1,4) = 1.98$, $p = .102$. A series of *post hoc* t-tests was used to directly compare the groups at each block. None of these comparisons revealed a reliable difference between the Instantaneous and Delay groups. Confirming that the participants improved with practice, however, there was a significant effect of block, $F(1,4) = 13.92$, $p < .0001$.

The data were also analyzed in terms of percent improvement, defined as the difference between block 5 and block 1 absolute error scores, divided by the block 1 score (Figure 3.3E). A two-sample t-test was conducted on the percent improvement scores. Consistent with the raw data, there was no difference between the groups on this measure, $t(29) = .01$, $p = .91$.

To test for target-specific differences in performance, the two groups' asymptotic performance (block 5) was compared at each of the four targets (Figure 3.3 C, D). There was no effect of group, $F(1,3) = .75$, $p = .39$, nor was there a group x target interaction, $F(1,3) = 1.27$, $p = .29$. However, there was an effect of target, $F(1,3) = 55.04$, $p < .0001$, consistent with the speed-accuracy tradeoff observed across the experiment. No effects of group or target were observed when a similar analysis was performed on the percent improvement data.

In summary, delaying feedback by 1 s did not have a measurable impact on learning in the shuffleboard task. This result is in contrast to the significant cost of delayed feedback that has been observed in visuomotor adaptation tasks (e.g. Kitazawa et al., 1995). These results suggest that temporal constraints may differ between tasks involving adaptation of a spatial transformation (e.g., visuomotor rotation) and a spatiotemporal mapping (e.g., movement speed or gain).

3.3.2 Experiment 2

Experiment 2 investigated the effect of modifying the simplified task to reintroduce the temporal variation that occurs ecologically in shuffleboard when played with a real object. Absolute error was compared between a group that received unpredictably timed feedback (Random group) and a group that received feedback that was predictable and congruent with ecological shuffleboard experiences (Physics group). The primary goal of this comparison was to

Figure 3.3 Experiment 1 Results
A. Absolute error as a function of task block.
B. Absolute error as a function of task block, normalized to block 1 performance.
C. Absolute error as a function of target distance over five task blocks.
D. Absolute error as a function of target distance during blocks 1 and 5.
E. Percent improvement in absolute error from block 1 to block 5.

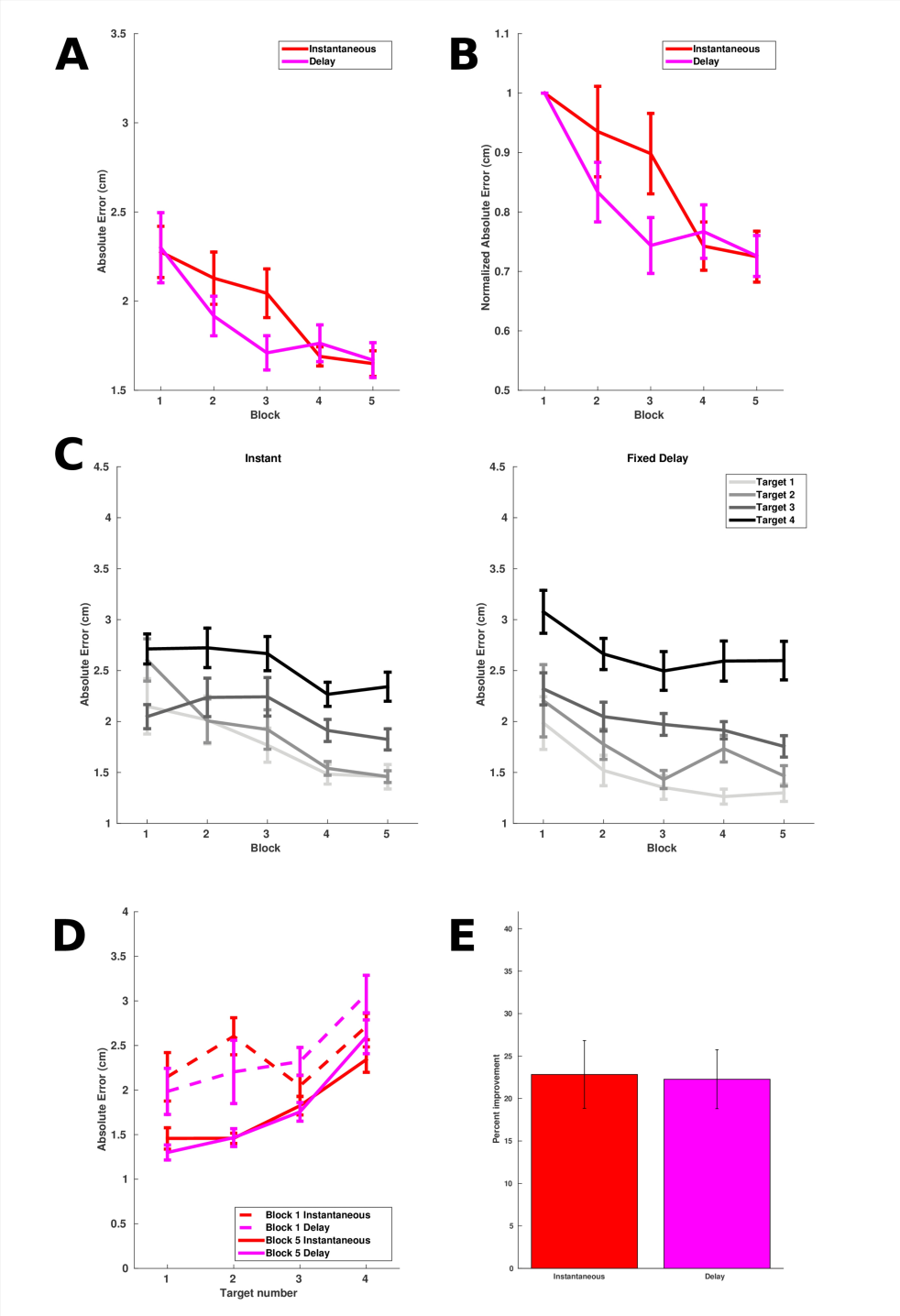

determine the roles of temporal prediction in feedback processing. In this comparison, superior performance with predictable timing would indicate reinforcement of spatial feedback by temporal signals.

A secondary goal was to determine whether the negative results obtained in Experiment 1 could be attributed to the non-ecological nature of the Instantaneous and Delay timing schemes. To determine whether ecological validity shapes task performance, a third group was introduced (Reverse Physics group). This group was given feedback with timing that was predictable, but non-ecological. The Physics (ecologically timed) and Reverse Physics (non-ecologically timed) groups were compared to each other. In this comparison, superior performance with ecologically timed feedback (Physics group) would suggest an important role for previous real-world experience in the use of temporal predictions. Equivalent performance between the two timing schemes would suggest that predictability alone, and not previous experience, is the key factor driving enhancement of performance with learning. To examine whether there is a general advantage of predictable feedback timing, ecological or otherwise, the Physics and Reverse Physics groups were also merged and compared to the Random group.

A tertiary goal was to dissociate movement speed from feedback latency through the introduction of the Reverse Physics group, as these factors are confounded in the Physics group (and in real-world shuffleboard). By incorporating a group whose shortest-latency feedback occurs following the fastest movements and whose longest-latency feedback occurs following the slowest movements, the effects of feedback latencies can be disentangled from known those of speed-accuracy tradeoffs (Fitts 1954). More specifically, if failure in Experiment 1 to replicate the interference due to long-latency feedback (Kitazawa et al., 1995) is due to the non-ecological nature of the Instantaneous and Delay timing schemes, a cost of longer latencies could be detected in Experiment 2, particularly where feedback timing is ecological (Physics group). However, such a cost could be clearly attributed to feedback latency and not to simple known speed-accuracy tradeoffs only if it is evident when long latencies are applied to the fastest, most difficult movements (Physics group) as well as to the slowest, least difficult movements (Reverse Physics group).

As in Experiment 1, all three groups reduced their error over five task blocks; this was evident both in the raw (Figure 3.4A) and normalized (Figure 3.4B) data, and was consistent across all targets (Figure 3.4C). A two-way mixed effects ANOVA was conducted on the raw absolute error scores, with factors of group and block. There was a significant effect of group, $F(2,4) = 4.78$, $p = .013$. *Post hoc* two-sample t-tests indicated that the Physics group differed significantly from the Random group during block 4, $t(29) = -2.69$, $p < .01$, and during block 5, $t(29) = -2.42$, $p < .05$, and a trend during block 2, $t(29) = -1.87$, $p = .07$. The Random group did not differ significantly from the Reverse Physics group during any block, although there was a trend in block 4, $t(31) = -1.8$, $p = .08$. The Physics group did not differ significantly from the Reverse Physics group during any block. Confirming that participants improved with practice, there was a significant effect of block, $F(2,4) = 23.38$, $p < .0001$. We next assessed the effect of predictability by combining the Physics and Reverse Physics groups' absolute error scores and comparing them to the Random group. Again, there was a significant effect of group, $F(1,4) = 156.76$, $p < .0001$, and a significant effect of block, $F(1,4) = 23.82$, $p < .0001$. There was also a significant group x block interaction, $F(1,4) = 7.14$, $p < .0001$. *Post hoc* t-tests indicated that the two groups differed significantly during block 4, $t(46) = 2.54$, $p < .01$, with a trend in block 5, $t(46) = 1.87$, $p = .07$.

Figure 3.4 Experiment 2 Results
A. Absolute error as a function of task block.
B. Absolute error as a function of task block, normalized to block 1 performance.
C. Absolute error as a function of target distance over five task blocks.
D. Absolute error as a function of target distance during blocks 1 and 5.
E. Percent improvement in absolute error from block 1 to block 5.

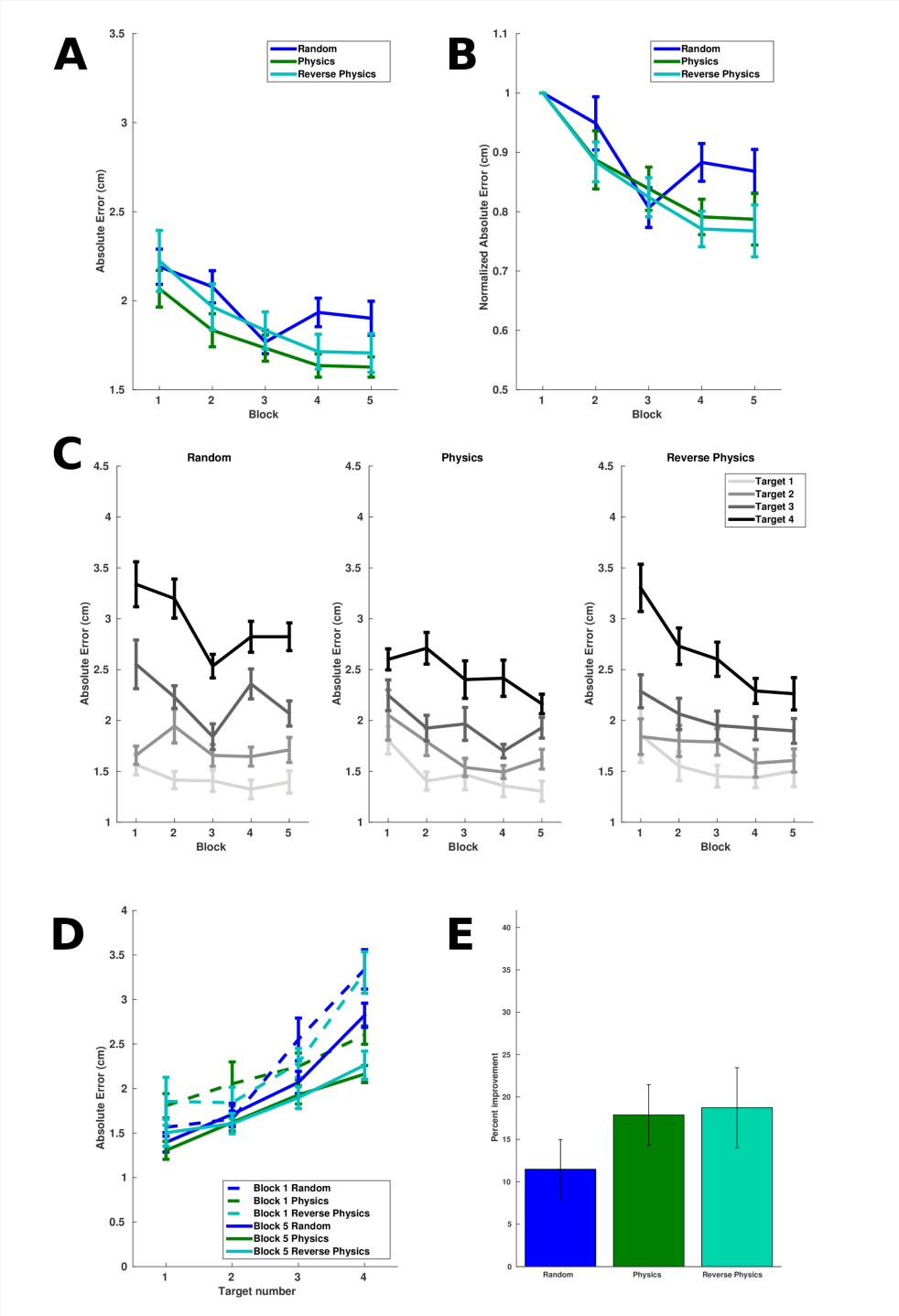

The groups were also compared in terms of percent improvement (Figure 3.4E). A one-way ANOVA revealed no difference between the groups' percent improvement, $F(2,47) = 0.97$, $p = .39$. There was also no difference when the Physics and Reverse Physics groups' data were combined and then compared to the non-predictable Random group, $t(46) = 1.40$, $p = .17$. Despite the abovementioned difference in asymptotic error between the Physics and Random groups, normalizing for baseline performance in this way results in a difference that is far from significant. It is important to note that, while asymptotic error may illustrate the level of performance that is possible with predictably timed feedback, between-group differences are at least partly attributable to differences in baseline performance. Given this, we emphasize that our timing manipulations did not affect learning, despite facilitating improved performance near the end of the session.

To test for target-specific differences in performance, the asymptotic performance (block 5) of the two predictably timed feedback groups (Physics and Reverse Physics) at each of the four targets was compared using a two-way mixed effects ANOVA. Because feedback latency is only regular for Physics and Reverse Physics, we confined our analysis to these two groups. There was a significant effect of group, $F(1,30) = 4.75$, $p < .05$. There was also a significant effect of target, $F(1,3) = 28.67$, $p < .0001$, confirming that as in Experiment 1, faster movements to farther targets resulted in larger errors (Figure 3.4 C,D). However, there was no group x target interaction, $F(1,3) = 0.61$, $p = .61$. A similar analysis compared the groups' percent improvement: there was no main effect of group, $F(1,3) = .006$, $p = .94$. There was also no main effect of target, $F(1,3) = 1.99$, $p = .12$, or group x target interaction, $F(1,3) = 2.10$, $p = .106$, on percent improvement scores. A series of *post hoc* t-tests was performed on both the asymptotic performance and percent improvement to directly compare the groups at each block. None of these comparisons revealed any reliable differences between the Physics and Reverse Physics groups.

In summary, our results indicate firstly that unpredictable feedback timing (Random group) imposes a cost on performance relative to predictable feedback timing (Physics and Reverse Physics groups). This cost did not become evident until late in training, when performance approached asymptotic levels. Indeed, participants in the Random group performed similar to the predictable groups in the first three blocks (Figure 3.4A), suggesting that early learning may be less susceptible to the cost of unpredictable feedback timing. Secondly, the cost of unpredictable feedback timing is evident regardless of whether that predictability aligns with previously experienced physical mappings, suggesting that the regularity of feedback timing, rather than the veridicality of this timing, drives relative enhancements in performance. When comparing predictable (Physics and Reverse Physics merged) to non-predictable (Random) timing schemes as a whole, there was no difference. Thirdly, there were no target-specific gains in performance to indicate that feedback latency impacted speed-accuracy tradeoffs in the predictably timed groups. In the most extreme case, the effect of feedback timing might overcome the effect of speed-accuracy tradeoffs (Fitts 1954) in the Reverse Physics groups, reversing the slope of the absolute error plotted as a function of target distance relative to the Physics group (Figure 4D). However, the lack of a group x target interaction indicated that speed-accuracy tradeoffs outweighed the effects of our timing manipulations.

3.3.3 Experiment 3

Experiment 3 addressed one limitation of Experiment 2: the temporal ranges used exceeded a putative limit of around 600 ms for error-based learning due to long-term depression in the cerebellum (Schneiderman & Gormezano 1964; Kitazawa et al., 1995; Howard et al., 2012). In addition to exceeding these temporal limits on learning, the long-latency timing schemes may also have failed to engage cerebellar mechanisms involved in subsecond timing (Ivry & Keele 1989). In Experiment 1, the Delay group consistently received feedback at 1 s, 400 ms later than the 600 ms limit. In Experiment 2, a suprasecond range was employed to make the differences in feedback timing more salient. This ensured that participants were able to form associations between their movements and the resulting feedback latencies, but it also resulted in all three groups in Experiment 2 receiving feedback later than the 600 ms limit on roughly half the trials. For the Random group, this latency could surpass 600 ms on any trial. For the Physics group, exceeding this limit occurred primarily for the two farther targets, and for the Reverse Physics group this occurred primarily at the two closer targets. Therefore, Experiment 3 sought to reduce the possible impact of cerebellar non-engagement at long latencies by compressing the range of feedback times to be within this 600 ms limit. As a secondary goal, Experiment 3 also sought to render the delays less salient in order to limit the influence of high-level cognitive recall in making and using temporal predictions. It may be the case that rather than learning a continuous distribution of feedback latencies in Experiment 2, participants formed temporal predictions that were specific to each target. By compressing the temporal range of latencies in Experiment 3, we sought to prevent participants from forming such representations.

As in Experiments 1 and 2, all three groups reduced their error over five task blocks, and again, this reduction in error was evident both in the raw (Figure 3.5A) and normalized (Figure 3.5B) data. This effect was consistent across all targets (Figure 3.5C)A two-way mixed effects ANOVA was conducted on the raw absolute error scores, with factors of group and block. There was a significant effect of group, $F(2,4) = 55.39$, $p < .0001$, a significant effect of block, $F(2,4) = 40.40$, $p < .0001$, and a significant interaction between block and group, $F(2,4) = 6.90$, $p = < .0001$. As confirmed by *post hoc* t-tests, this interaction was primarily driven by the poor baseline performance of the Short Physics group, an anomaly that leads us to interpret all comparisons to this group with caution. The Short Random group differed significantly from the Short Physics group during block 4, $t(38) = 2.39$, $p < .05$, with a trend during block 1, $t(38) = 1.90$, $p = .06$. However, the Short Random group's performance was superior to the Short Physics group's in this block, an effect that runs counter to our prediction that compressed predictability would be advantageous over nonpredictive feedback. The Short Physics group also differed significantly from the Short Reverse Physics group only during block 1, $t(37) = 2.65$, $p < .005$. Here again, the Short Physics group's absolute error was dramatically higher than the Short Reverse Physics group's during either block. The Short Random and Short Reverse Physics groups did not differ significantly during any of the 5 blocks. Assessing the effect of predictability by combining absolute error scores of the Short Physics and Short Reverse Physics groups' and then comparing them to the Short Random group produced similar results: There was a significant effect of group, $F(1,4) = 228.86$, $p < .0001$, a significant effect of block, $F(1,4) = 38.09$, $p < .0001$, and a significant group x block interaction, $F(1,4) = 11.51$, $p < .0001$. *Post hoc* t-tests compared the groups' performance at each block and indicated that the two groups differed during block 1 only, $t(53) = 2.29$. This effect reflects elevated baseline performance in the Short Physics group and cannot be interpreted as a learning difference.

The groups were also compared in terms of percent improvement (Figure 3.5E). In a one-

Figure 3.5 Experiment 3 Results
A. Absolute error as a function of task block.
B. Absolute error as a function of task block, normalized to block 1 performance.
C. Absolute error as a function of target distance over five task blocks.
D. Absolute error as a function of target distance during blocks 1 and 5.
E. Percent improvement in absolute error from block 1 to block 5.

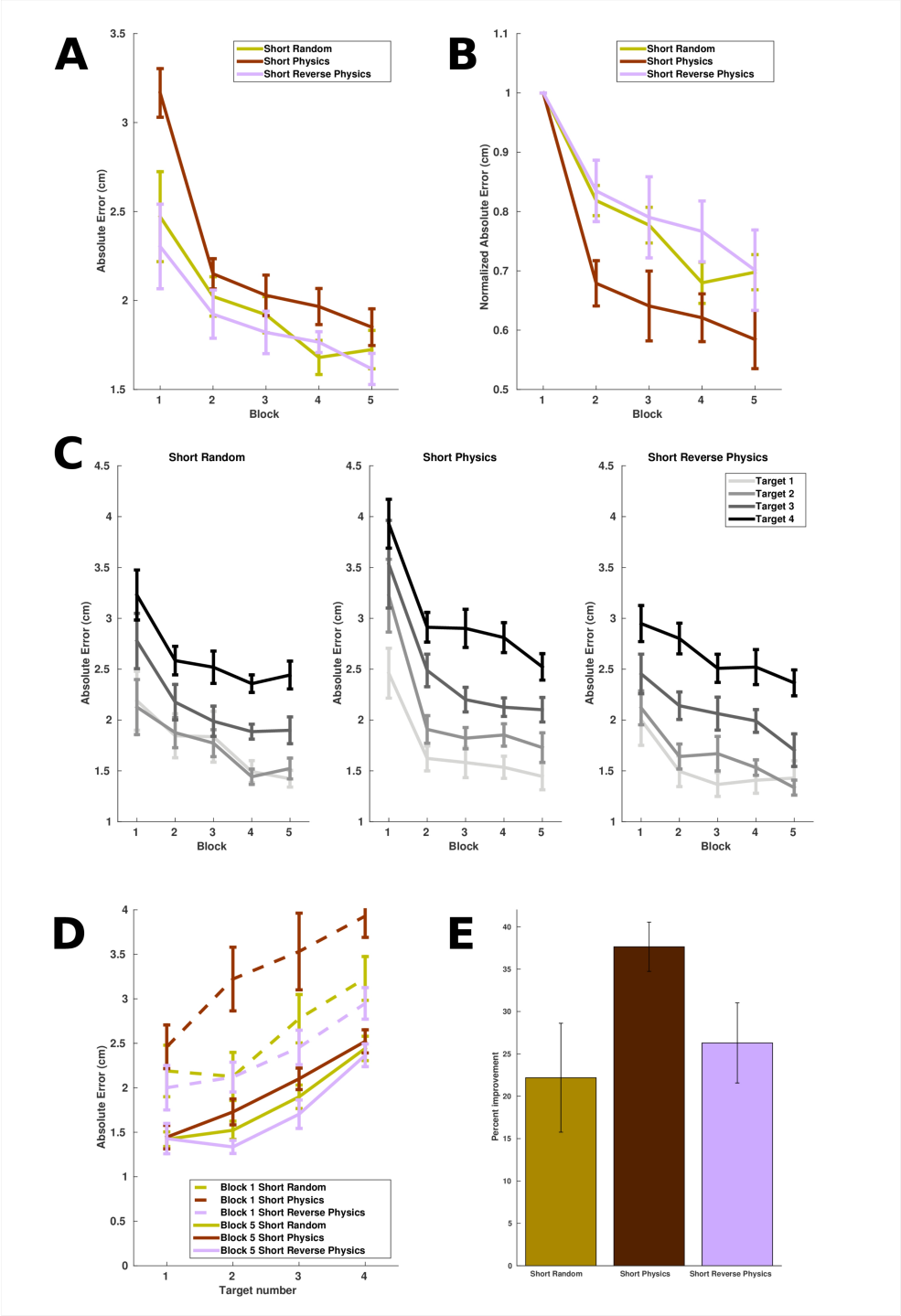

way ANOVA, the groups differed, $F(2,52) = 3.49$, $p < .05$. However, this effect was again driven by the Short Physics group's high error during block 1. There was no difference between the combined Short Physics and Short Reverse Physics group and the non-predictable Short Random group, $t(53) = 1.46$, $p = .15$.

To identify target-specific differences in performance, asymptotic performance (block 5) of the two predictably timed feedback groups (Short Physics and Short Reverse Physics) at each of the four targets was compared using a two-way mixed effects ANOVA. As in Experiment 2, the analyses of target-specific effects was restricted to only these two groups, testing whether reversing the latencies for the four targets between the two groups altered the main effect of target distance. There was a significant effect of group, $F(1,30) = 48.18$, $p < .0001$, and of target, $F(1,3) = 46.71$, $p < .0001$. The latter effect confirms that, as in Experiments 1 and 2, faster movements to farther targets resulted in larger errors (Figure 3.5 C,D). There was also a significant interaction of group and target, $F(1,3) = 4.48$, $p < .005$. A similar analysis compared the groups' percent improvement: there was a significant effect of group, $F(1,3) = 14.92$, $p < .0005$, but no main effect of target, $F(1,3) = .69$, $p = .56$, and no interaction, $F(1,3) = .47$, $p = .70$. A series of *post hoc* t-tests was performed on both the asymptotic performance and percent improvement to directly compare the groups at each target location. There was a difference in asymptotic performance at the second target from the release line, $t(37) = 2.0$, $p < .05$, reflecting the lower asymptotic error at this target in the Short Reverse Physics group. This result differs from the expected superior performance of the Short Reverse Physics group at the farther targets. There was also a difference in percent improvement at the farthest target from the release line, $t(37) = 2.16$, $p < .05$. However, this difference was driven once again by the elevated baseline at this target in the Short Physics group.

In summary, at the short latencies employed in Experiment 3, the manipulations of feedback timing had no effect. We predicted that if short latencies and predictable, ecological timing schemes provided the most redundantly informative error signals, the Short Physics group would benefit the most from the increased cerebellar engagement in predicting feedback delays. However, this group's baseline performance (block 1) was elevated for reasons beyond our explanation, thereby precluding the possibility of a definitive conclusion. At present, we can only speculate that this difference may have arisen through the random assignment of participants to groups, i.e., unskilled or unmotivated participants were assigned to the Short Physics group. Nevertheless, in Experiment 3, the Short Reverse Physics and Short Random groups performed roughly equivalently. In Experiment 2, the Physics and Reverse Physics groups performed roughly equivalently. Given this equivalence, we then assume that the reduced salience of the narrowed temporal window in Experiment 3 makes it unlikely that any differences between the Short Physics and Short Reverse Physics groups' performance are the result of our temporal manipulations. We therefore take the Short Reverse Physics group as the sole uncontaminated indicator of performance due to predictable feedback timing as compared to unpredictable (Short Random) timing, and conclude that compressed predictability confers no advantage compared to a compressed unpredictable timing scheme. At a minimum, it appears that within cerebellar timescales, there is not an important role for temporal prediction in movement speed learning.

3.4 Discussion

Temporal constraints affect learning in numerous types of error-based learning, typically

by diminishing learning when the interval between events that are relevant for learning extends beyond a few hundred milliseconds (Schneiderman & Gormezano, 1964; Kitazawa et al., 1995; Howard et al., 2012). However, unlike studies with fixed, arbitrary delays, players of real-world shuffleboard may exploit a temporal feature of the movement itself to create useful temporal predictions. Specifically, faster movements create sensory consequences that are more extended in both time and space.

Such delays are neither available nor informative in tasks that require adjustments to movement direction. However, when delays are available and informative, we hypothesized that maintaining performance in the face of these delays might rely upon cerebellar temporal processing mechanisms. Spatial and temporal prediction errors may reinforce each other to facilitate the formation of internal models of the effects of movement speed in the brain. Alternatively, shuffleboard players might rely upon extracerebellar mechanisms to improve task performance. This seems plausible given the nature of the task, because movement direction and speed are thought to be specified independently in the brain (Vindras & Viviani, 2002; Vindras et al., 2005). Many properties of movement direction learning do not generalize to movement speed learning (Bock 1992; Krakauer et al., 2000, 2004), and such discrepancies may be attributable to the recruitment of extracerebellar structures governing movement speed (Turner & Desmurget, 2010).

Surprisingly, the results of three experiments indicate that learning to adjust movement speeds on a trial-by-trial basis is not sensitive to feedback timing. In Experiment 1, we demonstrated that learning was not impaired by delayed feedback. In Experiment 2, we demonstrated that predictable timing schemes resulted in lower asymptotic error. However, normalizing to baseline levels of revealed that predictable timing did not result in greater improvements in performance. Furthermore, there was no effect of ecological validity of the timing schemes on asymptotic performance, ruling out effects of previous experience and/or increased realism in enhancing performance relative to unpredictable timing schemes. In Experiment 3, the effects of predictability seen in Experiment 2 were eliminated by using a narrower range of feedback times thought to recruit cerebellar processing mechanisms. The absence of an effect of predictability at these timescales suggests that any beneficial effect of predictably timed feedback derives from cognitive, likely attentional, mechanisms (cf. Large & Jones, 1999).

3.4.1 Putative cerebellar constraints on learning: behavioral dissociations

The costs associated with delays in visuomotor rotation learning is thought to derive from the circuitry of the cerebellum. More specifically, efference copies of motor commands must be followed within roughly 600 ms by an error-triggered complex spike in order for the synapses involved in motor representations to be eligible for learning via long-term depression (Ito 2002; Ohyama et al., 2003). If error-based feedback arrives too late, no learning can occur. By this logic, susceptibility of motor learning to a delay cost may be a signature of cerebellar involvement in any given task. Delaying feedback has been shown to diminish trial-by-trial learning in a visuomotor rotation paradigm (Kitazawa et al., 1995), similar to limitations seen in other forms of sensorimotor learning (Schneiderman & Gormezano, 1964; Howard et al., 2012; Howard et al., 2013). However, we failed to find a similar cost of delayed feedback in our shuffleboard task. In particular, delaying feedback presentation by 1 s did not adversely affect

movement speed learning (Experiment 1). Moreover, the lack of a cost of longer delays seen in Experiment 1 was replicated in the target-specific analyses of Experiments 2 and 3. Specifically, shorter feedback latencies at the farther targets (Reverse Physics and Short Reverse Physics groups) did not overpower the dominant effect of speed-accuracy tradeoffs: larger errors were always produced at faster speeds/farther targets, regardless of whether feedback latencies were long or short.

Delayed feedback produces diminished learning in visuomotor rotation paradigms, and delays are known to interfere with learning whenever they come between events relevant for learning (Schneiderman & Gormezano, 1964; Smith 1968; Howard et al., 2012). The discrepancy between our findings and those of previous studies may be attributed to differences in task demands between learning to produce movements in certain directions and at certain speeds. It may be the case that cerebellar involvement is minimal for processing errors of movement speed and that an alternative, extracerebellar mechanism is used for evaluating and responding to feedback. Alternatively, the cerebellum may indeed be involved in the task, based on its hypothesized role in timekeeping (Ivry & Spencer, 2004) to learn from errors in the prediction of feedback delays (Miall et al., 1993). We tested this by employing temporally informative feedback delays in Experiments 2 and 3, and found that the advantage of predictable feedback timing, regardless of ecological validity, was limited to situations where predictability was achieved through delays extending beyond the temporal limits of cerebellar processing (Experiment 2 but not Experiment 3). Thus, our results do not support a role for a separate temporal prediction in cerebellar error processing, suggesting instead that movement speed learning relies primarily on extracerebellar mechanisms.

The effects of temporal predictability at long latencies in Experiment 2 may be due to conflicts between the Random timing scheme and participants' past experience, in which larger force impulses cause pucks to travel for greater amounts of time. Alternatively, these effects could arise from the inability of participants to anticipate feedback in the Random timing condition. The similar benefits arising from the Physics and Reverse Physics conditions relative to Random timing support the latter hypothesis. The results indicate that, to facilitate learning, predictable feedback timing need not align with veridical or previously experienced temporal mappings (Experiment 2).

Despite this lack of effect of previous experience, we note that analysis of block-specific (asymptotic) effects on error shows that the cost of unpredictable feedback timing emerges late in learning. This cost could be a fatigue effect, resulting from the additional cognitive effort required to process unpredictably timed feedback. Alternatively, the fact that error reduction for the Physics and Reverse Physics conditions did not occur until blocks 4 and 5 may reflect participants' developing familiarity with the predictable temporal mappings. It may be the case that there is one system for early learning that is less temporally sensitive and another system for later fine-tuning of learning that shows temporal sensitivity.

In Experiment 3, we tailored the range of feedback intervals to fit within putative cerebellar limits (cf. Howard et al., 2012), thereby rendering the differences in timing less perceptible. Thus, any effects of predictability are more likely to be attributable to the non-cognitive, unconscious mechanisms within the cerebellum than they would have been with longer intervals. We hypothesized that short-latency predictable feedback timing could produce an error signal that was optimized for both cerebellar processes and temporal feedback predictions. Instead, we found that the benefit of predictable feedback timing seen in Experiment

2 was not evident in Experiment 3, indicating that this benefit relied on salience of the predictable delays. However, the elevated baseline error in the Short Physics group leaves a residual ambiguity, as asymptotic performance in this group is similar to the other groups, while the reduction in error over the five blocks is much greater. Had the Short Physics and Short Reverse Physics groups differed in a reliable way, this would have provided evidence for a role for ecological validity (or of previous experience with temporal mappings) at a cerebellar timescale, despite the lack of such an effect at more cognitive timescales. However, no such effect was found. Our findings are consistent with temporal predictability appears to facilitating learning from feedback through improved attentional capture.

3.4.2 Alternative neural circuitry involved in movement speed learning: the striatum

There are many reasons why shuffleboard, and similar tasks which involve learning optimal movement speeds from trial-by-trial delayed feedback, are not subject to putatively cerebellar temporal constraints. First, it may simply be more difficult to modulate temporal and dynamic movement variables relative to spatial ones. That is, it may be harder to move at a certain speed rather than to or towards a certain location. Second, our results may have differed had our task required different movement dynamics. For instance, the use of a force field to simulate the resistance of a puck's mass may have created a more ecologically-sound environment and engaged different processes. Indeed, it remains unclear whether kinematic manipulations like visuomotor rotations are compensated by different mechanisms than dynamic manipulations like force fields (Criscimagna-Hemminger et al., 2010; but see Donchin et al., 2012; Schlerf et al., 2013). Further work is needed to address possible effects of task difficulty and movement dynamics.

A third possibility, however, is that learning in our shuffleboard task relies on extracerebellar mechanisms: participants may have learned to repeat successful actions rather than learning to correct for errors. That is, our task may engage reward-based learning and explicit memory retrieval rather than error-based learning and sensorimotor retuning (Krakauer & Mazzoni 2011). Because participants attempted to hit four discrete targets, they may have relied upon learning discrete hand speeds and corresponding delay ranges, rather than adjusting their movements adaptively in response to continuous spatial and temporal prediction errors. This selection-based account of learning (Shadmehr et al., 2010; Costa 2011; Krakauer & Mazzoni 2011) leads to the prediction that striatal mechanisms involved in reward learning and movement speed regulation shape performance when movements have temporally extended consequences.

Notably, Kitazawa and colleagues showed that even visuomotor rotation learning was not completely abolished when feedback was delayed beyond 500-600 ms. In fact, some learning still occurred when feedback was delayed by as much as 1000 to 5000 ms (Kitazawa et al., 1995), suggesting the existence of a secondary, less temporally sensitive, learning mechanism. It has been demonstrated that visuomotor rotation learning can be driven by either sensory or reward prediction error (Izawa & Shadmehr, 2011), with reward prediction error signals associated with the basal ganglia. This prediction error, driven by dopamine signaling in the striatum, has long-lasting impacts on learning, with activity in these striatal neurons actually increasing over post-reward intervals as long as 16 s (Fiorillo et al., 2008).

The striatum's role in controlling movements provides further reason to assign it a role in

trial-by-trial learning in the shuffleboard task. This structure has been implicated in controlling the speed and timing of movements, possibly through dopaminergic modulation of the gain of a perceptual reference signal (Yin 2014). In humans, Parkinson's disease has long modeled the syndrome associated with striatal dysfunction: Parkinson's patients show hypometria, hypophonia, micrographia, and bradykinesia (Hallett & Khoshbin, 1980; Berardelli et al., 2001; Pfann et al. 2001; Desmurget et al., 2003; Viviani et al. 2009). This is in accord with a role for the basal ganglia in scaling the force, or vigor, of movements (Desmurget et al., 2003; Turner et al., 2003; for review, see Turner & Desmurget, 2010). In primates, spiking activity in the primary output nucleus of the sensorimotor striatum, the globus pallidus internus (GPi), scales with movement amplitude and velocity (Turner & Anderson, 2005). Furthermore, inactivation of the GPi causes slowing and hypometria of movements in monkeys (Desmurget & Turner, 2008).

A PET study in humans found cerebellar activations during rotation learning and striatal activations during gain learning (Krakauer et al., 2004), supporting the notion that direction and speed may be specified independently and by distinct neural systems. However, there is neuroanatomical evidence that the cerebellum and basal ganglia are directly connected through the thalamus (for review, see Bostan et al., 2013). The interaction of distinct neural systems during error- and reward-based learning paradigms is a topic of much debate (for example, see Smith et al., 2006; Inoue et al., 2015). For instance, a fast, cerebellar program may drive improvements in performance early in learning and a slow, striatalprogram may drive improvements late in learning (Shadmehr et al., 2010). Conversely, the striatum may drive early selection of actions while the cerebellum refines late specification of actions: consistent with this view, one study found a role for the basal ganglia in visuomotor rotation learning only after restricting the analysis to the early stages of learning (Seidler et al., 2006).

We infer that the absence of effects of simple delayed feedback indicates an extracerebellar locus of trial-by-trial movement speed learning. The temporal imprecision of striatal circuits, combined with the association of these circuits with movement speed regulation, make this structure an attractive candidate for improving trial-by-trial performance. Further imaging studies are needed to directly assess the underlying mechanisms.

3.5 Conclusions

We developed a novel shuffleboard task to examine temporal constraints in the learning and regulation of movement speed. The main finding from this study is that we failed to identify strong temporal constraints; in particular, task performance did not suffer when feedback presentation was delayed by 1 s. However, predictable feedback timing conferred an advantage both when the mapping was predictably congruent with real-world task analogues and when this mapping was reversed. The advantage was revealed by comparison to feedback timing that was randomized, and thus rendered unpredictable, within an identical temporal range. More speculatively, the advantage conferred by this predictability may be extracerebellar, possibly a striatal, origin. When predictability was restricted to a cerebellar timescale, performance was not dramatically enhanced relative to a non-predictable timing scheme within this same temporal range. Thus, while a role for temporal prediction may exist in tasks like shuffleboard, bocce, golf, archery, and other games with long delays between action and outcome, further study is needed to determine whether this role generalizes to other tasks based on movement amplitude and speed as well as to tasks based on movement direction.

Chapter 4: Involvement of dorsal striatum but not cerebellum in trial-by-trial learning of movement speed

4.1 Introduction

In learning to produce novel movements, people process multiple types of feedback. Although current neural models of motor learning encompass a distributed network of brain structures, the functional and computational contributions of the components of this network to feedback processing remain unclear (for review, see Shadmehr et al., 2010 and Krakauer & Mazzoni, 2011). Feedback may come in the form of rewards, increasing the probability of selecting actions that were previously successful, or lack of reward, decreasing the probability of selecting actions that were not successful (Sutton & Barto, 1998; Schultz, 1998; O'Doherty et al., 2004; Daw et al., 2006; Glascher et al., 2010). Feedback may also indicate the size and/or direction of errors, influencing the coordination of future actions by triggering adjustments in movement parameters according to the nature of the error experienced (Shadmehr & Mussa-Ivaldi, 1994; Thoroughman & Shadmehr, 2000; Fine & Thoroughman 2006, 2007; Tanaka et al., 2009). Behaviorally, people can learn motor tasks using feedback about either errors or rewards, although only error-based feedback causes the sensory recalibration that is thought to drive performance changes in motor adaptation tasks (Izawa & Shadmehr, 2011).

Evidence from neuroimaging and patient studies has implicated a number of cortical and subcortical sites in human motor learning (Martin et al., 1996; Desmurget et al., 2003; Desmurget et al., 2004; Krakauer et al., 2004; Grafton et al., 2008; Tunik et al., 2009; Viviani et al., 2009; for review, see Doyon et al., 2003, O'Doherty, 2004; Seidler, 2010), including the striatum and the cerebellum (for review, see Doya, 2000; Shadmehr & Krakauer, 2008). Neuroimaging studies have demonstrated that both structures are active during motor learning tasks and undergo changes in activation as skill develops (Imamizu et al., 2000; Seidler et al., 2004; Diedrichsen et al., 2005; Seidler et al., 2006; Schlerf et al., 2012). Furthermore, patients with damage to either the striatum or the cerebellum exhibit deficits on a wide variety of motor control and motor learning tasks like sequence learning and visuomotor or force field adaptation (Pascual-Leone et al., 1993; Martin et al., 1996; Gabrieli et al., 1997; Doyon et al., 1997; Doyon et al., 1998; Desmurget et al., 2004; Maschke et al., 2004).

These two brain structures are thought to drive two distinct systems for learning. Mismatches between the actual and intended consequences of an action register as sensory prediction errors, triggering complex spikes in the cerebellum (Marr, 1969; Albus, 1971; Ito, 1984). Meanwhile, unexpected rewards create a reward prediction error, reflected in the firing of dopaminergic cells in the striatum (Schultz et al., 1997; Sutton & Barto, 1998; Schultz, 1998). Neuroanatomically, both structures are well-positioned to influence behavior through plasticity within their extensive, somatotopically organized loops with motor and non-motor cortical structures (for review, see Alexander & Crutcher, 1990; Houk & Wise, 1995; Middleton & Strick, 2000). However, these structures may also interact directly rather than operating purely in independently: recent neuroanatomical tract tracing studies have revealed that the two are bidirectionally connected through the thalamus (for review, see Bostan et al., 2013).

Error-based and reward-based learning differ in terms of their feedback signals and neural circuitry, but also in terms of the tasks typically used to model them. Behavioral studies and computational models of error-based learning typically rely on tasks which provide vectorial

feedback, either during a movement or upon completion of a movement, about the direction and magnitude of errors within a given workspace (Shadmehr & Mussa-Ivaldi, 1994; Thoroughman & Shadmehr, 2000; Mazzoni & Krakauer, 2006; Fine & Thoroughman 2006, 2007; Cheng & Sabes 2007; Grafton et al., 2008). According to these models, trial-by-trial learning involves correcting for some proportion of a movement error's magnitude on subsequent trials (Thoroughman & Shadmehr, 2000; and for review, see Thoroughman et al., 2007). In contrast, reward-based learning is often examined by having participants learn from the success or failure of choices between two or more differently rewarding stimuli (O'Doherty et al., 2004; Daw et al., 2006; Glascher et al., 2010). In this case, contributions of the motor system are often minimal, as proportions of decisions in favor of each alternative are analyzed as a function of changes in the probability, rate, or size of rewards.

Studies which point to a role for the cerebellum in error-based learning have traditionally relied on spatial error signals that cause people to alter their movement direction (Martin et al., 1996; Donchin et al., 2003; Grafton et al., 2008; Taylor et al., 2010; Criscimagna-Hemminger et al., 2010; Schlerf et al., 2013). The tasks used in these studies, including visuomotor and force field adaptation paradigms, impose directional perturbations on participants' feedback, measuring the resulting incremental adjustments to motor programs that occur over tens of trials. As learning proceeds, the heading angle or force of participants' movements changes direction in a trial-by-trial fashion as movements become aligned with the goal.

As people learn new motor skills, however, movement direction is not the sole parameter that is altered in response to feedback. For instance, when using a new computer mouse for the first time, a person may have to adjust the gain, or speed-to-distance mapping, of their movements. Behavioral and neuroimaging studies have revealed important distinctions between movement direction and speed (or between movement direction and amplitude or gain, as these covary) in terms of learning rate, generalization, and neural activations (Bock 1992; Pine et al., 1996; Krakauer et al., 1999; Krakauer et al., 2000; Vindras & Viviani, 2002; Turner et al., 2003; Krakauer et al., 2004; Diedrichsen et al., 2005; Vindras et al., 2005). Taken together, these results suggest that movement direction and speed are specified independently in the brain. Given that error-based and reward-based learning are viewed as less independent than previously imagined, both behaviorally (Izawa & Shadmehr, 2011) and neuroanatomically (for review, see Bostan et al., 2013), we asked whether direction and speed are adjusted by distinct or overlapping systems for trial-by-trial motor learning.

While the cerebellum is thought to be critical for updating movements in tasks with directional errors (Martin et al., 1996; Donchin et al., 2012; Grafton et al., 2008; Taylor et al., 2010), the striatum has been implicated in the regulation of movement vigor (Turner et al., 2003; Krakauer et al., 2004; Spraker et al., 2010; Beierholm et al., 2013; and for review, see Shadmehr & Krakauer, 2008 and Turner & Desmurget, 2010). Vigor, for a given amount of friction or resistance, is a measure of movement speed or of the magnitude of force impulses applied, and therefore a covariate of amplitude or gain. Vigor may be implicitly altered through sensitivity to reward, as in cases where people are faster to reach or saccade to more rewarding stimuli (Mazzoni et al., 2007; Xu-Wilson et al., 2009; Beierholm et al., 2013), but it may also be learned, as a scaling factor for movements in gain adaptation paradigms (Bock 1992; Pine et al., 1996; Krakauer et al., 2000; Turner et al., 2003; Desmurget & Turner, 2010). Importantly, however, movement speed itself is typically not the substrate of trial-by-trial adjustments in motor learning studies.

Nevertheless, there exist many real-world tasks in which people scale the speed or amplitude of their motor output to displace an object by a certain distance from one trial to the next (for example, shuffleboard, bocce, frisbee, or pushing a child on a swing). Studies of learning to produce movements with a certain speed or amplitude have relied on gain adaptation paradigms. Studies of gain adaptation of either saccades or reaches impose perturbations on participants' movement amplitude or speed. In contrast with directional tasks like visuomotor or force field adaptation, people can learn a new scaling factor relatively quickly and can generalize it globally across workspaces, sometimes in a single trial (Bock 1992; Pine et al., 1996; Krakauer et al., 1999; Krakauer et al., 2000). Studies of motor learning have emphasized responses to directional errors, possibly because the process driving gain adaptation is fast and therefore not as amenable to study through the use of trial-by-trial experimental interventions.

We sought to explore a less-studied aspect of movement learning, asking whether the neural sites active during trial-by-trial learning of movement speed are similar to or distinct from the cerebellar sites previously identified for learning movement direction (Diedrichsen et al., 2005; Schlerf et al., 2012). To address this question, we used functional magnetic resonance imaging (fMRI) to scan the brains of healthy participants as they played a virtual shuffleboard game. In this task, participants produced hand movements in which their hand speed determined the distance traveled by a virtual “puck.” The participants attempted to choose the appropriate speed to hit one of three targets that varied in distance. Thus, the task used movement speed rather than movement direction as a substrate for trial-by-trial learning.

In imaging performance of this task, several design considerations facilitated estimation of effects of interest in the brain. We used a movement localizer that was independent of the main task to identify movement-responsive regions. We also inserted no-feedback trials in the main task runs to allow us to subtractively identify feedback-responsive regions. A fast event-related design with frequent changes in target location and a random perturbation schedule ensured that error-based corrections persisted throughout the scan session despite the typical fast time course of gain adaptation (Bock 1992; Krakauer et al., 2000; Desmurget et al., 2000). To make the game challenging and engage error-based learning mechanisms throughout the scanning session, feedback was perturbed on some of the trials. These perturbations also allowed us to precisely measure participants' responsivity to these errors. Finally, both binary and parametric measures of task performance were used to quantify two distinct types of behavioral responses in the brain. Specifically, performance was analyzed both in terms of trial success (hit or miss) and in terms of trial accuracy (error size). We hypothesized that responses would exhibit trial-by-trial modulation by error size, consistent with some models of error-based learning (Thoroughman & Shadmehr, 2000).

We compared our imaging results to three possible outcomes. First, we tested whether, when the presence of errors is prolonged over time through the use of perturbed feedback, cerebellar regions involved in processing errors of direction would also be activated by errors of speed. Such a result would suggest that the cerebellum processes errors about either movement speed or direction, provided these errors persist long enough to drive improvements in motor precision. Second, given the independent coding of direction and speed, the shuffleboard task could instead recruit the striatum to modulate vigor. Such a result would suggest that the role of the cerebellum in error-based learning may be limited to tasks which require corrections to movement direction. Finally, we tested if the task could recruit the striatum not because of the use of speed as a substrate for learning but because of the mechanism used for learning: task

performance may in fact proceed via reinforcement learning rather than sensorimotor adaptation of internal models of gain.

4.2 Material and methods

4.2.1 Participants

Twenty healthy right-handed adults participated in this study (one excluded due to poor task performance; of those remaining, 8 female, mean age 27.5 years). All had normal or corrected-to-normal vision and completed a color blindness test prior to the study. The participants provided written informed consent under a protocol approved by the University of California, Berkeley Institutional Review Board. All participants were compensated for their time and received additional bonus pay based on their task performance. Participants were informed of the bonus pay only after informed consent was obtained.

4.2.2 Experimental setup

Prior to scanning, participants were fitted with a custom bite bar. During the scanning session, the bite bar was mounted to the head coil to minimize head movement. Physiological signals were recorded during scanning using a BIOPAC physiological monitoring system (www.biopac.com). Heartbeat was measured with a photoplethysmograph placed on the participant’s left index finger, and respiration was measured with a pneumatic pressure sensor placed several centimeters below the sternum and held in place by an elastic strap. Visual stimuli were backprojected onto a screen mounted inside the bore of the magnet and viewed via a mirror mounted to the head coil. From a supine position, participants held a robotic manipulandum (www.fmrirobot.org) in their right hand. The manipulandum, which recorded hand position at 1000 Hz, was positioned over the participant’s abdomen and could be freely moved in a plane parallel to the scanner bed. Before scanning, participants completed a training session in which they held the manipulandum from a standing position while viewing stimuli on a 27.5 x 34 cm LCD monitor.

4.2.3 Task: Overview

Participants were told they would be playing a virtual shuffleboard game. As in real-world shuffleboard games, the speed of the hand at the moment of release determined how far the puck would travel. Participants attempted to cause virtual pucks to land on targets presented at one of three locations in the workspace (Figure 4.1). In our virtual simulation of this game, the visible workspace in the scanner subtended 20 degrees of visual angle along the vertical axis and 36.2 degrees along the horizontal axis. This workspace corresponded to 36.7 x 66.4 cm in the robotic manipulandum's native space, which had a 1:1 mapping with hand movements (when the puck was under the participant's control). The puck was displayed as a white dot with a 1 cm diameter (1.1 degrees of visual angle). The targets were displayed as blue circles with a diameter of 4 cm (3.7 degrees of visual angle). The three target locations were at 7 cm, 12 cm, and 17 cm (5.5, 10.0, and 14.3 degrees of visual angle) above a blue line, the release line. This line was positioned 10 cm (8.3 degrees of visual angle) above the puck's start location on each trial. To

Figure 4.1 Task
A. Target and puck at the onset of a Feedback trial
B. Target and puck at the onset of a No Feedback trial
C. Example feedback on a trial in which the puck missed the target
D. Example feedback on a trial in which the puck hit the target
E. Relationship between hand speed and feedback distance, in hand space and the manipulandum's native workspace. Targets are to scale; centers are marked with yellow rings for illustrative purposes only.

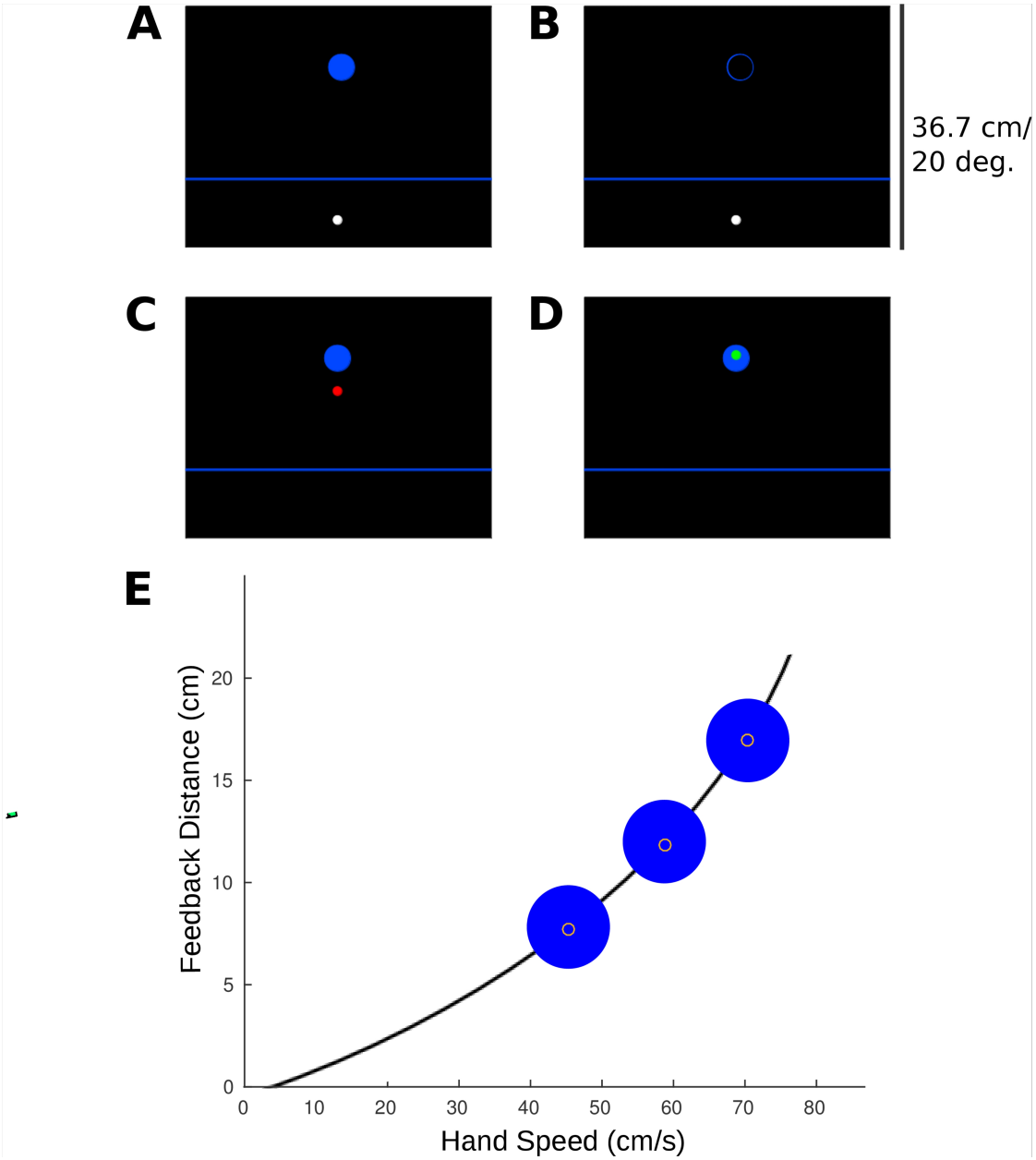

cross this line, the participant had to move the manipulandum at least 10 cm on each trial, although the actual movements were slightly larger due to follow through after crossing the release line.

At the onset of each trial, a white puck appeared at the start location, simultaneously with the appearance of one of the three targets. The participant was instructed to make an out-and-back movement in the direction of the target, primarily by flexion about the elbow. They were to adjust the movement speed to create a desired "force" that would cause the virtual puck, when "released," to land on the target. The puck remained visible until the hand reached the release line. At this point, the cursor jumped to its final position, determined as a function of hand velocity (see below). The puck was constrained to move only along the y-axis (vertically on the screen), ignoring any small lateral deviations in the hand trajectory along the x-axis (horizontally on the screen). Participants were informed of this constraint and were instructed to minimize movements along the x-axis. They were instructed to make a smooth out-and-back movement, returning the hand to the vicinity of the start location after each "throw." Because the puck distance was based on the velocity at the release line, the movement always extended beyond this point. Return movements were terminated with the hand hovering over the navel as the participant lay in a supine position. The trial ended when the hand position did not change by more than 1 cm over a 500 ms period. To avoid imposing demands on participants to find the start location, the start position for each trial was automatically adjusted to the final hand position from the previous trial, and the workspace was recalibrated about this point. The inter-trial interval (ITI, defined as the time elapsed between target onsets) was 3 s, with a random amount of jitter between 0 and 500 ms added to the onset of each trial.

We did not impose any delay between the point at which the hand reached the release line and the reappearance of the puck at its final position. This, of course, is unlike a natural shuffleboard task in which the participant would observe the puck as it traversed the workspace. One alternative would have been to animate the puck's trajectory on-screen. However, we opted to use a no-delay approach to facilitate perturbation of the feedback position of the puck on some trials (see below). Another alternative would have been to use endpoint-only feedback, but randomly vary the interval between movement and feedback, a method that would have allowed us to separately model movement and feedback in an event-related design. However, sensorimotor learning can be subject to temporal constraints, with reduced learning as feedback is delayed (Kitazawa et al., 1995; Howard et al., 2012). The results presented in Chapter 3 suggest that this may not be the case for the shuffleboard task; nevertheless, to avoid any possible effects of feedback delay introduced by this particular study design, we opted to treat the movement and feedback as a single entity rather than separating the two in time.

Spatial feedback in the form of puck location was reinforced with color feedback that indicated trial success. The puck reappeared as red if it landed outside of the target region and green if it landed within the target boundaries (Figure 4.1B,C). This feedback was presented on the screen for 350 ms. Thus, participants received feedback only about the puck's endpoint (the location where the puck would have come to rest). Participants received five cents bonus pay for each trial on which the puck hit the target but received no feedback about the bonus pay until after the conclusion of the experiment.

Participants' hand speeds were determined by calculating the time it took to traverse a 5 cm (4.1 degree) region adjacent to the release line (cf. Chapter 3). The virtual distance traveled by the puck was proportional to the square of the hand speed (Figure 4.1E). Given the diameter

of the target, the range of hand speeds required to hit the three targets was 38.9-52.1, 55.6-64.7, and 67.6-75.0 cm/s. We also set boundary conditions in terms of the displayed position of the puck. Specifically, a hand speed of 5.0 cm/s or less caused the puck to land at the release line, and a speed of 87.2 cm/s caused the puck to land at the upper edge of the monitor. If a participant produced a speed that caused the puck to "land" at a location beyond the edge of the monitor, a warning was displayed instead to tell them to slow down.

Trials were counterbalanced within each run such that each of the three target locations was presented an equal number of times, and the transitions between target locations (including a condition in which the target location did not change from one trial to the next) occurred with nearly equal frequency. Of nine possible transitions between targets (including target location repetitions), the distribution of transitions within any given run was balanced such that there were 16 instances of each possible transition per run, with the exception that one transition occurred only 15 times. This exception was required to maintain an even number of target presentations. Nine possible task runs were created, each missing a single instance of one of the nine transitions. For each participant, five of these runs were selected at random for the scan session.

Feedback in the form of the red or green puck and distance traveled was provided on 75% of trials. On the remaining 25%, no feedback was provided. Participants were cued at the onset of each trial as to whether the trial was a feedback trial (Figure 4.1A, filled target at trial onset) or no-feedback trial (Figure 4.1B, hollow target at trial onset). We opted to provide these cues rather than simply withholding feedback without warning because the latter situation could produce an unwanted prediction error signal (the absence of an expected feedback signal). Participants were informed that they would receive bonus pay for producing the correct movement speed on no-feedback trials. We note, however, that despite this instruction, participants' errors were slightly larger on no-feedback trials than on feedback trials (Figure 4.2A).

On some feedback trials, visual perturbations were applied to the location of participants' feedback. This was done for two reasons. First, to ensure that our effects are due to true error processing-related activity in the brain, perturbations reduced the correlation between movement speed and error size (Figure 4.5). Second, perturbations provided a way to maintain a relatively constant proportion of errors throughout the scan session, ensuring that errors were not experienced solely within the early portion of the scan session (Figure 4.2A). Note that this manipulation has the effect of creating trials in which the participant produced the correct hand speed but received an error, as well as trials in which they produced the incorrect hand speed but were given feedback indicating the trial was successful. We will refer to errors as either visual error (the difference between the puck's perturbed, on-screen location and the target) or motor error (the error based on their unperturbed hand speed, which was not seen by participants). However, the analyses will focus on visual errors, based on the assumption that this corresponds to the participants' belief about their performance. This assumption is confirmed by the participants' responses to a questionnaire which probed their awareness of the perturbations (described in section 4.2.6).

One of three perturbations was applied on each feedback trial: positive, negative, and zero. In the zero-perturbation condition, the feedback was veridical and based on the hand speed at the release line. In the positive-perturbation condition, the feedback distance was increased relative to the veridical mapping, while in the negative-perturbation condition, it was decreased.

The type of perturbation was randomly determined on each trial, with the constraint that each run contained an equal number of each perturbation type. The size of the perturbation was 20% of the distance between the target and the center of the screen. The selection of this perturbation size was based on pilot studies in which we sought to maximize the size of the perturbation while avoiding participants becoming aware of the perturbation as assessed by a post-experiment questionnaire.

Because perturbations were measured from the center of the screen, the proportional size of the perturbation increased with target distance (5.7%, 11.7%, and 14.1% of the target distance from the release line at the near, middle, and far targets, respectively). In our behavioral studies with the shuffleboard task (see Chapter 3), our results have always been consistent with Fitts' Law (Fitts, 1954), with larger errors associated with faster movements. Even when this relationship between performance and movement speed is taken into account, the scaling of the perturbations with target distance ensured that participants would perceive that their performance was disproportionately poor at the far target and disproportionately good at the close target. Therefore, increasing the proportionate size of the perturbation with target distance had the effect of exaggerating the effect of Fitts' Law.

This was done in part to reverse the speed-accuracy tradeoff described in Seidler et al., 2004, a study which allowed movement vigor to be increased as participants attempted to hit larger (easier) targets. In contrast, we are interested in studying the process of learning to specify particular movement speeds. A cost of this approach, however, is that the perturbations become less effective at reducing the correlation between speed and error size for the closest target compared to the farthest target (Figure 4.5). However, differences in performance across targets were accounted for in the fMRI analysis either by z-scoring the distribution of error sizes for each target or by isolating data within target distances (Section 4.2.13).

4.2.4 Task: Training

All participants completed a training session outside the scanner immediately before scanning. This session familiarized the participants with the robotic manipulandum and the task. First, the experimenter explained the natural translation from movement speed to puck distance in real-world shuffleboard, demonstrating by pushing a real puck along a table. The experimenter then explained how to use the manipulandum to control the on-screen puck. Participants were told that their hand speed would be measured at the release line, similar to a police officer using a radar gun to measure speed, and that their hand speed would translate into the puck's travel distance. The red and green feedback for misses and hits was explained, as well as the filled and hollow circles for feedback and no feedback trials. Critically, participants were not informed of the perturbations.

Following these instructions, the participant observed as the experimenter completed a practice run of the task. The participant then completed the same practice run. The practice run consisted of twenty trials, a truncated version of the actual task runs. The practice run, like the task runs, included feedback and no feedback trials at all targets. Feedback was unperturbed during this practice run. In two cases, the participant was asked to repeat the practice based on concerns with their performance.

After completing the practice run, the experimenter re-emphasized that the participants should keep their movements as smooth as possible, cross the release line on every trial, and

avoid double reaches within a trial. They were also informed that they would receive five cents for each time they succeeded in hitting the target. Participants were not given any information about their cumulative task performance at any point during the scan session.

4.2.5 Task: Scanning

The scanning session consisted of an anatomical scan and six functional scans: five task runs and one localizer run. Each participant completed an additional practice run during the anatomical scan. Each task run lasted 7 minutes and 44 seconds (232 volumes), while the localizer run lasted 5 minutes and 40 seconds (170 volumes). The localizer run was always obtained after the task runs.

The five task runs consisted of ten seconds of rest followed by 144 trials, with an inter-trial interval (ITI) of 3 s. Trial onsets alternated between being synchronized with the beginning of a volume acquisition or to the middle of the acquisition. The ITI was randomly jittered (between 0 and 500 ms was added to the onset of each 3 s trial). There were a total of 720 trials per participant over five task runs.

For the localizer run, the participants were informed that they would not receive feedback on any of the trials and that they should aim to reach with a consistent, comfortable speed on each trial. This run consisted of 9 blocks of 6 no-feedback trials (hollow blue ring targets, all at the middle target distance), each of which lasted 18 seconds, with rest periods lasting 20 seconds in between each block.

Because we were primarily interested in comparing trials with errors of differing sizes, we did not include null events in the task design. Instead, task runs contained no-feedback trials, providing a basis for subtractively isolating fMRI responses related to feedback processing. The localizer run, comprised entirely of no-feedback trials with rest periods, provided a basis for isolating pure movement-related responses.

4.2.6 Post-scanning questionnaire and interview

After the scan session, participants completed a questionnaire (Table 4.1). They were first asked to describe the task in their own words. This allowed us to assess general comprehension of the task. Participants were then asked to indicate their level of agreement with each of ten questions (0 to 100% agreement). The first of these were basic, checking for potential across-participant covariates like arm fatigue and confidence, although none of these measures were used as covariates in any behavioral or imaging analysis. The last two questions were of greatest interest, probing participants' awareness of the perturbations. The first asked whether the program “seemed glitchy” and the second asked whether they were “sometimes surprised” to see where their puck landed.

The experimenter then conducted a brief oral interview. Participants were told that there had been two groups of participants: For the manipulated group, the puck would sometimes land at a location that did not correspond to hand speed; for the non-manipulated group, the puck always landed at a location that corresponded to hand speed. Participants were asked to indicate their group assignment. If they reported the manipulated group, they were asked to indicate when they had first suspected the feedback had been altered: early in the experiment, late in the experiment, while filling out the questionnaire, or only when the experimenter indicated that

feedback had been manipulated for some participants.

4.2.7 Imaging parameters

Data were collected on a 3 T MAGNETOM Trio scanner (Siemens Healthcare, Erlangen, Germany) at the Henry H. Wheeler, Jr. Brain Imaging Center at the University of California, Berkeley. A 12-channel transverse electromagnetic send-and-receive radiofrequency head coil was used. One high-resolution T1-weighted MPRAGE anatomical volume (TR = 1900 ms; TE = 2.52 ms; 1 × 1 × 1 mm voxels; acquisition matrix 256 x 256; field of view 25 x 25 cm) was acquired for each participant. Multi-slice echo-planar imaging (EPI) was used to collect functional imaging data (gradient-echo EPI sequence; TR = 2000 ms; TE = 23 ms; 36 ascending sagittal slices; 3.1 x 3.1 x 3.0 mm voxels; flip angle = 90°; acquisition matrix 64 x 64; field of view 20 x 20 cm; 232 volumes per task run, 170 volumes per localizer run).

4.2.8 Physiological monitoring and analysis

Physiological nuisance covariates were generated using the procedure outlined in Chapter 2. Analog TTL signals generated by the scanner were recorded to temporally align physiological measurements with the EPI time series. Cardiac and respiratory data were recorded at 125 Hz. For fMRI analysis, physiological regressors were created using the Physiological Log Extraction for Modeling (PhLEM) v1.0 toolbox for SPM8 (Verstynen & Deshpande, 2011). The PhLEM package marks respiration and heartbeat events using an automatic peak detection algorithm. Based on visual inspection of the data, it was not necessary to manually perform corrections of the heart rate and respiration waveforms for any participant.

The heart rate and respiration time series were computed following the methods described in Chang et al. (2009) and in Chapter 2. Heart rate was calculated in units of beats per minute. This time series was then shifted by 0-11 TRs to produce 12 time series lags of 0-22 seconds (HR regressors). The respiration time series was computed using a measure of respiratory variation (RV) that was obtained by computing the standard deviation of the respiration waveform within a 6-s sliding window centered on each 2-s TR. This time series was then shifted by 0-11 TRs to produce 12 respiration volume (RV) regressors. Although there exist basis functions that model the relationship between changes in these physiological processes and the BOLD signal (Birn et al., 2008; Chang et al., 2009), we opted to avoid constraining the hypothesized shape of this relationship, instead adopting the more flexible and exhaustive model containing a series of lagged regressors as in Chapter 2. We did this to avoid the assumption that basis functions based on resting state data are generalizable and effective in the removal of effects of task-related changes.

Regressors to estimate the effects of respiratory and cardiac phase were made using the RETROICOR method as described in Glover et al. (2000) and in Chapter 2. The first two harmonics of the heartbeat and respiration events were computed, and both sine and cosine waveforms were included, for a total of eight phase regressors.

4.2.9 fMRI data preprocessing

Functional imaging data were preprocessed and analyzed using SPM8

(www.fil.ion.ucl.ac.uk/spm) and Matlab (www.mathworks.com/products/matlab). The first five volumes of each run were discarded to remove T1 equilibration effects. Images were slice-time corrected using sinc interpolation. Each volume was then realigned using a two-pass procedure: firstly to the first image of its run, and secondly to the mean image across all runs. All functional images were then coregistered to an anatomical scan and smoothed with a Gaussian kernel (FWHM = 5 mm).

4.2.10 Exclusion criteria: participants and individual trials

One participant's dataset was excluded because her mean absolute error on the shuffleboard task was greater than two standard deviations above the group mean across all runs and all target distances.

Three types of trial were excluded from any of the behavioral and fMRI analyses that included error size as a variable. These trials were not excluded from factorial analyses that defined trial types based on stimulus presentation alone, independent of the response. These trial types were as follows: 1) Trials with excessive movement speed which generated a feedback distance (sometimes perturbed) that was beyond the upper edge of the screen (and followed by the “too fast” warning). These trials were infrequent (mean = 5.5 of 720 trials, sd = 6.3, minimum = 0 trials, maximum = 13 trials). 2) No response trials or trials in which the hand failed to cross the release line. These were also infrequent (mean = 1, maximum = 8). 3) Double reach trials in which the participant's hand path entered the 5 cm window preceding the release line (the window that was used to obtain a measure of hand speed) and then reversed towards the start position before a second reversal to cross the release line. Again, there were very few of this type of trial for each participant (mean = 1, maximum = 5).

4.2.11 Behavioral analyses: Performance metrics and responsivity to perturbations

For each trial, signed and absolute error were defined as the difference (or absolute value of the difference) between the puck and target locations, both relative to the release line. For each run and target location, the mean percentage of successful trials (percent hits) was calculated. Both metrics were calculated in terms of the real (unperturbed) motor error and the presented (perturbed) visual error.

Signed and absolute error were measured in units of centimeters. However, for imaging analyses involving error scores, z-scored values were used in the regressors. Z-scores were computed by first grouping data according to the target distance, and then by separating feedback and no-feedback trials, resulting in six different conditions. A Fisher Z-transform was then applied to the error size distribution for each condition. Signed and absolute error were z-scored separately, as were real and visual error.

As an indicator of error-based learning in the shuffleboard task, participants' responsivity to the perturbations was measured by measuring changes in performance across successive trials. For this analysis, motor distance is defined as the distance at which the puck would have been presented on an unperturbed trial (this distance is fully determined by hand speed). This was calculated for each trial N, and the mean change in motor distance between trial N and trial N+1 was calculated as a function of perturbation type on trial N.

4.2.12 Selection of movement variables for parametric modulations

Five movement-related variables were recorded for each trial. These were used to create regressors that, when added to models as parametric modulators, controlled for unwanted sources of variance in the imaging data. These variables were reaction time (the interval between presentation of the target and puck and the initiation of movement in each trial), time to line (the time between movement initiation and release line crossing), movement duration (the time between movement initiation and release line crossing), hand speed (see above), and movement amplitude (the distance, in centimeters, covered by the hand prior to reversing trajectory).

These variables were calculated separately for the following trial types in different contrasts (Appendix, Supp. Figure 4.1): hits vs. misses, feedback vs. no-feedback trials, target location, and run number. The correlation of each of these variables with each other, as well as with feedback distance and absolute and signed visual and motor error, was examined across all targets and for each target location separately (Appendix, Supp. Figure 4.2). This was done to search for collinearity among regressors of interest which could have negatively impacted our ability to estimate effects of interest (Dale 1999; Monti, 2011). Note that some correlations are only meaningful for a specific target location: For instance, due to the non-uniformity of proportional perturbation size (as outlined in section 4.2.3 and in Figure 4.5), the effectiveness of the perturbations in reducing the correlation between hand speed and error can only be assessed within each particular target location.

All five variables were used as parametric modulators in preliminary models which included only a single modulator for all trial onsets. In each of these models, group-level one-sample t-tests were conducted on participants' parameter estimates. The effects of reaction time and hand speed were relatively strong and widespread compared to the statistical maps for the other movement variables. Furthermore, the other variables' maps contained activation peaks that coincided substantially with either the reaction time or speed maps.

Five additional models were then fit in which all five movement regressors were included. Each of these five models was used to estimate the effect of a single movement regressor, which was serially orthogonalized with respect to the preceding regressors. Note that, by definition, the time to line and speed variables are strongly negatively correlated. However, both were examined because speed was not measured across the entire approach trajectory to the line, but only at a small window preceding it. Therefore, for these variables, additional models were fit in which only one or the other was included. One-sample t-tests on the parameter estimates for the final regressor in each model produced statistical maps representing the effect of this variable, after controlling for the four others. Of these maps, those showing the effects of reaction time and speed contained substantially more significant voxels compared to those showing the effects of time to line, movement duration, and movement amplitude (these results are not shown). Within the maps for reaction time and speed, the effects remained relatively widespread, even after controlling for other movement variables. For this reason, reaction time and hand speed were selected to be used as parametric modulators in all imaging analyses. Although not shown, all analyses were repeated without these modulators, and the results were compared to determine whether any effects of interest may have been removed by this correction. Where this correction had a clear impact, it is noted in the text.

4.2.13 Imaging analyses

Following preprocessing, fMRI data were analyzed using generalized linear models at the first (individual) level and a random effects analysis at the second (group) level. All first-level analyses employed the canonical hemodynamic response function (HRF) as a basis function to generate regressors of interest and included head motion parameters and physiological variables (heart rate and respiration and their phases) as nuisance covariates. Following first-level model implementation, contrasts of interest were computed for each individual. The resulting t-statistic maps were spatially normalized to MNI space using the SPM8 and the Spatially Unbiased Infra-tentorial (SUIT) toolbox in SPM8 (www.icn.ucl.ac.uk/motorcontrol/imaging/suit.htm, Diedrichsen et al., 2009), resampled to the resolution of the atlas space (1 mm isotropic), and smoothed with a Gaussian kernel (FWHM = 5 mm), before being entered into a group-level one-sample t-test with participants entered as random factors.

The movement localizer run was analyzed using a block design to identify areas active in the contrast of Move > Rest. The only covariates used in this analysis were the nuisance covariates (head motion and physiological regressors). For the main task runs, both factorial and parametric designs were used in generalized linear models (GLMs). The former were employed to make preliminary comparisons between trial types and the latter to measure effects of error size (both signed and absolute). All factorial and parametric analyses were conducted first without and then with reaction time and hand speed entered as parametric modulators. When the effect of interest was assessed parametrically, these corrective modulators were entered prior to the regressors of interest, and the regressors of interest were then serially orthogonalized in SPM. This approach may have increased the rate of false negative findings due to the correlation between hand speed and error (Figure 4.4).

In general, analyses were conducted in two parallel forms. Some analyses estimated the effects of one or more contrasts by modeling trials at all target locations as a single condition. Other analyses estimated effects by modeling trials at each target as a separate condition (for a total of six separate conditions for all contrasts comparing two conditions in a factorial design) taking the conjunction of effects at each of the three target locations. When trials at different targets were modeled as a single condition, the error sizes used in the regressors were always z-scored (within target, and separately for the feedback and no-feedback trials within each target). This approach effectively avoids misattributing activations to a given contrast which may actually be driven by differences in performance or movement variables across target locations (Figure 4.2D).

Regions involved in feedback processing were defined by comparing feedback trials to no-feedback trials, both across target locations and within each target. Note that the differences in reaction time, but not speed (Figure 4.4) across this contrast make the use of these variables as corrective parametric modulators particularly important. Successful and unsuccessful trials (hits and misses) were also compared, across all target locations and within each target. Isolating the effect of this contrast within each target is particularly important, as participants' performance varied as a function of target location due to the motor requirements and differences in proportional perturbation size at each target.

Parametric regressors were used to assess effects of both signed and absolute error size. Similar to factorial analyses, parametric effects were estimated both within and across targets. In “target z-scored” models, error sizes were z-scored within trials at each target and then used to create a single regressor for all trials at all targets. In “target isolated” models, trials at each target

were modeled as separate conditions, each with parametric modulators (reaction time and speed) for only the trials at that target, before taking the conjunction of the resulting statistical maps to identify effects that were common across targets. This analysis of error sizes is agnostic to each trial's classification as a hit or miss, instead treating error sizes as part of an error size continuum. Therefore, in a separate analysis, data from each target location were further split into hits and misses to test for effects of error size that may only have been apparent for trials that were processed as errors.

Clusters of activation surviving the $p < .05$, family-wise error (FWE) corrected criterion are presented in Table 4.2. Activations with peaks reaching the $p < .001$, uncorrected threshold are reported in Table 4.3. All images were thresholded at $t(18) = 3.61$, $p < .001$, uncorrected. The peak t-statistic and cluster-level FWE corrected p-values are reported in the text below. These two metrics correspond to the height and extent thresholds, respectively, although it should be noted that many of these activations failed to reach cluster-level significance. Because many peaks exceed the height threshold for significance ($p < .001$, uncorrected) but do not exceed the extent threshold (cluster-level $p < .05$, FWE corrected), all peak of activations with a cluster-level significance of $p < .90$ are reported.

4.3 Results

4.3.1 Task performance in the scanner

Participants' performance was analyzed as a function of target and of task block (Figure 4.2). Percent hits are plotted as a function of block (Figure 4.2A) and target (Figure 4.2D). Z-scored absolute error scores are also plotted as a function of block (Figure 4.2C); the z-scored visual error, motor error on feedback trials, and motor error on no feedback trials all decreased over the course of five blocks. The visual absolute error values on feedback trials were entered into a two-way repeated measures ANOVAs with factors of block and target location. As seen in Figure 4.2B, there was a significant main effect of block, $F(4,72) = 2.75$, $p = .03$. As seen in Figure 4.2E, there was also a significant main effect of target location, $F(2,36) = 50.77$, $p < .0001$. There was no significant target x block interaction, $F(8,144) = 1.25$, $p = .27$. The visual absolute error is also plotted as a function of block, broken down by target distance (Figure 4.2F).

Participants' responsivity to perturbations was plotted separately for each target location (Figure 4.3). Responsivity was defined as the sign of the change in motor distance (the unperturbed feedback location, unseen by participants) from one trial to the next (from any given trial N to trial N+1), as a function of perturbation (negative, zero, and positive). These shifts are plotted in terms of both the raw and z-scored motor distance at each target separately (Figure 4.3A,B) and by target transition type (Figure 4.3C,D). The raw motor distances provide evidence that participants respond to changes in target distance (Figure 4.3A,C), as these changes are larger than the changes following perturbations. Examining changes in the z-scored distances demonstrates that participants adjust for errors by altering their motor output in response to perturbed feedback (Figure 4.3B,D). Specifically, if the perturbation on trial N is negative, motor distance shifts positively from trial N to trial N+1, and vice versa.

Relationships between task conditions and movement variables to be used as parametric modulators of task effects were also investigated (Figure 4.4). Reaction time did not differ

Figure 4.2 Motor (unperturbed) and visual (perturbed) performance metrics
A. Participants increased percent hits over five task runs.
B. Participants reduced absolute error over five task runs.
C. Same as B, z-scored within target.
D. Percent hits scaled inversely with target distance.
E. Absolute error scaled with target distance.
F. Absolute error (visual error, FB trials only) plotted separately for each target, over five task runs.

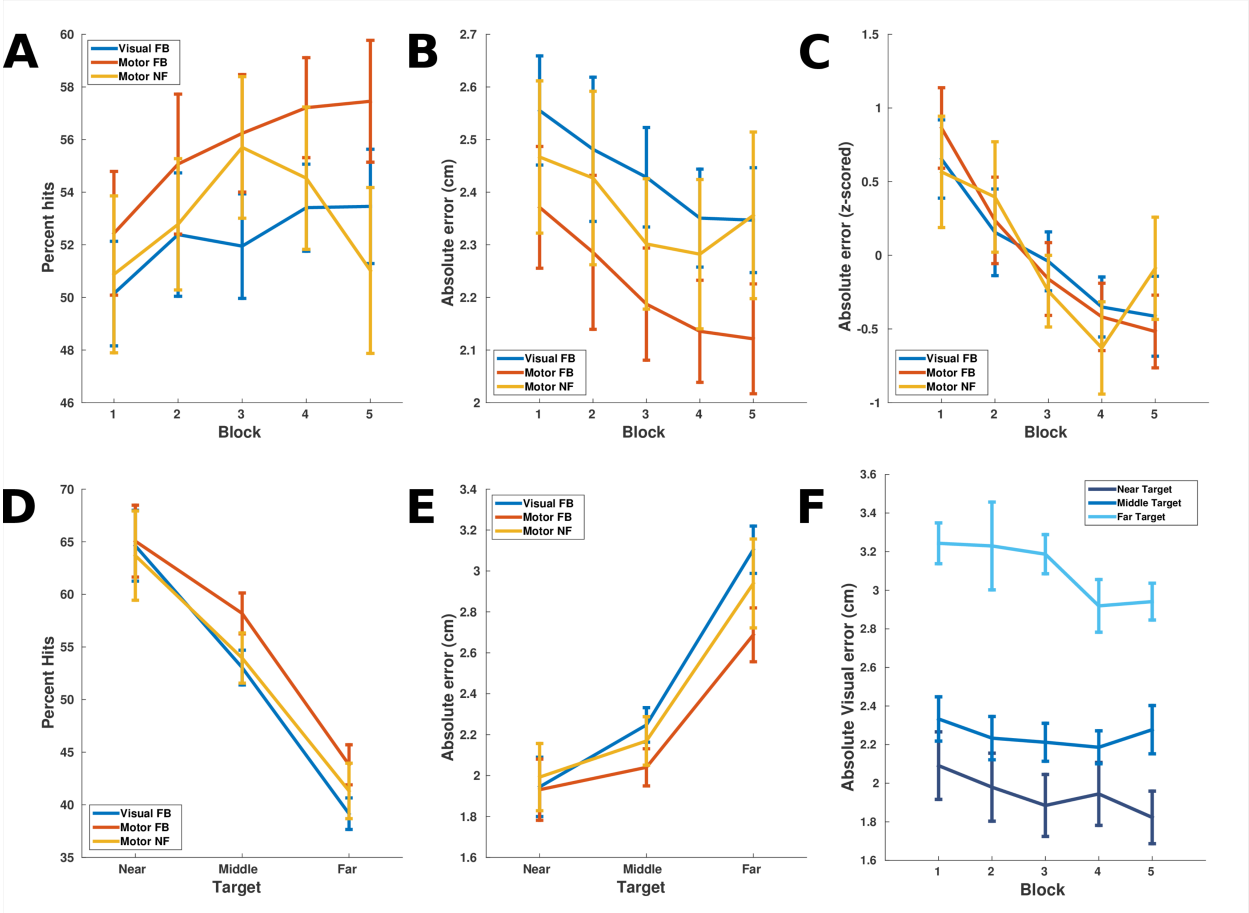

reliably across target (Figure 4.4A), across trial outcome (hits and misses), or across feedback condition (feedback and no feedback trials), nor was reaction time correlated with signed or absolute visual error (Figure 4.4B). Hand speed, in contrast, varied reliably as a function of target distance (Figure 4.4C) and was slightly greater for misses at the near target, but was not different across feedback condition in any target. The correlation between hand speed and visual error was small when plotted across all targets (Figure 4.4D), but clustering of curves indicates that within a given target distance and perturbation type, hand speed is highly determinative of visual error.

The effect of the perturbations in converting motor errors to visual errors is summarized for each target in Figure 4.5, and correlations between movement and task variables are further explored in the Appendix.

Figure 4.3 Responsivity to perturbations: raw and z-scored, by target and transition
A. Participants responded to perturbations by adjusting their motor distance (the unperturbed feedback puck distance specified by their hand speed) from trial N (blue) to trial N+1 (red). Perturbations on trial N are indicated on the x-axis (Negative, Zero, Positive). Note that participants were not presented feedback at the motor distance, but instead viewed feedback with a visual perturbation added. Motor distance (y-axis) is shown here as a depiction of participants' changes in behavior in response to perturbations (x-axis).
B. Same as A, with motor distances z-scored within target prior to classification according to trial N, N+1.
C. Participants responded to target location and transitions between targets. Titles above each panel indicate target location on trial N and trial N+1.
D. Same as C, with motor distances z-scored within target prior to classification according to trial N, N+1.

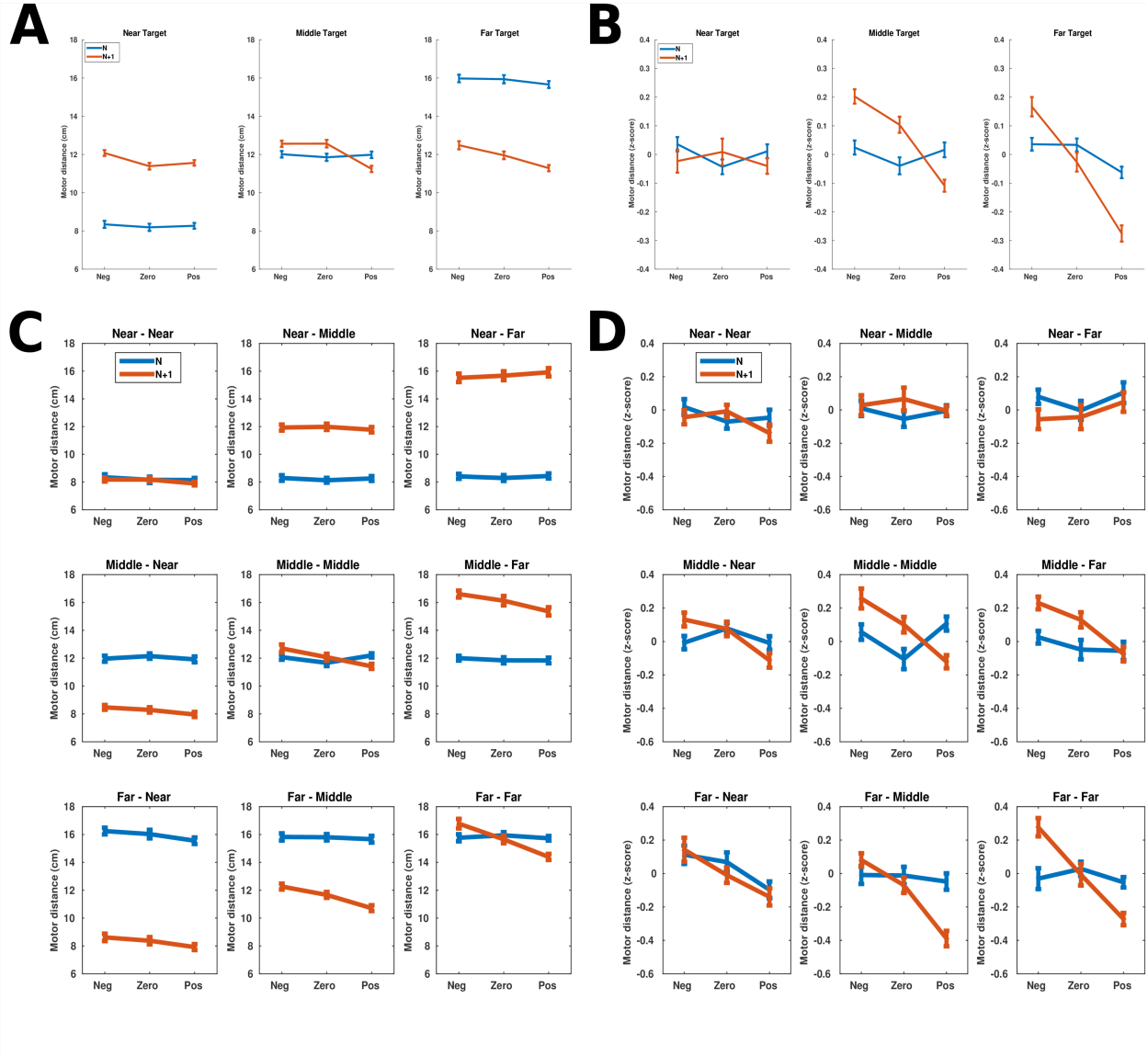

Figure 4.4 Relationship between trial type, behavioral variables of interest, and movement variables

Note: vertical stacking of data points in scatterplots results from all trials on which a "too fast" warning was displayed being set to a feedback distance 2 cm (6.6 degrees) beyond the screen's edge.

A. Reaction time as a function of trial success (top) and feedback condition (bottom).

B. Correlation between reaction time and visual error (top) and absolute visual error (bottom).

C. Hand Speed as a function of trial success (top) and feedback condition (bottom).

D. Correlation between hand speed and visual error (top) and absolute visual error (bottom).

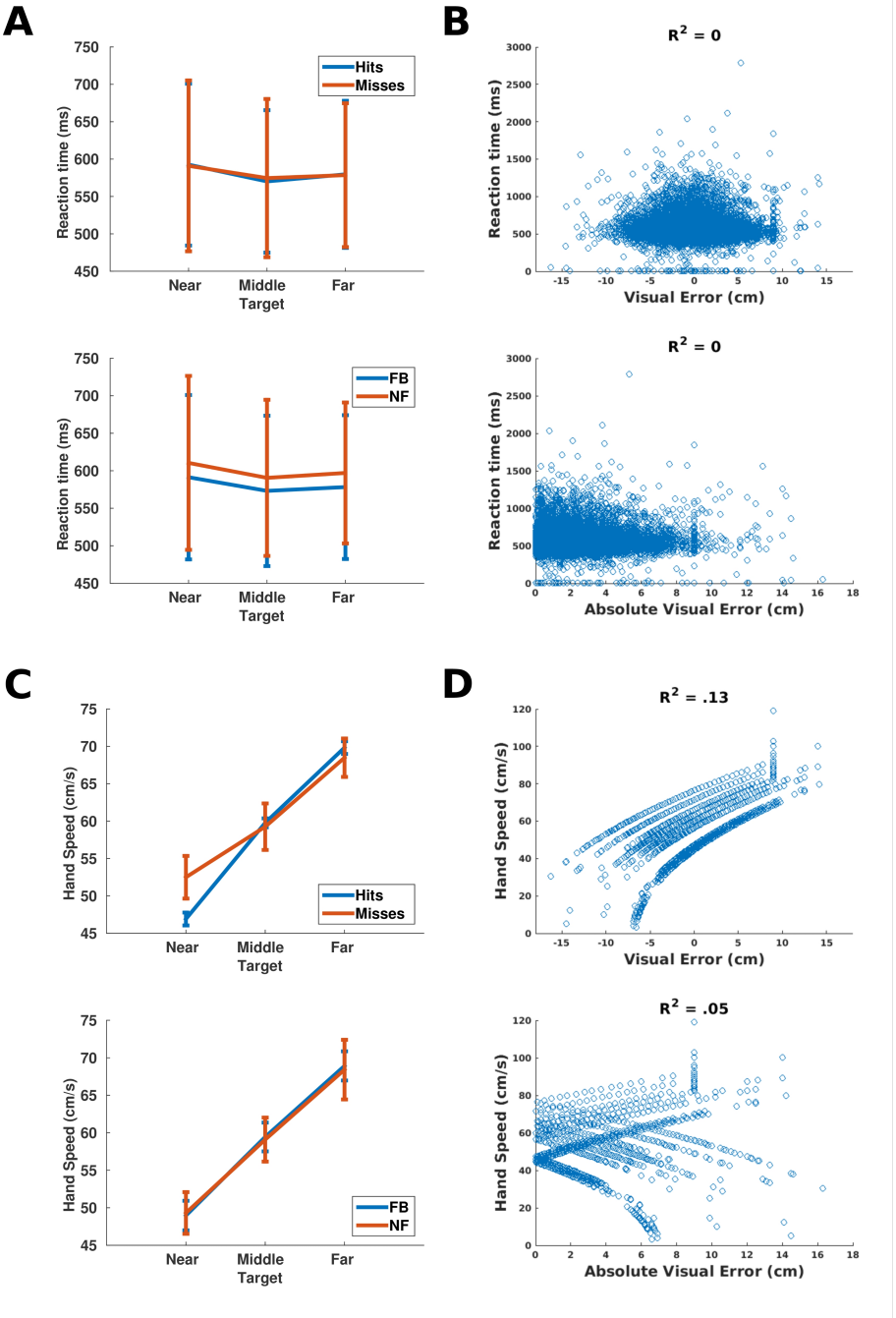

Figure 4.5 Perturbations reduce correlation between hand speed and feedback distance
A, B, C: For the near (A), middle (B), and far (C) targets, the relationship between visual (perturbed) error and motor (unperturbed) error, signed (top) and absolute (bottom). Data cluster in three lines corresponding to the negative, zero, and positive perturbation conditions.

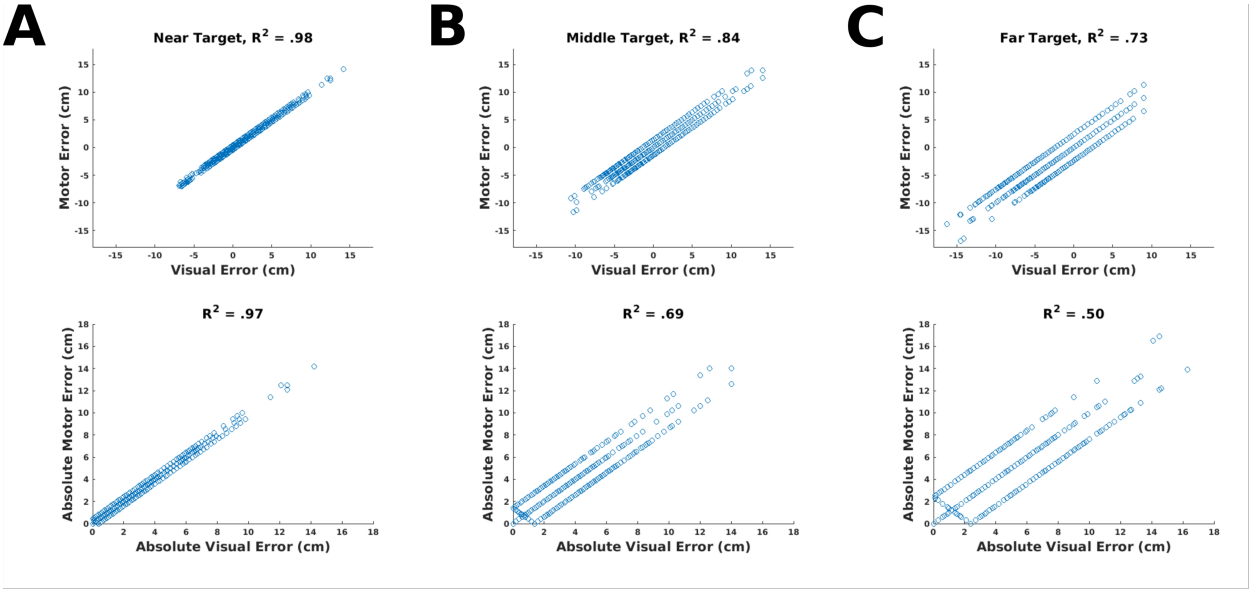

4.3.2 Post-scanning questionnaire and interview

The population mean and standard deviation for each questionnaire item were calculated and are reported in Table 4.1. Responses to post-questionnaire interview items are also reported in Table 4.1. For each questionnaire item, each participant indicated their agreement with the statement as a percentage between zero and 100% (zero indicating strongest disagreement and 100 indicating strongest agreement). Although no questionnaire data were included in the fMRI analyses, the responses provide insight into task performance. Due to the heterogeneity of the questionnaire items, results are reported in Table 4.1 for illustrative purposes only.

Most importantly, questionnaire items 9 and 10 probed participants' awareness of the perturbations. These questions were answered before the post-questionnaire interview which explicitly asked participants to guess whether their feedback had been perturbed or not. On average, participants were nearly perfectly neutral in stating agreement with item 9, which indicated that they were sometimes surprised to see their puck's landing place (item 9, mean = 51.3%, sd = 22). However, these responses do not indicate the source of the surprise. Item 10 stated that the puck's location seemed attributable to glitches, and participants were on average less in agreement with this item than item 9, suggesting that errors were attributed largely to their own performance rather than to glitches (item 10, mean = 22.9%, sd = 21.2).

Given a two-alternative forced choice of whether they thought their feedback had been manipulated or not, only three of 19 participants thought their feedback had been manipulated (Table 4.1, post-questionnaire interview item 1). Of these, one said they had thought this early on in the experiment, while two said they thought this later in the experiment. No participant reported that they were made to think their feedback had been manipulated while filling out the

Table 4.1 Questionnaire and post-questionnaire interview items and responses
Participants' responses to questionnaire items indicate their estimated percent agreement with each statement. Interview items indicate the number of participants choosing each of two options. Note that for interview item 2, participants also had the option to choose “while filling out the questionnaire” or “only once the experimenter mentioned it,” however, no participant selected either response.

	Questionnaire		
Question		**Mean**	**Std dev**
1	I was able to stay alert and focused throughout the experiment.	85.8	9.9
2	My arm got tired by the end of the experiment.	18.3	24.3
3	I was motivated to perform well in this experiment.	87.2	18.7
4	I was motivated by the money I was earning.	44.2	30.4
5	By the end of the experiment, I felt like I was doing a better job of correcting my mistakes.	61.6	28.1
6	I had trouble remembering not to expect feedback on the empty circle (no feedback) trials.	8.7	18.9
7	The empty circle (no feedback) trials were frustrating. I couldn't tell how I was doing.	45	28.1
8	The task seemed realistic: the puck landed where I would expect it to if this were a real shuffleboard table.	59.5	26.6
9	I sometimes felt surprised to see where my puck landed.	51.3	22
10	The program seemed glitchy—It didn't always measure my speed accurately.	22.9	21.2
	Post-questionnaire Interview		
		Manipulated N	**True N**
1	There were two groups: one with manipulated feedback and one with true feedback. Which group do you think you were in?	3	16
		Early N	**Late N**
2	If manipulated, when in the experiment did you first think something was wrong?	1	2

questionnaire or during the interview, although these were included as possible choices.

A minority of participants guessed that their feedback had been manipulated. Furthermore, participants did not indicate a high level of agreement with the statement that the program had seemed glitchy, and on average, they neither agreed nor disagreed that their feedback appeared surprising to them. The questionnaire and interview results therefore indicate that participants saw the feedback presented as caused by their own movements, with any surprising variance attributed not to glitches or experimenter manipulations but to their own performance. The questionnaire data indicate that this self-attribution of errors was likely maintained throughout the experiment.

4.3.3 Imaging: Movement localizer

Activations for the contrast Move vs. Rest during the movement are summarized in Table 4.3 and Figure 4.6. Because not all peaks that survived $p < .001$ (uncorrected) were also significant after cluster correction, all results reported here list both peak-level t-statistics and cluster-level p-values. In comparing movement epochs to rest epochs, no clusters survived the family-wise error corrected threshold, $t(18) = 7.91$. However, the modest effect size is likely due to the use of a single localizer run. At $p < .001$ (uncorrected), however, peaks of activation were found in the right anterior lobe of the cerebellum, $t(18) = 7.59$, $p = .091$, the left precentral gyrus (primary motor cortex), $t(18) = 7.39$, $p = .13$, the right middle occipital gyrus (visual cortex), $t(18) = 5.08$, $p = .16$, and the right cerebellum lobule VIIIb, including parts of the vermis (posterior lobe), $t(18) = 4.33$, $p = .34$. Deactivations during movement, relative to rest, appeared in the right (ipsilateral) postcentral gyrus (primary somatosensory cortex), possibly reflecting intermanual inhibition, as well as throughout large swaths of visual cortex.

Table 4.2 Clusters of activation, p < .05, family-wise error corrected

Effect	Threshold	T-statistic at peak	Cluster-level p(FWE)	Coordinate	Number of voxels	Region name
FB > NF (target isolated)	6.68	7.42	0.0001	-14 6 14	94	Left caudate head
NF > FB (target isolated)	6.68	8.16	0.0001	52 4 4	41	Right superior temporal gyrus
Hit > Miss (target isolated)	6.58	7.94	0.0001	-16 12 2	293	Left putamen
		7.92	0.01	-10 56 0	17	Left superior frontal gyrus
		7.89	0.0001	22 16 -2	317	Right putamen
Anticorrelation: Unsigned error (target z-scored)	6.65	7.31	0.003	-18 -16 20	34	Left putamen

Table 4.3 Activations centered on peaks reaching p < .001, uncorrected

Regions that appeared in Table 4.2 are starred if they survived family-wise error correction. Note that the peak coordinate and region name may change, as multiple family-wise error corrected clusters may be part of one broader swath of activation. Where areas encompass multiple structures, the region name reflects the area as a whole instead of the peak.

Effect	Threshold	T-statistic at peak	Cluster-level p(FWE)	Coordinate	Number of voxels	Region name
Move > Rest (localizer)	3.61	7.59	0.09	8 -54 -12	1398	Right cerebellum lobule V
		7.39	0.13	-38 -32 68	1565	Left precentral gyrus
		5.08	0.16	36 -90 -2	869	Right middle occipital gyrus
		4.33	0.34	26 -52 -54	104	Right cerebellum lobule VIIIb
FB > NF (target isolated)	3.61	7.42	0.0001	-14 6 14	5459	Bilateral striatum*
		5.82	0.004	46 -66 -2	941	Right inferior temporal gyrus
		4.12	0.16	32 -70 32	319	Right precuneus
		3.93	0.12	10 -56 70	371	Right postcentral gyrus
		3.86	0.52	-12 28 4	148	Left anterior cingulate gyrus
		3.79	0.1	28 -28 4	391	Right thalamus (pulvinar)
NF > FB (target isolated)	3.61	8.16	0.14	52 4 4	346	Right superior temporal gyrus*
		5.83	0.13	36 40 36	356	Right superior frontal gyrus
Hit > Miss (target isolated)	3.61	7.94	0.0001	-16 12 2	11549	Bilateral striatum*
		4.82	0.14	32 -92 -8	383	Inferior occipital gyrus
		4.78	0.1	-10 48 44	441	Left superior frontal gyrus*
		4.27	0.63	-32 -66 62	123	Left superior parietal lobule
		4.22	0.5	46 -60 56	162	Right inferior parietal lobule
		4.14	0.27	42 -76 -32	268	Right cerebellum lobule VIIa
Anticorrelation: unsigned error (target z-scored)	3.61	7.31	0.0001	-18 -16 20	6068	Bilateral striatum*
		5.47	0.4	32 38 -20	192	Right inferior frontal gyrus
		5.26	0.56	20 -26 -12	138	Right parahippocampal gyrus
		5.16	0.52	28 -90 -8	148	Right inferior occipital gyrus
Anticorrelation: unsigned error (target isolated)	3.61	4.44	0.12	-22 6 -4	386	Left putamen
		4.34	0.17	22 8 -4	330	Right putamen
		3.62	0.46	32 -90 -10	174	Right inferior occipital gyrus
Anticorrelation: unsigned error on misses (target z-scored)	3.61	4.59	0.9	-12 68 6	47	Left superior frontal gyrus
Anticorrelation: unsigned error on misses (target isolated)	3.61	4.08	0.98	'-42 -52 -30	15	Left cerebellum lobule VIIa/Crus 1
Anticorrelation: unsigned error on hits (target isolated)	3.61	3.91	0.97	30 -56 -32	18	Right cerebellum lobule VI
Correlation: Signed error (target z-scored)	3.65	5.08	0.6	46 -72 40	123	Right inferior parietal lobule
		4.83	0.94	-12 30 -6	32	Left anterior cingulate gyrus
Anticorrelation: Signed error on misses (target z-scored)	3.61	5.33	0.6	-10 -92 32	130	Left cuneus
		4.28	0.92	-14 -12 72	36	Left superior frontal gyrus

Figure 4.6 Movement localizer
Images show activations and deactivations for the contrast Move > Rest during the localizer run. Colorbar at bottom, lower threshold: t(18) = 3.61, p < .001, uncorrected, upper threshold: t(18) = 7.91, p < .05, family-wise error corrected.
A. Left primary motor cortex (M1, precentral gyrus) was activated by movements of the contralateral (right) hand. Deactivations appeared in the ipsilateral central gyrus and frontal and parietal areas.
B. Posterior regions of visual cortex, near the middle occipital gyrus, were activated, while swaths of visual cortex and right inferior frontal gyrus/posterior insula were deactivated.
C. Regions of the cerebellum, including the right anterior lobe, vermis, and right posterior lobe were activated by arm movements. Ventralmost and dorsalmost portions of the activations lie within two somatotopic regions of the cerebellum (Schlerf et al., 2010), and the medial portion is consistent with an oculomotor role for the vermis (for review, see Kheradmand & Zee, 2011).

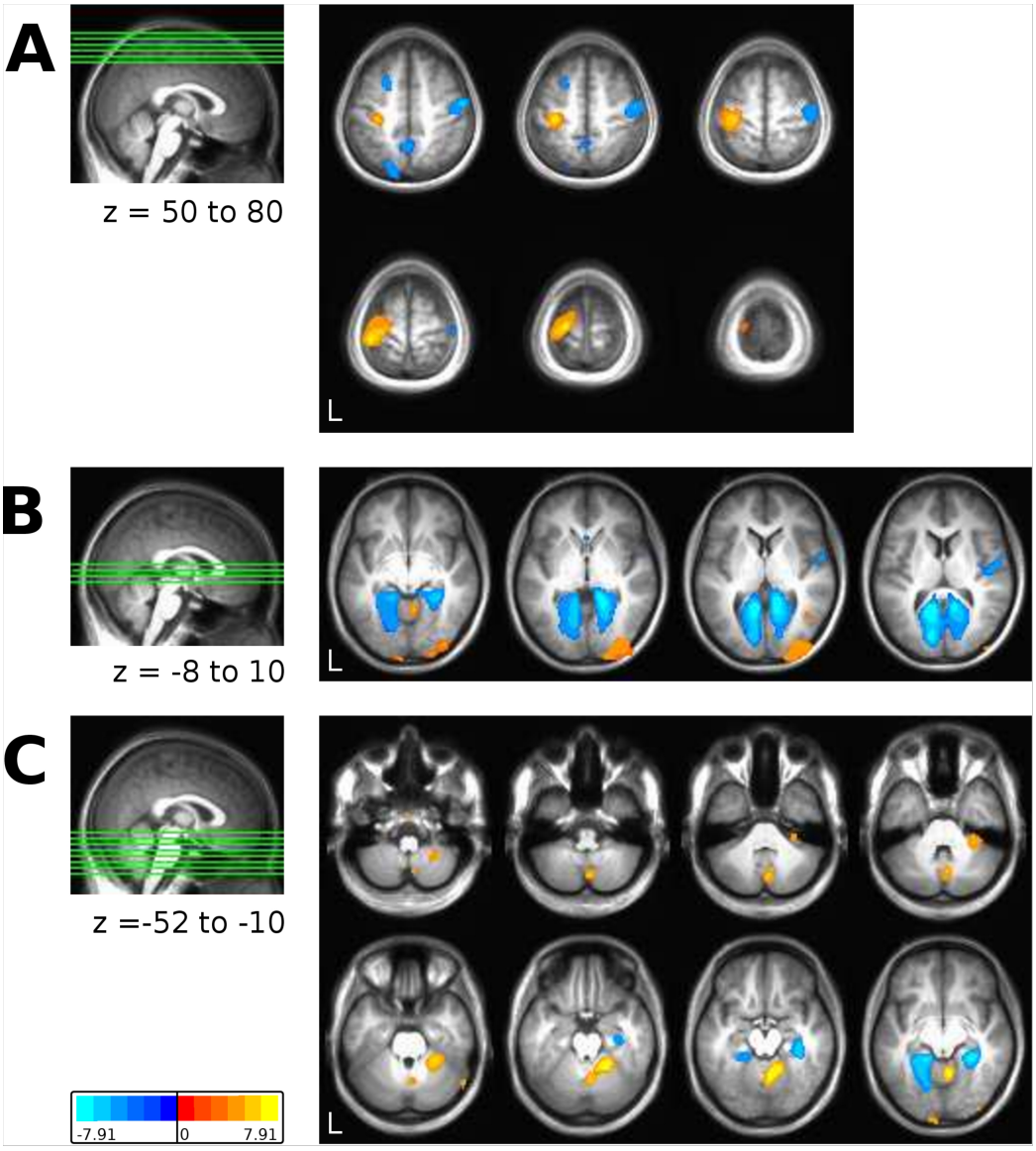

Activations within this run, despite being measured in an independent data set, are not further addressed, as the primary effects of interest in analyses of feedback processing lie outside of these movement-related areas.

4.3.4 Imaging: Factorial effects of interest

Comparisons between Feedback and No feedback were made using two-sample t-tests applied as a contrast of the two conditions. Details on location and extent of the activations can be found in Table 4.2 and Table 4.3. Because not all peaks that survived $p < .001$ (uncorrected) were also significant after cluster correction, all results reported here list both peak-level t-statistics and cluster-level p-values.

The contrast Feedback > No feedback was used to identify feedback processing regions. Feedback and No Feedback trials were compared for each target location, and the conjunction of the three single-target maps was calculated. These comparisons are summarized in Figure 4.7. Within the Feedback > No feedback contrast, one cluster survived at a threshold of $p < .05$, FWE-corrected, in the left head of the caudate nucleus, $t(18) = 7.42$, $p < .001$, FWE-corrected. Six regions of activation were identified at $p < .001$ (uncorrected). The first, which corresponds to the cluster that was significant following FWE correction, spread bilaterally across the striatum, $t(18) = 7.42$, $p < .0001$. The five additional activations were located in the right inferior temporal gyrus, $t(18) = 5.82$, $p < .004$, the right precuneus, $t(18) = 4.12$, $p = .16$, the right postcentral gyrus, $t(18) = 3.91$, $p = .12$, the left anterior cingulate gyrus, $t(18) = 3.86$, $p = .52$, and the right pulvinar nucleus of the thalamus near the hippocampus and brainstem, $t(18) = 3.79$, $p = .1$). Thus, feedback about movement outcomes activated regions outside of those identified in the localizer run, indicating that structures like the striatum and motor and non-motor regions of parietal and frontal cortex, are recruited for the evaluation of movement success or failure.

Within the No feedback > Feedback contrast, one cluster survived at $p < .05$, FWE-corrected, in the right superior temporal gyrus, $t(18) = 8.16$, $p < .0001$, FWE-corrected. Two regions of activation were identified at $p < .001$ (uncorrected). Of these, one corresponded to the right superior temporal gyrus region; at this more lenient criterion, the cluster-level FWE-corrected p-value was .14. The second was a region in the right superior frontal gyrus, $t(18) = 5.83$, $p = .13$. These deactivations may reflect self-monitoring processes activated in the absence of feedback.

Successful and unsuccessful trials (hits and misses) were also compared for each target location, and the conjunction of the three single-target maps was calculated (Figure 4.8). For the Hits > Misses contrast, three clusters survived at $p < .05$, FWE: the left putamen, $t(18) = 7.94$, $p < .0001$, the left superior frontal gyrus, $t(18) = 7.92$, $p < .01$, and the right putamen, $t(18) = 7.89$, $p < .0001$. When the criterion was relaxed to $p < .001$, uncorrected, two corresponding regions were identified, one corresponding to a swath of the striatum which encompassed the left and right putamen clusters, $t(18) = 7.94$, $p < .0001$, and one corresponding to the left superior frontal gyrus cluster, $t(18) = 4.78$, $p = .1$. Four additional activations were identified at this threshold in the right inferior occipital gyrus, $t(18) = 4.82$, $p = .14$, the left superior parietal lobule, $t(18) = 4.27$, $p = .63$, the right inferior parietal lobule, $t(18) = 4.22$, $p = .5$, and the right posterior cerebellum, $t(18) = 4.14$, $p = .27$. Taken together, these results indicate that the striatum responds robustly to successful actions, and a network of cortical and cerebellar sites mimic this pattern to a lesser extent.

Figure 4.7 Feedback (FB) vs. No feedback (NF) trials
All images show activations and deactivations for the contrast Feedback > No Feedback during task runs. Colorbar at bottom, lower threshold: t(18) = 3.61, p < .001, uncorrected, upper threshold: t(18) = 6.68, p < .05, family-wise error corrected. Compared to no feedback trials, feedback trials activated regions of the striatum bilaterally (with a cluster in the head of the left caudate nucleus surviving at p < .05, FWE-corrected), the right inferior temporal gyrus, precuneus, and postcentral gyrus, small regions of the frontal cortex in and around the left anterior cingulate gyrus, and the right pulvinar nucleus of the thalamus (near the hippocampus and brainstem). Compared to feedback trials, no feedback trials activated the right superior temporal gyrus and the right superior frontal gyrus (with the right superior temporal gyrus cluster surviving at p < .05, FWE-corrected).

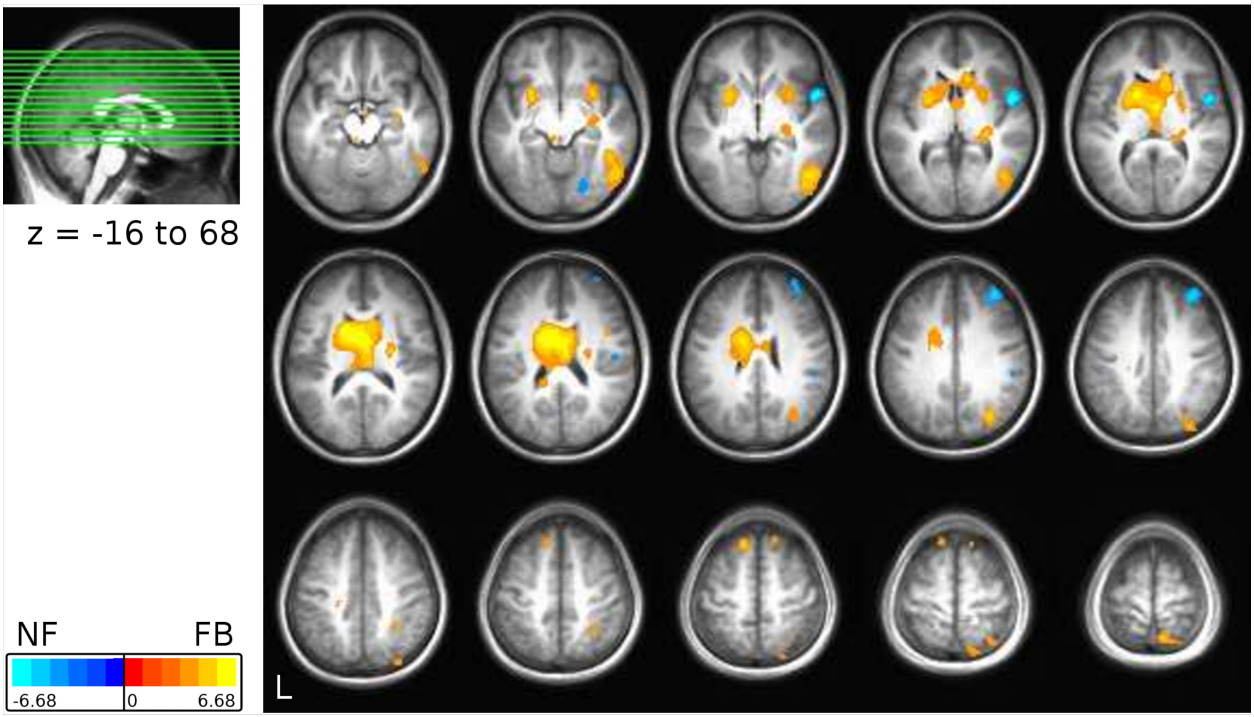

No clusters responded more to misses than to hits at p < .05, FWE-corrected. Furthermore, no activations peaks fitting this pattern at p < .001 (uncorrected) were identified. This is somewhat surprising, given the robust response to errors identified by previous studies in the striatum (Diedrichsen et al., 2005) and the cerebellum (Diedrichsen et al., 2005; Schlerf et al., 2012).

4.3.5 Imaging: Parametric effects of interest

Parametric effects of signed and absolute error size were assessed by including parametric modulators for each condition in GLMs and conducting one-sample t-tests on the parameter estimates for the regressor of interest. All effects were tested using regressors that had been orthogonalized with respect to the reaction time and speed modulators. Details on location

Figure 4.8 Hit trials vs. Miss trials
All images show activations and deactivations for the contrast Hits > Misses during task runs. Colorbar at bottom, lower threshold: t(18) = 3.61, p < .001, uncorrected, upper threshold: t(18) = 6.68, p < .05, family-wise error corrected.
A. Compared to misses, hits activated a broad swath of the striatum, bilaterally, a region of orbitofrontal cortex in the medial aspect of the superior frontal gyrus, bilaterally, and the right inferior occipital gyrus. Three clusters survived at p < .05, FWE-corrected: one in the left putamen, one in the right putamen, and the orbitofrontal cluster.
B. Compared to misses, hits activated a region of the right posterior cerebellum. This peak surpassed p < .001 (uncorrected), but the region did not survive FWE correction.
C. Compared to misses, hits activated smaller areas in the frontal and parietal lobes bilaterally. These peaks surpassed p < .001 (uncorrected), but the regions did not survive FWE correction.

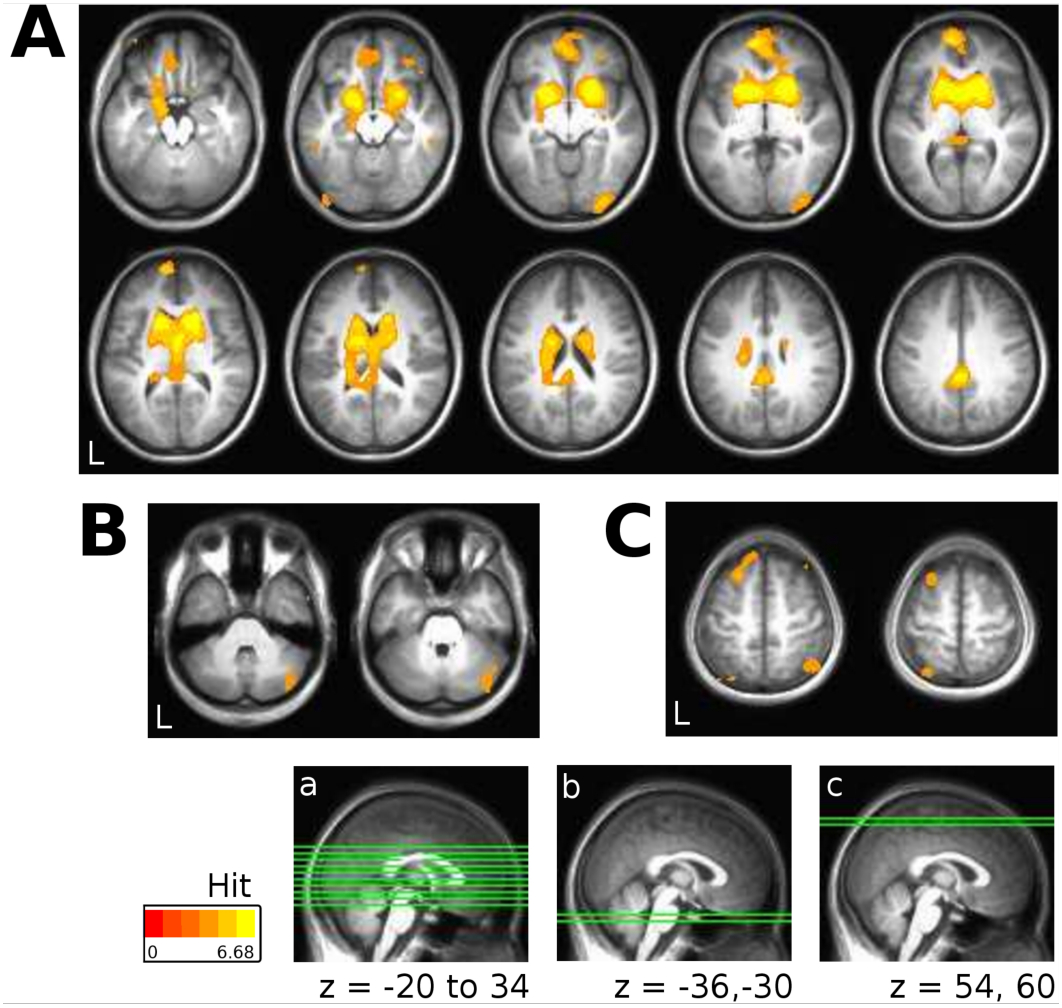

and extent of the activations can be found in Tables 4.2 and 4.3. Because not all peaks that survive p < .001 (uncorrected) were also significant after cluster correction, all results reported here list both peak-level t-statistics and cluster-level p-values.

One cluster survived these analyses at $p < .05$, FWE-corrected, in the left putamen, $t(18) = 7.31$, $p < .003$, FWE-corrected. This cluster's activity was anticorrelated with absolute error size when errors were normalized within each target and then compared across all targets. Note that this analysis treats error size as a continuum; it is agnostic regarding whether trials were classified as hits or misses. After relaxing the criterion to $p < .001$, uncorrected, four regions were identified, one corresponding to the left putamen cluster (Figure 4.9A). At this threshold, the putamen cluster expanded to include areas of the striatum bilaterally, $t(18) = 7.31$, $p < .0001$. The three additional activations were located in the right inferior frontal gyrus, $t(18) = 5.47$, $p = .4$, the right parahippocampal gyrus, $t(18) = 5.26$, $p = .56$, and the right inferior occipital gyrus, $t(18) = 5.16$, $p = .52$.

A similar set of regions exhibited activity that was anticorrelated with absolute error (Figure 4.9B): the left putamen, $t(18) = 4.44$, $p = .12$, the right putamen, $t(18) = 4.34$, $p = .17$, and the right inferior occipital gyrus, $t(18) = 3.61$, $p = .46$. Note that these regions are very similar to the significant clusters identified in the Hits > Misses contrast as well as the significant cluster in the left putamen obtained using the target z-scored model. However, the more restrictive approach of taking the conjunction of three target-specific maps reveals a more focal region of the putamen, and not the striatum as a whole. Taken together, these analyses indicate that regions of the striatum as well as a region of visual cortex in the right hemisphere reliably respond more to small errors and to hits. As in the factorial analyses, no regions were identified as responding more to larger errors, or misses.

We also investigated whether effects of absolute error were present within hits and misses separately. When z-scoring error sizes, activity in the medial aspect of the left superior frontal gyrus was anticorrelated with absolute error only for misses; that is, activity was greater for miss trials that were nearly hits than for misses with larger errors, $t(18) = 4.59$, $p = .9$ (Figure 4.9C). Using single-target models, activity in two small regions of the cerebellum was anticorrelated with error size, one in the hits condition and one in the misses condition (Figure 4.9D). The left posterior cerebellum responded more to near-hits than to misses with larger errors, $t(18) = 4.08$, $p = .98$, while the right posterior cerebellum responded more to perfect hits than to hits that were nearly misses, $t(18) = 3.91$, $p = .97$. Note, however, that these effects are far from significant. They are reported here to clarify that the general effects of anticorrelation with absolute error are likely to be driven by the distribution of error sizes as a whole, rather than reappearing as a robust sensitivity to error size when trials were counted as misses.

Finally, effects of signed error were identified. Because signed error is highly correlated with hand speed, particularly at the near target (Figure 4.5), these effects could not be estimated using single-target models. However, using target z-scored models, activity in two regions was positively correlated with signed error; that is, activity in these regions was greater for overshoots than for undershoots (Figure 4.10A and B). Note that this includes hit trials, although the z-scored error sizes for these trials will by definition be smaller than for miss trials. These activations were located in the right inferior parietal lobule, $t(18) = 5.08$, $p = .6$, and the left anterior cingulate gyrus, $t(18) = 4.83$, $p = .94$. When analyzing hits and misses separately, two additional regions were identified as having activity that was anticorrelated with signed error on miss trials only; that is, activity in these regions was greater for undershoots than for overshoots when the participant missed the target (Figure 4.10C and D). These activations were located in the left cuneus, $t(18) = 5.33$, $p = .6$, and the left superior frontal gyrus (within the primary motor cortex activation for the contrast Move > Rest in the localizer run), $t(18) = 4.28$, $p = .92$. Note

Figure 4.9 Parametric effect of absolute error

All images show linear anticorrelations with visual absolute error on feedback trials only during task runs. Colorbars, lower threshold: t(18) = 3.61, p < .001, uncorrected, upper threshold: t(18) = ~6.62, p < .05, family-wise error corrected.

A. Using the target z-scored model, activity in regions of the striatum, bilaterally, the right inferior frontal gyrus, the right parahippocampal gyrus near the brainstem, and the right inferior occipital gyrus was anticorrelated with absolute error. A cluster in the left putamen survived at p < .05, FWE-corrected.

B. Using single-target models produced similar, but more focal results. Activity in the left putamen, right putamen, and right inferior occipital gyrus was anticorrelated with absolute error.

C. Segregating hits and misses in the target z-scored model revealed that on miss trials only, activity in the left superior frontal gyrus was anticorrelated with absolute error.

D. Segregating hits and misses in the target isolated model revealed that on miss trials only, activity in the left posterior cerebellum, and on hit trials only, activity in the right posterior cerebellum, was anticorrelated with absolute error.

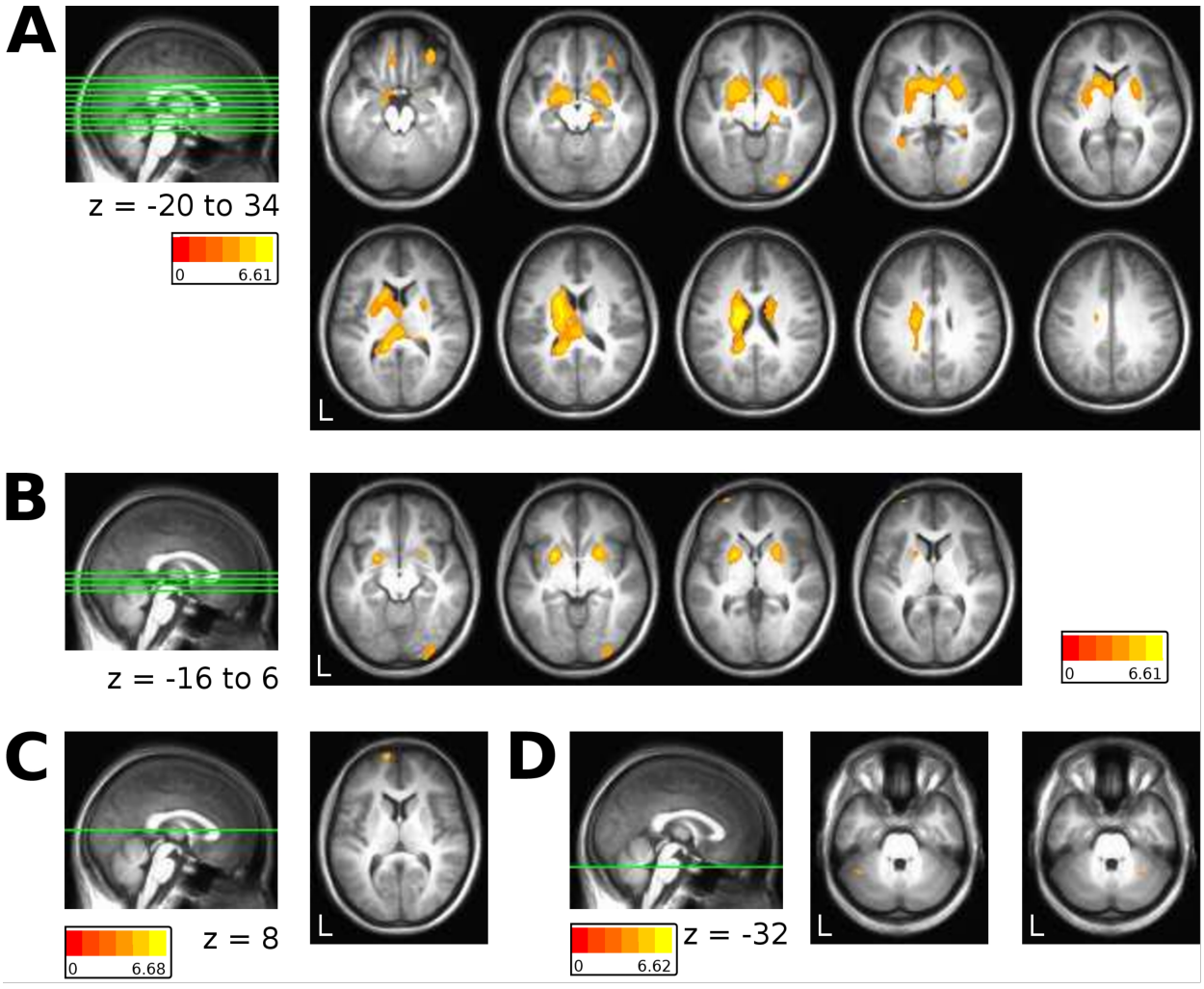

Figure 4.10 Parametric effect of signed error
All images show linear correlations and anticorrelations with visual signed error on feedback trials only during task runs. Note that the same color scheme is here used for both positive and negative correlations. Colorbars, lower threshold: t(18) = 3.61, p < .001, uncorrected, upper threshold: t(18) = 6.63/6.84, p < .05, family-wise error corrected.
A, B. In the target z-scored model, activity in the right inferior parietal lobule (A) and the left anterior cingulate gyrus (B) was positively correlated with signed error. That is, these regions responded more to overshoots.
C,D. In the target z-scored model, activity in the left superior frontal gyrus (C) within the primary motor cortex activation (localizer run), and in the left cuneus (D), was negatively correlated with signed error. That is, these regions responded more to undershoots.

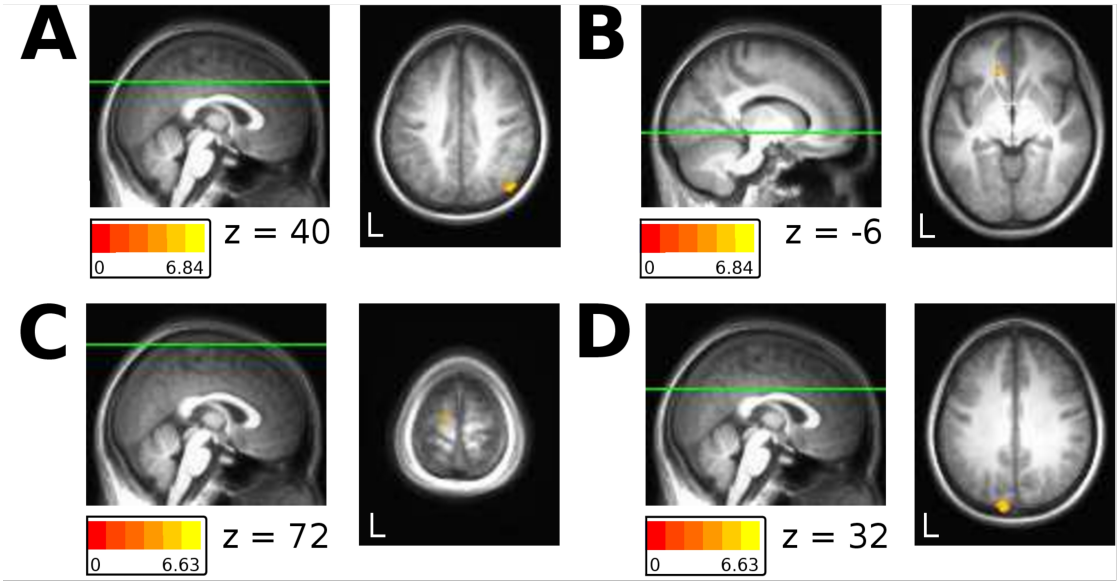

again, however, that while these peaks of activation (t-statistic) reach p < .001, uncorrected, these effects are far from significant at the cluster level and are reported here to highlight the dearth of regions whose activity was correlated with signed error after removing the effects of reaction time and hand speed.

4.3.6 Imaging: Reaction time & hand speed

To account for both linear and quadratic effects, reaction time and hand speed were included in all analyses as first-and second-order parametric modulators of the mean of each condition's parameter estimate. For analyses using parametric regressors to estimate effects of interest, reaction time and hand speed were entered first into the GLM. Using serial orthogonalization of regressors in SPM8, this approach ensured that any variance attributable to either reaction time or hand speed was removed prior to estimating the effect of interest. For this reason, effects are listed in Table 4.4 as “controlling for” each other. Removing this control and estimating the effect of each separately produces similar results (data not shown).

We also directly measured the effects of reaction time and speed (Table 4.4 and Figures

Table 4.4 Regions modulated by reaction time and hand speed, p < .001, uncorrected
The starred region name indicates a cluster which also survived family-wise error correction, p < .012, although the p-value starred represents the p-value larger cluster thresholded at p < .001, uncorrected.

Effect	Threshold	T-statistic at peak	Cluster-level p(FWE)	Coordinate	Number of voxels	Region name
Correlation: Reaction time (controlling for Speed)	3.61	6.16	0.02	'-40 -34 64	720	Left precentral gyrus
		5.97	0.0001	'-34 -92 -18	1588	Left inferior occipital gyrus
		5.66	0.0001	-2 -82 46	2299	Left precuneus
		4.97	0.0001	46 -54 -34	1736	Right cerebellum lobule VIIa/Crus 1
		4.95	0.39	-2 -102 8	205	Left cuneus
		4.91	0.007	4 8 50	919	Right medial frontal gyrus
		4.78	0.54	-46 54 16	150	Left middle frontal gyrus
		4.76	0.15	38 54 22	357	Right middle frontal gyrus
		4.53	0.83	'-12 -98 -18	67	Left lingual gyrus
		4.42	0.59	44 8 32	135	Right middle frontal gyrus
		4.29	0.61	16 -2 70	127	Right superior frontal gyrus
		4.25	0.34	38 -4 66	225	Right middle frontal gyrus
		4.16	0.78	'-24 -28 -38	80	Left cerebellum lobule I-IV
		4.08	0.89	54 -36 26	48	Right inferior parietal lobule
		4.03	0.9	-18 36 -26	41	Left orbital gyrus
		4.01	0.41	42 18 -2	192	Right inferior frontal gyrus
Anticorrelation: Reaction time (controlling for Speed)	3.61	4.61	0.83	22 -38 18	67	Right caudate tail
		4.48	0.84	-10 58 10	64	Left superior frontal gyrus
		4.13	0.39	0 30 -8	201	Right anterior cingulate gyrus
		3.96	0.94	-6 16 12	30	Left caudate head
Correlation: Speed (controlling for RT)	3.61	5.87	0.002	12 -80 -10	1111	Left and right cuneus
Anticorrelation: Speed (controlling for RT)	3.61	6.76	0.008	24 -98 18	851	Right middle occipital gyrus
		6.5	0.001	-32 -30 70	2029	Left precentral gyrus
		4.8	0.2	16 -76 -50	299	Right cerebellum lobule VIIb/Crus 2
		4.66	0.3	-2 -102 2	237	Left cuneus
		4.2	0.3	2 -4 56	243	Right medial frontal gyrus
		4.03	0.86	-28 26 52	59	Left middle frontal gyrus
Correlation: Speed (controlling for RT), FB only	3.61	5.37	0.007	18 -80 -12	882	Right lingual gyrus
		4.06	0.94	-38 -90 18	32	Left middle occipital gyrus
Anticorrelation: Speed (controlling for RT), FB only	3.61	5.17	0.005	-42 -32 66	936	Left postcentral gyrus
		4.97	0.18	22 -98 16	314	Right middle occipital gyrus
		3.98	0.89	-24 30 46	50	Left middle frontal gyrus
Correlation: Speed (controlling for RT), NF only	3.61	7.36	0.008	10 -80 -8	833	Left and right cuneus
Anticorrelation: Speed (controlling for RT), NF only	3.61	5.64	0.03	20 -98 16	587	Right cuneus
		4.94	0.37	22 -70 -50	201	Right cerebellum lobule VIIb/Crus 2
		4.88	0.35	-20 -106 14	211	Left cuneus

4.11-4.13). These effects were estimated without z-scoring or otherwise transforming either variable. In each case, pooled single-target activation maps are similar to those estimated without isolating each target first. Therefore, all results presented here were estimated using all trials as a single condition in a GLM and applying a one-sample t-test as a contrast on the parametric modulators. Although both linear and quadratic effects of reaction time and speed were estimated and removed from all analyses, here we present only the linear effects. Adding quadratic effects of reaction time only minimally alters these maps, and adding quadratic effects of hand speed results in less focal activations throughout the brain (data not shown).

Because effects of reaction time and hand speed were eliminated from all the analyses presented so far, they are shown here to illustrate which regions were most susceptible to these effects. The effect of hand speed is also separately presented for feedback and no-feedback trials, given the positive and negative correlations with hand speed in visual cortex.

Figure 4.11 Effects of reaction time, after controlling for effects of hand speed
Images show linear correlations and anticorrelations with reaction time, after controlling for hand speed, on all trials during task runs. Colorbar at bottom, lower threshold: $t(18) = 3.61$, $p < .001$, uncorrected, upper threshold: $t(18) = 6.65$, $p < .05$, family-wise error corrected. Activity was positively correlated with reaction time in both anterior and posterior regions of the cerebellum, occipital cortex, medial and lateral frontal and parietal cortices. Activity was negatively correlated with reaction time in a medial region of the frontal lobe as well as a region in the tail of the right caudate nucleus.

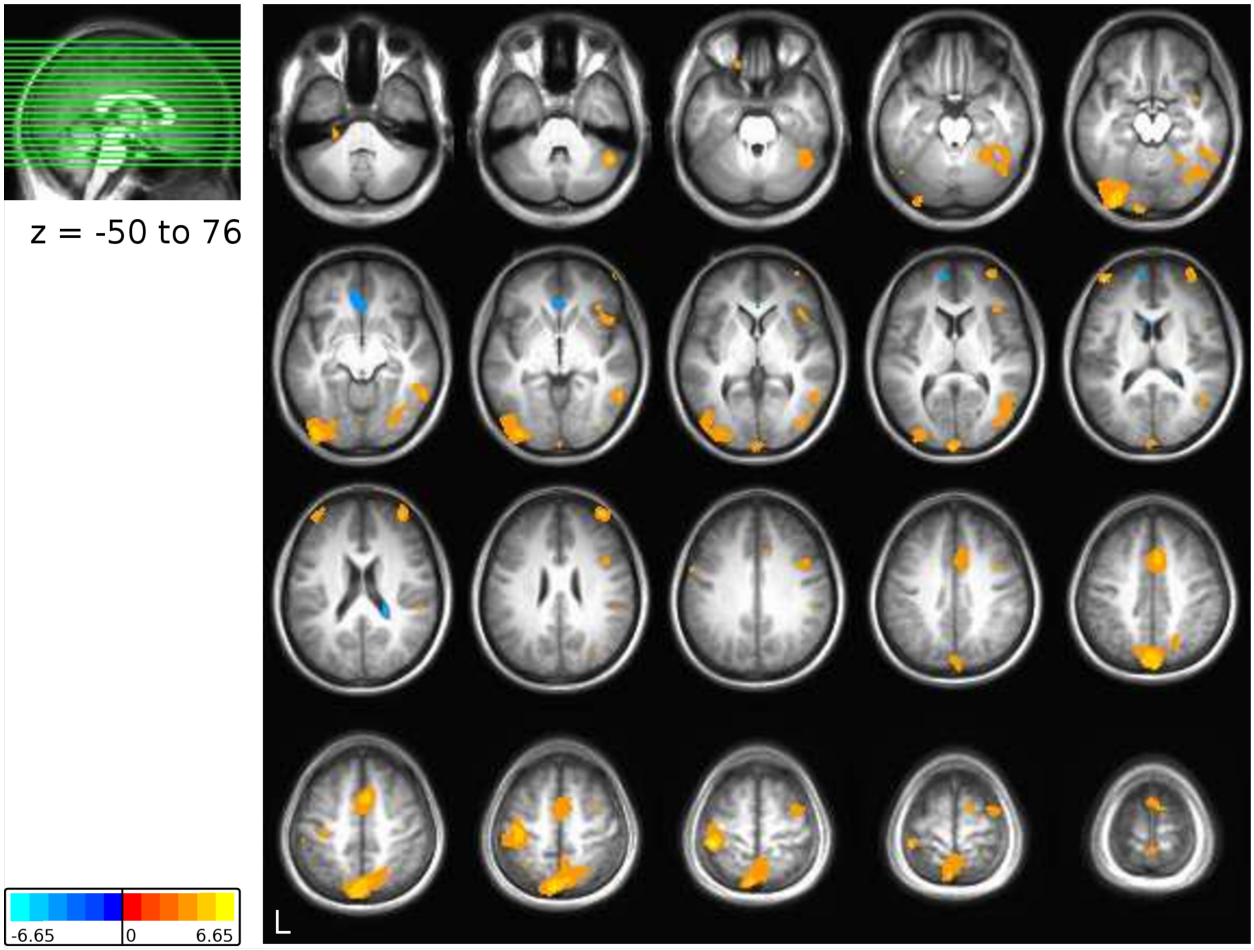

No clusters exhibited activity that was correlated with reaction time at $p < .05$, FWE-corrected. Relaxing the criterion to $p < .001$ (uncorrected) revealed widespread correlations with reaction time throughout the brain, including sixteen peaks of activation with a cluster-wise FWE corrected p-value of .9 or less in motor, visual, and prefrontal and parietal areas as well as the cerebellum (Table 4.4 and Figure 4.12). Although activity that correlates with reaction time is typical of time-on-task BOLD responses in general, four peaks of activation had activity that was anticorrelated with reaction time. These were located in the head and tail of the caudate nucleus and in areas of prefrontal cortex.

No clusters were found with activity correlated with hand speed at $p < .05$, FWE-

Figure 4.12 Effects of hand speed, after controlling for effects of reaction time
Images show linear correlations and anticorrelations with hand speed, after controlling for reaction time, on all trials during task runs. Colorbar at bottom, lower threshold: $t(18) = 3.61$, $p < .001$, uncorrected, upper threshold: $t(18) = 6.65$, $p < .05$, family-wise error corrected. Activity was positively correlated with hand speed in a region of visual cortex, while in a neighboring region, activity was negatively correlated with hand speed. Additional negative correlations with hand speed were found in the right posterior cerebellum and left primary motor cortex, extending into premotor regions.

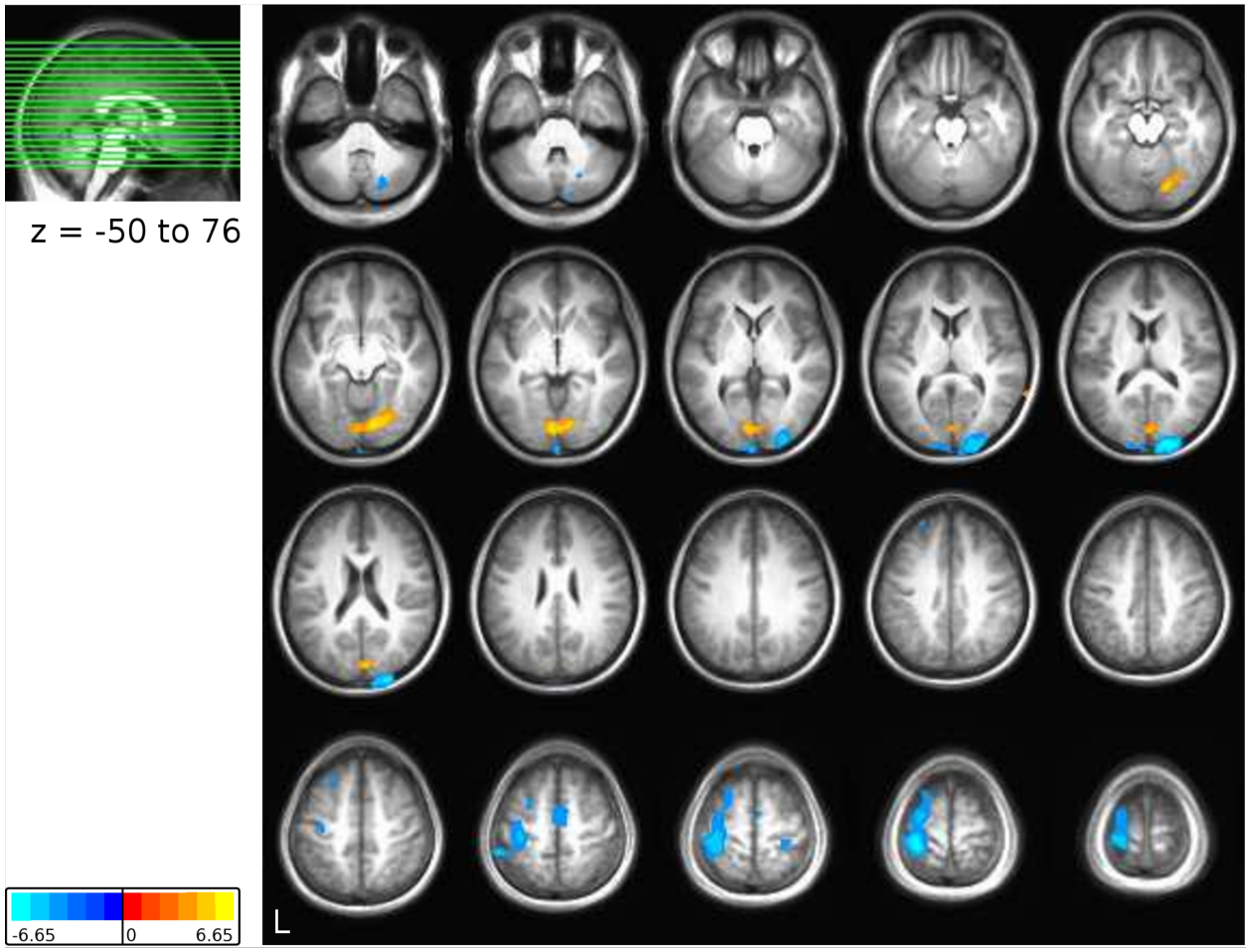

corrected. However, activation peaks surpassing $p < .001$ (uncorrected) were found in visual cortex (Figure 4.13). A bilateral region of visual cortex was positively correlated with hand speed (right and left cuneus in Table 4.4), while activity in two nearby regions of visual cortex was negatively correlated (right and left cuneus in Table 4.4). While precise retinotopic mappings would be needed to confirm the precise location of visual field representations, these regions can be said to crudely correspond to regions of visual cortex (Sereno et al., 1995), and the sign of the activations suggests that the location of feedback in the visual field determines which portion of the visual field representation is activated.

In addition to anticorrelations with hand speed in the right and left cuneus, activity in four additional areas was anticorrelated with hand speed: motor, premotor, and visual cortical areas,

Figure 4.13 Effects of hand speed by feedback condition, after controlling for effects of reaction time

Images show linear correlations and anticorrelations with hand speed, after controlling for reaction time, broken down by feedback condition. Colorbar at bottom, lower threshold: $t(18) = 3.61$, $p < .001$, uncorrected, upper threshold: $t(18) = 6.65$, $p < .05$, family-wise error corrected.
A. For feedback trials only, correlations with hand speed were evident in visual cortex, and anticorrelations were evident in adjacent visual cortex and primary motor cortex.
B. For no feedback trials, correlations and anticorrelations within visual cortex, as well as a region of the cerebellum near the vermis, were evident.

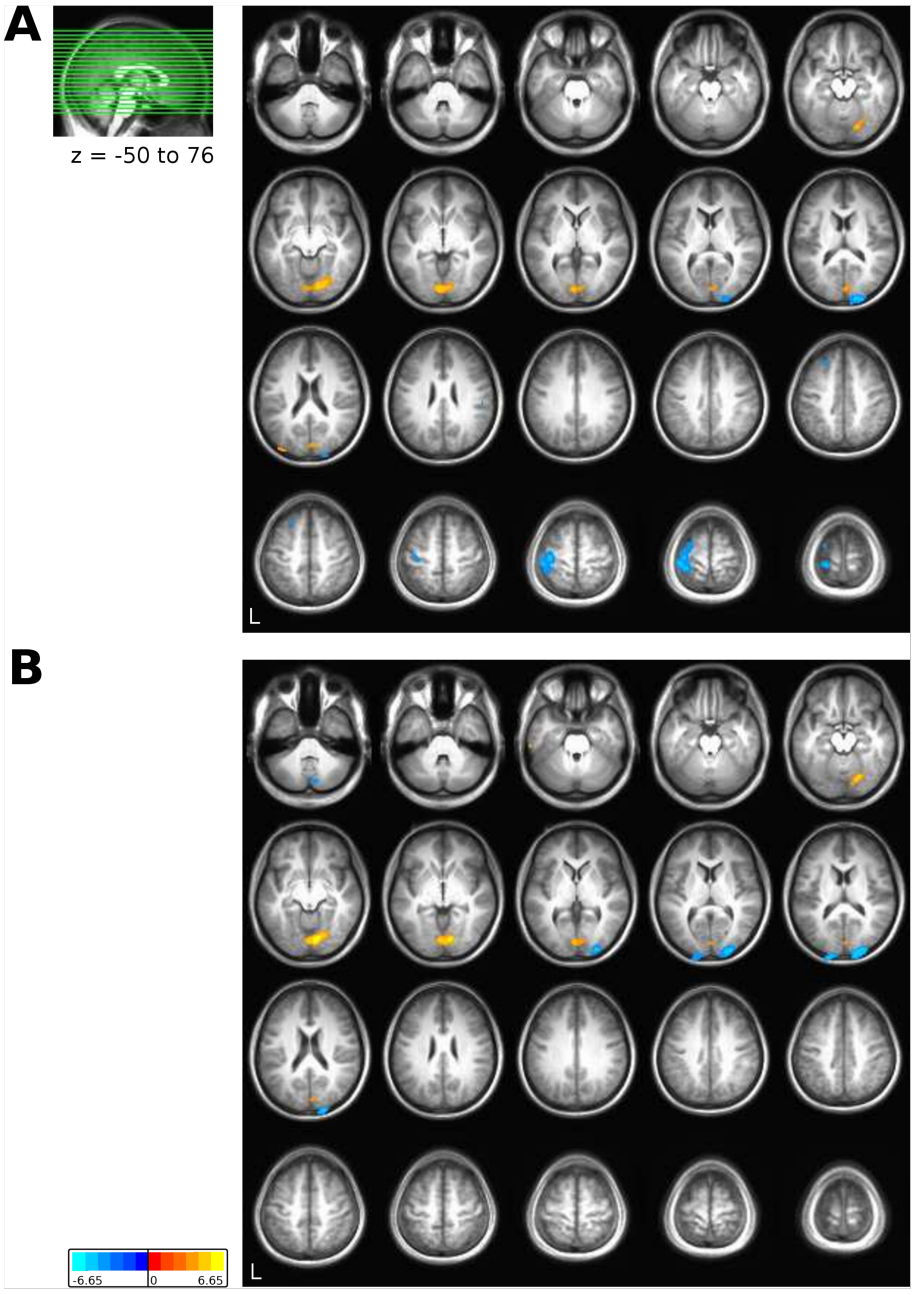

as well as a region of the posterior cerebellum, suggesting that these anticorrelations are produced by the greater control exerted in slowing down hand speed. This may occur because movements made at slower hand speeds take longer, because they are more difficult, because they require a greater number of corrective submovements, or because they require greater top-down control to inhibit movement speed.

Breaking the effect of hand speed down by feedback and no feedback trials produced similar results as the analysis of hand speed across all trials (Table 4.4 and Figure 4.13). Surprisingly, it is the putatively retinotopic activations that are preserved in the no-feedback trials. Meanwhile, unlike the combined feedback/no feedback trials, no feedback trials alone did not show anticorrelation in primary motor cortex, but there was an anticorrelation in the cerebellum. This change suggests, firstly, that the effects of hand speed in visual cortex are not due to feedback location in the visual field, but rather possibly due to the movement of the puck itself and/or predictive imagery generated by the participant. Secondly, regarding the differences in motor cortex and the cerebellum, it may be the case that slower movements only cause greater activations when movements are directed towards a goal about which feedback will be received. According to this interpretation, the anticorrelation with hand speed could be explained by participants' greater caution on feedback trials, as evidenced by their decline in accuracy on no feedback trials (Figure 4.2A).

4.4 Discussion

In a task where participants use vectorial feedback about their movement speed to update the gain, or scaling factor, of subsequent movements to produce appropriate speeds, we found little evidence for the engagement of cerebellar error processing mechanisms. Indeed, no region showed greater activity on miss trials compared to hit trials. However, evidence for the engagement of the brain's reward circuitry was found in multiple analyses. Specifically, regions of the striatum, dorsal to the nucleus accumbens, had greater activity on feedback trials than on no-feedback trials. These regions also had greater activity on hit than miss trials, and this activity was anticorrelated with absolute error (responses were greater for small errors than for large errors). This correlation was strongest in the bilateral putamen after separately analyzing effects for each target and then taking the conjunction of the resulting three within-target statistical maps. These effects persisted after controlling for reaction time and hand speed.

4.4.1 Behavioral evidence for error-based learning in shuffleboard task

We obtained clear evidence for error-based learning in trial-by-trial analysis of motor output. Participants responded to errors by appropriately adjusting their gain on the subsequent trial (Figure 4.3). Note that this responsivity is not simply a change in movement speed from one trial to the next, as such changes may occur in response to either a perturbation or a change in target distance. We confirmed that participants responded to both of these (Figure 4.3). Plotting raw motor distance scores as a function of target and transitions between targets demonstrated that participants change their hand speed with target distance (Figure 4.3A). Normalizing the data by z-scoring the distribution of motor distances produced at each target location revealed sensitivity to perturbations in terms of changes in gain, as participants' within-target normalized motor distance increased following negative perturbations and decreased following positive

perturbations (Figure 4.3B). This pattern of behavior is consistent with models of error-based learning in which people reduce the error experienced on any given trial by some proportion of the error size on the next trial (Thoroughman & Shadmehr 2000). We also note that a majority of participants (16 of 19) reported that the perturbations did not cause them to attribute errors to influences beyond their own motor skill.

Persistent errors throughout the experimental session allowed us to measure and compare responses to errors of movement speed to responses to errors of movement direction that have been described in previous studies (Turner et al., 2003; Krakauer et al., 2004; Diedrichsen et al., 2005). However, recent work has revealed that humans' responses to errors vary widely as a function of error size and schedule (Smith & Shadmehr, 2004; Berniker & Kording, 2008, 2011; Wei & Kording, 2009; Marko et al., 2012; Schlerf et al., 2013; Castro et al., 2014; Herzfeld et al., 2014), making it likely that alternative perturbation sizes and schedules in this task would influence participants' responses. The use of frequently shifting goal target locations and random perturbations in the present study may have prevented participants from forming clear exemplars of desired movement speeds at each target. As a result, our shuffleboard task prolonged the period of learning beyond what is typical in gain adaptation studies (Bock, 1992; Pine et al., 1996; Vindras & Viviani, 2002). This allowed us to measure BOLD responses to a range of experienced errors over time, although the mean error size was greater for earlier runs than for later runs (Figure 4.2). As in Chapter 3 and previous pilot experiments, participants reduced their absolute error and achieved an increasing proportion of hit trials over the course of the experiment (Figure 4.2). However, performance was relatively stable over the scan session, as the perturbed feedback imposed limits on participants' ability to improve performance. Learning curves were relatively flat, with the mean percentage of hits showing a modest increase from 52% in block 1 to 57% in block 5 (Figure 4.2A).

Previous work (Chapter 3) measured responses to errors in the absence of perturbations and in environments where target location changed less frequently: for instance, among four target distances, a change occurred only every twelve trials in Chapter 3. Though not shown, plots of absolute error (learning curves) across these twelve-trial “miniblocks” were steepest in the first two trials, becoming relatively flat for the remaining ten trials. By frequently changing target distance and perturbing participants' visual feedback, we created a unique environment to prolong trial-by-trial gain adjustments. Nevertheless, outside of disease states in which performance is very noisy and the use of highly sensitive controllers such as our robotic manipulandum, such an unstable environment is uncommon in real-world settings. Because gain is typically unlikely to change in a trial-by-trial fashion, it is possible, then, that our participants' responsivity to perturbations (which we take as indicative of error-based learning) reflects a behavior that is seldom subject to human control.

Participants' performance reproduced one feature of real-world shuffleboard performance and of motor control in general: Accuracy (measured as both visual and motor error) was negatively correlated with target distance (Figure 4.2D and E), consistent with established speed-accuracy tradeoffs (Fitts, 1954). This effect was increased by the perturbations. Thus, the use of three target distances created three distinct distributions of error sizes that scaled with hand speed. In analyses of imaging data, normalizing within these distributions allowed us to detect error and reward processing mechanisms that are common to multiple levels of skill in a single task. However, this approach may have resulted in a failure to detect effects of signed error at the near target after correcting for hand speed (see correlation between hand speed and visual error,

Figure 4.4), as the proportionally smaller perturbations did not effectively dissociate visual from motor errors (Figure 4.5).

4.4.2 Striatal reinforcement but not cerebellar error signals

Despite the evidence showing that participants adjusted their behavior appropriately from trial to trial based on the error feedback, we did not observe error-related activity in any brain regions, including the cerebellum. As expected, the right anterior lobe of the cerebellum, corresponding to the right hand representation in the motor region of the cerebellum (Kelly & Strick 2003; Krienen & Buckner 2009) was more active during movements than during rest in the localizer run (Figure 4.6), confirming cerebellar involvement in movement during task performance. However, it is in this region that previous studies of error-based learning have found evidence for error responsivity in the form of greater activation on error trials compared to correct trials (Diedrichsen et al., 2005; Schlerf et al., 2012). Although our movement localizer results indicate that the BOLD signal in this region was sufficiently robust to allow detection of effects of interest, our analysis of error-related activity contained no such difference. In particular, we did not find elevated activity in this region on miss trials compared to hit trials, nor did we find a positive correlation with absolute error.

In contrast, activity in dorsal striatal regions was greater for feedback trials than no feedback trials, greater for hits than misses, and anticorrelated with absolute error across all trials. Importantly, these effects localized primarily to the dorsal striatum (caudate nucleus and putamen), rather than the ventral striatum (nucleus accumbens), suggesting that these effects represent changes in motor pathways rather than simple reinforcement signals generated in the nucleus accumbens (for review, see O'Doherty et al., 2004; Haber 2011). However, these striatal activations are also not likely to reflect movement alone, as neither the caudate nor the putamen were more active during movement than rest in the localizer. Furthermore, were these activations representative of movement alone, it is unlikely that the activations for feedback trials relative to no feedback trials, activations for hit trials relative to miss trials, and correlations with absolute error would have emerged, given that movement variables like reaction time and hand speed do not differ across these comparisons (Figure 4.4).

To determine whether the sensitivity to error size represents a true sensitivity to non-binary information in reward outcomes or was simply driven by the same difference that was evident in the hits vs. misses comparison, further ROI-based analyses are necessary. Indeed, when error size was analyzed separately for hits and for misses, no striatal sensitivity to error size remained (Figure 4.9C & D shows only small effects in the left superior frontal gyrus and cerebellum). Thus, the anticorrelation with absolute error is unlikely to reflect a stronger response to small errors *per se*; rather, this response is may be driven by these trials' binary classification as hit trials.

Activity was sensitive to trial outcome or error size in several other regions. A region of orbitofrontal cortex was more active on hit than miss trials, reflecting the engagement of frontal mechanisms for processing abstract rewards (O'Doherty et al., 2001). A region of the right posterior cerebellum was also more active during hit than miss trials. Furthermore, activity in a small region in the left posterior cerebellum was anticorrelated with absolute error on miss trials only, while activity in a similarly small region in the right posterior cerebellum was anticorrelated with absolute error on hit trials only (Figure 4.9D). However, after family-wise

error correction, these clusters were far from significant. It may be the case that the regions of the posterior cerebellum where activity was correlated with reaction time (Figure 4.11) and anticorrelated with hand speed (Figure 4.12) represent peaks in a larger region for which the effects of these movement variables were removed, and with them, the effects of interest. To investigate this possibility, we examined the unthresholded Feedback > No Feedback maps, with all trials entered as a single condition or as three separate conditions (trials at each of the three targets comprising a condition), with and without corrective parametric modulators for reaction time and speed included in the model. Before applying the correction, activity in the right anterior lobe was slightly greater for no feedback than feedback trials. However, after applying the correction, this pattern was reversed. These differences are far from significant even for an uncorrected threshold. However, given the error responses previously described in this region (Diedrichsen et al., 2005; Schlerf et al., 2012), our results suggest that correction for reaction time and hand speed was more likely to reveal feedback-related responses than to obscure them.

The lack of error-related cerebellar activation, and the presence of reward-related activation of striatal and cortical sites, may be attributable to one or both of two particularities of the shuffleboard task. First, it may be the case that this task requires learning to select, rather than to coordinate, appropriate actions. In this case, error feedback would be less essential, with participants instead relying on reinforcement of successful action selections (making reinforcement of action selection and error-based learning of action coordinations analogous to the contributions of explicit and implicit processing as outlined in Taylor et al., 2014). As an example of this type of learning, one study found that in visuomotor rotation learning, people can learn from reward-only feedback, but no sensory recalibration occurs (Izawa & Shadmehr, 2011). It may be the case that the gain changes driving movement speed learning do not recalibrate sensory models of the consequences of actions, but instead represent the retrieval and use of previously rewarded gains.

Second, the shuffleboard task requires learning of movement speed, rather than direction, and therefore may not be amenable to modification by cerebellar circuitry. According to one model of visuomotor rotation learning, sensory recalibration in this task proceeds through cerebellar error signals that modify connection weights between visually tuned neurons in parietal cortex and directionally tuned neurons in primary motor cortex (Tanaka et al., 2009). Such modifications to motor plans, that occur by altering the mapping between actions and directional outcomes, may not extend to modifications to speed-to-distance (gain) mappings. Given the relatively fast time course of gain adaptation compared to visuomotor rotation learning (Bock, 1992; Pine et al. 1996; Krakauer et al. 1999; Krakauer et al. 2000), such a trial-by-trial mechanism may be of little use.

Taken together, our results indicate that the striatum is involved in processing feedback about movement speed in the shuffleboard task. We interpret this activation as likely functionally reinforcing the selection of previously successful actions. Indeed, this interpretation is anecdotally supported by our participants' open-ended questionnaire and interview responses, which commonly contained mention of attempting to remember the appropriate speed when they happened to successfully hit a target.

In comparison, other neuroimaging studies have identified regions very similar to ours in which activity is sensitive to error size/type (Diedrichsen et al., 2005), movement speed (Turner et al., 2003), or both (Seidler et al., 2004). In one fMRI study, bilateral regions of the putamen were suppressed during errors of execution (visuomotor rotation or force field), while these types

of errors activated the cerebellum (Diedrichsen et al., 2005). The suppression in the putamen is consistent with a reward-based interpretation of striatal processing. Importantly, in this same study, the putamen was activated by a different kind of error: the prediction error that results from a mid-trial change in goal location, measured as the difference between the actual and anticipated (at trial onset) goal location. The regions of the putamen that showed these effects were nearly identical to regions whose activity was anticorrelated with absolute error in the present study (Figure 4.9B).

In a PET study, activity in similar bilateral regions of the putamen was found to be correlated with visuomotor gain (Turner et al., 2003). However, Turner et al. (2003) also found that activity in a region of the right posterior lobe of the cerebellum was similarly correlated with visuomotor gain. In the present study, by contrast, the striatum was not significantly modulated by hand speed or signed visual error, possibly owing to the rapid, event-related design used being less powerful than the block design used by Turner et al. (2003).

In another fMRI study (Seidler et al., 2004), striatal and cerebellar responses of these regions scaled oppositely with both error and speed. Consistent with both Turner et al. (2003) and Diedrichsen et al. (2005), activity in a striatal region was correlated with movement speed and anticorrelated with error. However, Seidler et al. (2004) varied target size and allowed participants' movement speeds to increase naturally for larger, easier-to-hit targets. This positive correlation between speed and accuracy captures reward-related increases in vigor (Mazzoni et al., 2007; Xu-Wilson et al., 2009; Beierholm et al., 2013), while at the same time reversing the speed-accuracy tradeoff in the present data. Seidler et al. (2004) found that a region of the anterior lobe of the cerebellum showed an effect opposite that of the striatum, becoming more activated as smaller targets required slower movements with more online feedback control. In our task, slower movements were associated with smaller errors, and we found striatal sensitivity to error size but not movement speed. Similarly, in our study, greater movement speed was associated with greater errors, leaving open the possibility that the negative correlation between cerebellar activity and movement speed canceled error-related activations.

4.4.3 Contributions of multiple learning systems: Credit assignment of errors and the regulation of movement variability

The apparent sensitivity of striatal activity to error size may in fact be driven by a truly continuous distribution of responses across error sizes. However, the correlation between error size and striatal activity may simply be driven by larger responses for hits than for misses. Nevertheless, the behavioral data (Figure 4.3) indicate that participants do, at a minimum, take into account the direction of errors and adjust accordingly on the next trial. Therefore, errors are indeed being used to drive behavior, but this error processing did not cause a measurable increase in the cerebellar BOLD signal. This discrepancy between behavioral and imaging results is likely to reflect the unique aspects of a task in which movement speed, thought to be regulated by the striatum, is subject to trial-by-trial adjustments.

One possible explanation for the lack of recruitment of cerebellar error processing mechanisms would be that participants did not truly self-attribute the errors as presented on screen, which may be a critical driver of cerebellar involvement. This possibility is of particular concern because performance on motor learning tasks is known to be affected by credit assignment. Studies of visuomotor adaptation to abrupt and gradual perturbations in healthy

participants have shown that large (abrupt) and small (gradual) errors produce different amounts of adaptation (Torres-Oviedo & Bastian 2012; Wong & Shelhamer 2011), duration of aftereffects (Hatada et al. 2006; Huang & Shadmehr 2009), and patterns of generalization (Malfait & Ostry 2004; Kluzik et al. 2008; Torres-Oviedo & Bastian 2012). Credit assignment has been invoked to explain differing responses to large and small errors. However, within this framework, differing predictions emerge. Studies which compare movements before and after the application of single-trial perturbations have shown that large errors are discounted (Wei & Kording 2009; Marko et al., 2012; Criscimagna-Hemminger et al., 2010). This may occur either because large errors are viewed as rare, random occurrences or because it seems unlikely that motor processes under volitional control could have produced such errors. In contrast, studies of adaptation where perturbations may be transient or persist over time suggest that people change their behavior more in response to large or persisting errors (Schlerf et al., 2013; Gibo et al., 2013; Herzfeld et al., 2014). This may occur because these errors are likely to signal changes in the world that must be compensated, while small errors may arise from incorrigible motor noise.

While we cannot analyze credit assignment on a trial-by-trial basis, a majority of our participants indicated that they self-attributed errors (Table 4.1), accepting a high level of motor noise due to the high gain of the manipulandum and their lack of experience with the task (Figure 4.1E). In this unique task environment, participants are responsive to errors despite high motor noise, inconsistent error directions induced by the random perturbations, and the persistence of errors across the experiment. Errors processed by the cerebellum may provide a gating signal that indicates whether there is a mismatch between predicted and actual sensory consequences of a movement; if there is, any rewards received are not likely to be self-attributable.

According to one view, novel situations should cause the striatum to upregulate variability (in other words, explore) in order to facilitate learning about the novel situation (Costa 2011). Behaviorally, the susceptibility of adaptation to the stability of an environment supports this claim (Gibo et al., 2013; Herzfeld et al., 2014). The striatum has been implicated in upregulating movement variability when reward is low (and, conversely, when error is high), and Parkinson's disease patients fail to respond to such a change in reward (Pekny et al., 2015). While decreases in tonic dopamine reduced patients' ability to increase exploration in response to low reward in Pekny et al. (2015), another study showed that increases in tonic dopamine led to increased exploration (Beierholm et al., 2013). The regulation of variability, then, may reflect a balance struck by the striatum between careful exploration of novel motor patterns when a person's internal models of the world require improvement, and vigorous exploitation of established motor patterns when they do not.

4.4.4 Future directions

The present study focused on processing of trial outcomes (errors and rewards) in a movement speed task. Our analyses were designed to identify brain regions involved in error processing, rather than in the motor act of adjusting outputs in response to errors. The study design allowed for the identification of regions involved in movement (primary motor cortex and the right anterior lobe of the cerebellum, extending into the vermis and ventral posterior cerebellum), in feedback processing (primarily striatal regions), in the differential processing of successful and unsuccessful trials (primarily striatal regions), and in the processing of error size

(focal bilateral regions of the putamen).

It remains unclear, however, whether the relevant updates to motor plans (as implemented by adjusting a forward model, for example, see Tseng et al., 2007) are implemented at the moment of feedback delivery or at the time of the subsequent movement. However, future analyses of this data set will attempt to identify activations related to the implementation of a correction, and not simply the processing of feedback. First, region of interest-based analyses will be necessary to further characterize responses to errors themselves. By defining functional and anatomical regions of interest, striatal and other responses may be plotted according to error size, either confirming or denying the existence of non-binary reward responses driving the anticorrelations with absolute error.

Second, future work will also analyze fMRI responses to perturbations and, more generally, errors on subsequent trials. Classifying and analyzing any given trial N in terms of the response elicited on trial N+1 may reveal activations that scale with error responsivity. These activations may or may not covary with signed error; at present, there is little evidence of sensitivity to over- and undershoots, although this contrast is particularly susceptible to false negatives given that signed error is correlated with hand speed.

Third, future work will employ state-space models to produce trial-by-trial estimates of error responsivity. Using these estimates as parametric regressors may prove to be a more sensitive approach for identifying brain correlates of error responsivity.

Fourth, more specific factorial analyses will be used to identify differential recruitment of error and reward processing mechanisms in different contexts. For example, trials at the near target could be considered to be part of a high motor accuracy/high reward condition, while trials at the far target are more likely to be low accuracy/low reward. As motor responses to errors are highly dependent on a number of contextual factors, direct comparisons of these contexts may reveal, for instance, that errors are processed differently when they are rare compared to when they are common. Thus far, however, all analyses have assumed no influence of target-based context, taking the conjunction of effects at all three targets to represent task-related activity as a whole.

4.5 Conclusions

In a task designed to elicit trial-by-trial adjustments to movement speed, the present results suggest that the dorsal striatum is involved in reinforcing learning of movement speeds. Activity in the striatum was not, however, found to be modulated simply by movement speed. Furthermore, we found no evidence for the recruitment cerebellar error processing mechanisms, possibly due to the non-directional nature of motor errors.

Due to the novelty of the task, further experiments are needed to characterize both the behavioral and neural changes driving performance. However, this task constitutes an atypical environment in which movement speeds are adjusted continuously over the course of an experiment and in response to errors. Ultimately, task performance may rely on the reinforcement of motor memories. Given that the rates of errors and rewards negatively covary throughout motor tasks, errors may gate the reinforcement of these memories according to a credit assignment framework. Further work is needed to characterize these influences.

Neurally, we propose that the absence of cerebellar involvement may reflect a lack of stable contextual changes that, in tasks with directional errors, may induce exploratory motor

learning. It is possible that the use of movement speed as a substrate imposes a goal that is too uncommon to be subject to error-based fine-tuning. Alternatively, shifting the balance of credit assignment towards self over world in a high-error context may be generally atypical for healthy participants, unique to disease states, or specific to movement variables like speed which are not as subject to precise control. Our task may be used to model an atypical time course of processes similar to gain adaptation. Future work may benefit from such a deviation from directional error-based tasks, allowing researchers to dissociate multiple learning processes according to divisions of movement substrate, accuracy, time course of learning, and/or credit assignment for errors. At present, these results serve as a demonstration that error-based learning does not necessarily engage the cerebellum but can instead proceed in tandem with striatum-based reinforcement learning.

Chapter 5: Conclusion

There is a pervasive sense of iconoclasm among researchers of motor learning. Although the brain is generally considered the organ of thought, we insist that it is actually, in a sense, *for movement*. However, the reality is more complex. At times, organisms appear to be stimulus-bound, responding in stereotyped or otherwise automatized ways to inputs from the world. At other times, organisms are capable of generating astounding variability in their behaviors. Neuroanatomically, the basis for the precision and variability with which we complete movements is thought to lie in complex loops connecting cortical and subcortical structures. In approaching these processes experimentally, variables are painstakingly operationalized, paradigms are refined through endless iterations, and rigorous controls are put in place. Despite these efforts, methodological challenges and other practical concerns may stand in the way. The interplay of cognition and action remains as much a chicken-and-egg type problem as ever.

One such methodological challenge served as the launching point for my graduate school researdch. The first experiment in this dissertation (Chapter 2) was a methodological inquiry into what might have been a serious physiological confound for the interpretation of functional magnetic resonance imaging (fMRI) data. Moving forward, I set out to understand how motor learning proceeds using a novel shuffleboard task which I developed. The second experiment (Chapter 3) used this task to investigate a temporal constraint on learning which, at the time the experiment began, was regarded as a methodological obstacle to neuroimaging studies rather than an interesting component of motor learning in itself. Humbled by the complexity of this issue, I finally committed to a version of this task for use in a scanner environment. The last experiment (Chapter 4) draws on key insights from the previous two in order to better understand how people learn to produce movements of certain speeds. Although these three efforts may stand as independent contributions to scientific knowledge, addressing the methodological and behavioral aspects of movement speed learning was critically important to the eventual study of how the brain processes feedback.

In Chapter 2, I asked whether the increases in heart rate induced by a simple motor task could be causing seemingly task-related responses. Given that previous findings on the locus of error processing signals in the cerebellum had critically depended on the removal of this effect (Schlerf et al., 2013), it was in principle possible that physiological sources of noise had caused widespread contamination of fMRI data. At worst, fMRI researchers had been measuring these effects and mistaking them for true neural responses for as long as the method had existed. However, the measured responses of motor regions to movements were only slightly different when correcting for changes in heart rate. Nevertheless, comparing models with and without heart rate correction revealed that this correction had significantly improved model fit of BOLD responses for a majority of participants in the primary motor cortex and for a minority of participants in the cerebellar hand region. This was not the case for changes in respiration, which showed no task-related modulation. To prevent contamination of fMRI data in a study of motor learning, the suite of corrections developed in this experiment is used again in Chapter 4. It is my hope that the results of the experiment presented in Chapter 2 serve as evidence for the importance of physiological noise correction, and that the methods act as an example to others wishing to assess the efficacy of these corrections in their own experiments.

Chapter 3 presents an experiment designed to characterize temporal constraints on learning in a novel movement speed task based on real-world shuffleboard. Much of what is

known about human motor learning has come from experiments that use updated versions of one of several tasks: visuomotor rotation learning, force field learning, and sequence learning. Developed with a scanning environment in mind, the shuffleboard task modeled a learning environment in which movements and feedback about those movements are separated in time. Such a task might have been useful in measuring separate responses for the two event types. However, in visuomotor rotation learning, as in other sensorimotor learning tasks, learning is diminished when feedback is delayed (Kitazawa et al., 1995). Furthermore, the timing of feedback in real-world shuffleboard is correlated with movement variables. It seemed plausible, then, given that the cerebellum is thought to play a role in both temporal processing and prediction (for review, see Ivry & Spencer, 2004), that temporal predictions played a role in overcoming the cost of delay. A set of temporal manipulations was applied as participants learned. At sufficiently long delays, randomized feedback timing can cause a decrement in performance. However, given the lack of effect of the majority of our manipulations, this cost is small and likely to be caused by attentional lapses. To the extent that people do learn to produce movements of certain speeds, this learning appears unaffected by the temporal constraints on learning movements of certain directions. This learning must depend on a neural mechanism that is less temporally sensitive than cerebellar error-based learning. This prediction fit with what is known about the separate coding of movement direction and amplitude in the brain, but without neuroimaging data, our speculations on the neural origin of this behavioral dissociation could not be confirmed.

In Chapter 4, the shuffleboard task is used in the fMRI scanner to identify brain regions involved in processing feedback for movement speed learning. Data were processed using the physiological corrections developed in Chapter 2. Based on the mixed results of Chapter 3, the task was modified to eliminate delays between movement and feedback. The results of this imaging experiment failed to find evidence of cerebellar involvement in erorr processing, confirming a prediction drawn from the behavioral results in Chapter 3. If anything, a region of the posterior cerebellum was less active during errors than during successful trials; however, the removal of effects of movement variables like reaction time and hand speed may have also removed true effects. Instead of cerebellar involvement, robust activation of the dorsal striatum was found during feedback processing, this activation was greater for successful trials than errors, and in fact, this activation was correlated with error size across all successful trials and errors. Further analyses will be necessary to rule out alternative explanations and to elucidate the link between feedback processing and the actual implementation of updates to motor plans. However, at present, the results of Chapters 3 and 4 indicate that trial-by-trial learning of target movement speeds is likely to be dependent on striatal reinforcement learning mechanisms and not on motor adaptation processes thought to be cerebellum-dependent.

Taken together, these experiments address methodological and scientific issues. Within the field of human motor learning research, this work introduces a novel shuffleboard task which probes a less-understood aspect of skill learning, how people use reinforcement to regulate and vary movement speed. After identifying and minimizing the impact of physiological confounds and temporal constraints, a preliminary neuroimaging experiment has provided evidence that trial-by-trial reduction in error occurs in tasks where performance is not defined by reduction in directional error or sculpted by cerebellar error signals. The science of motor learning is far from settled in humans or any other organism. It is my hope that this dissertation contributes solutions and provocations that guide the ways in which future researchers approach this slippery topic.

References

Aguirre, G.K., Zarahn, E., D'esposito, M., 1998. The variability of human, BOLD hemodynamic responses. Neuroimage 8, 360–369. doi:10.1006/nimg.1998.0369

Albus, J.S., 1971. A theory of cerebellar function. Math. Biosci. 10:25-61.

Alexander, G.E., Crutcher, M.D., 1990. Functional architecture of basal ganglia circuits: neural substrates of parallel processing. Trends Neurosci. 13, 266–271.

Beierholm, U., Guitart-Masip, M., Economides, M., Chowdhury, R., Düzel, E., Dolan, R., Dayan, P., 2013. Dopamine modulates reward-related vigor. Neuropsychopharmacology 38, 1495–1503. doi:10.1038/npp.2013.48

Berardelli, A., Rothwell, J.C., Thompson, P.D., Hallett, M., 2001. Pathophysiology of bradykinesia in Parkinson's disease. Brain 124, 2131–2146.

Berniker, M., Kording, K., 2008. Estimating the sources of motor errors for adaptation and generalization. Nat. Neurosci. 11, 1454–1461. doi:10.1038/nn.2229

Berniker, M., Kording, K.P., 2011. Estimating the relevance of world disturbances to explain savings, interference and long-term motor adaptation effects. PLoS Comput. Biol. 7, e1002210. doi:10.1371/journal.pcbi.1002210

Birn, R.M., 2012. The role of physiological noise in resting-state functional connectivity. Neuroimage 62, 864–870. doi:10.1016/j.neuroimage.2012.01.016

Birn, R.M., Diamond, J.B., Smith, M.A., Bandettini, P.A., 2006. Separating respiratory-variation-related fluctuations from neuronal-activity-related fluctuations in fMRI. Neuroimage 31, 1536–1548. doi:10.1016/j.neuroimage.2006.02.048

Birn, R.M., Murphy, K., Handwerker, D.A., Bandettini, P.A., 2009. fMRI in the presence of task-correlated breathing variations. Neuroimage 47, 1092–1104. doi:10.1016/j.neuroimage.2009.05.030

Birn, R.M., Smith, M.A., Jones, T.B., Bandettini, P.A., 2008. The respiration response function: the temporal dynamics of fMRI signal fluctuations related to changes in respiration. Neuroimage 40, 644–654. doi:10.1016/j.neuroimage.2007.11.059

Bock, O., 1992. Adaptation of aimed arm movements to sensorimotor discordance: evidence for direction-independent gain control. Behav. Brain Res. 51, 41–50.

Bostan, A.C., Dum, R.P., Strick, P.L., 2013. Cerebellar networks with the cerebral cortex and basal ganglia. Trends Cogn. Sci. (Regul. Ed.) 17, 241–254. doi:10.1016/j.tics.2013.03.003

Brayanov, J.B., Press, D.Z., Smith, M.A., 2012. Motor memory is encoded as a gain-field combination of intrinsic and extrinsic action representations. J. Neurosci. 32, 14951–14965. doi:10.1523/JNEUROSCI.1928-12.2012

Buonomano, D.V., & Mauk, M.D., 1994. Neural Network Model of the Cerebellum: Temporal Discrimination and the Timing of Motor Responses. Neural Computation 6(1): 38-55.

Buxton, R.B., Frank, L.R., 1997. A model for the coupling between cerebral blood flow and oxygen metabolism during neural stimulation. J. Cereb. Blood Flow Metab. 17, 64–72. doi:10.1097/00004647-199701000-00009

Chang, C., Cunningham, J.P., Glover, G.H., 2009. Influence of heart rate on the BOLD signal: the cardiac response function. Neuroimage 44, 857–869. doi:10.1016/j.neuroimage.2008.09.029

Chang, C., Glover, G.H., 2009. Relationship between respiration, end-tidal CO2, and BOLD

signals in resting-state fMRI. Neuroimage 47, 1381–1393. doi:10.1016/j.neuroimage.2009.04.048
Chang, C., Metzger, C.D., Glover, G.H., Duyn, J.H., Heinze, H.-J., Walter, M., 2013. Association between heart rate variability and fluctuations in resting-state functional connectivity. Neuroimage 68, 93–104. doi:10.1016/j.neuroimage.2012.11.038
Cheng, S., Sabes, P.N., 2007. Calibration of visually guided reaching is driven by error-corrective learning and internal dynamics. J. Neurophysiol. 97, 3057–3069. doi:10.1152/jn.00897.2006
Costa, R.M., 2011. A selectionist account of de novo action learning. Curr. Opin. Neurobiol. 21, 579–586. doi:10.1016/j.conb.2011.05.004
Criscimagna-Hemminger, S.E., Bastian, A.J., Shadmehr, R., 2010. Size of error affects cerebellar contributions to motor learning. J. Neurophysiol. 103, 2275–2284. doi:10.1152/jn.00822.2009
Crone, E.A., Bunge, S.A., de Klerk, P., van der Molen, M.W., 2005. Cardiac concomitants of performance monitoring: context dependence and individual differences. Brain Res Cogn Brain Res 23, 93–106. doi:10.1016/j.cogbrainres.2005.01.009
Crone, E.A., van der Veen, F.M., van der Molen, M.W., Somsen, R.J.M., van Beek, B., Jennings, J.R., 2003. Cardiac concomitants of feedback processing. Biol Psychol 64, 143–156.
D'Esposito, M., Zarahn, E., Aguirre, G.K., Rypma, B., 1999. The effect of normal aging on the coupling of neural activity to the bold hemodynamic response. Neuroimage 10, 6–14. doi:10.1006/nimg.1999.0444
Dagli, M.S., Ingeholm, J.E., Haxby, J.V., 1999. Localization of cardiac-induced signal change in fMRI. Neuroimage 9, 407–415. doi:10.1006/nimg.1998.0424
Dale, A.M., 1999. Optimal experimental design for event-related fMRI. Hum Brain Mapp 8, 109–114.
Dale, A.M., Buckner, R.L., 1997. Selective averaging of rapidly presented individual trials using fMRI. Hum Brain Mapp 5, 329–340. doi:10.1002/(SICI)1097-0193(1997)5:5<329::AID-HBM1>3.0.CO;2-5
Damen, E.J., Brunia, C.H., 1987. Changes in heart rate and slow brain potentials related to motor preparation and stimulus anticipation in a time estimation task. Psychophysiology 24, 700–713.
Daw, N.D., O'Doherty, J.P., Dayan, P., Seymour, B., Dolan, R.J., 2006. Cortical substrates for exploratory decisions in humans. Nature 441, 876–879. doi:10.1038/nature04766
Desmurget, M. Grafton, S.T., 2000. Forward modeling allows feedback control for fast reaching movements. Trends Cogn. Sci. (Regul. Ed.) 4, 423–431.
Desmurget, M., Grafton, S.T., Vindras, P., Gréa, H., Turner, R.S., 2003. Basal ganglia network mediates the control of movement amplitude. Exp Brain Res 153, 197–209. doi:10.1007/s00221-003-1593-3
Desmurget, M., Grafton, S.T., Vindras, P., Gréa, H., Turner, R.S., 2004. The basal ganglia network mediates the planning of movement amplitude. Eur. J. Neurosci. 19, 2871–2880. doi:10.1111/j.0953-816X.2004.03395.x
Desmurget, M., Turner, R.S., 2008. Testing basal ganglia motor functions through reversible inactivations in the posterior internal globus pallidus. J. Neurophysiol. 99, 1057–1076. doi:10.1152/jn.01010.2007
Desmurget, M., Turner, R.S., 2010. Motor sequences and the basal ganglia: kinematics, not

habits. J. Neurosci. 30, 7685–7690. doi:10.1523/JNEUROSCI.0163-10.2010
Diedrichsen, J., Balsters, J.H., Flavell, J., Cussans, E., Ramnani, N., 2009. A probabilistic MR atlas of the human cerebellum. Neuroimage 46, 39–46. doi:10.1016/j.neuroimage.2009.01.045
Diedrichsen, J., Hashambhoy, Y., Rane, T., Shadmehr, R., 2005. Neural correlates of reach errors. J. Neurosci. 25, 9919–9931. doi:10.1523/JNEUROSCI.1874-05.2005
Donchin, O., Francis, J.T., Shadmehr, R., 2003. Quantifying generalization from trial-by-trial behavior of adaptive systems that learn with basis functions: theory and experiments in human motor control. J. Neurosci. 23, 9032–9045.
Donchin, O., Rabe, K., Diedrichsen, J., Lally, N., Schoch, B., Gizewski, E.R., Timmann, D., 2012. Cerebellar regions involved in adaptation to force field and visuomotor perturbation. J. Neurophysiol. 107, 134–147. doi:10.1152/jn.00007.2011
Doya, K., 2000. Complementary roles of basal ganglia and cerebellum in learning and motor control. Curr. Opin. Neurobiol. 10, 732–739.
Doyon, J., Gaudreau, D., Laforce, R., Castonguay, M., Bédard, P.J., Bédard, F., Bouchard, J.P., 1997. Role of the striatum, cerebellum, and frontal lobes in the learning of a visuomotor sequence. Brain Cogn 34, 218–245.
Doyon, J., Laforce, R., Bouchard, G., Gaudreau, D., Roy, J., Poirier, M., Bédard, P.J., Bédard, F., Bouchard, J.P., 1998. Role of the striatum, cerebellum and frontal lobes in the automatization of a repeated visuomotor sequence of movements. Neuropsychologia 36, 625–641.
Doyon, J., Penhune, V., Ungerleider, L.G., 2003. Distinct contribution of the cortico-striatal and cortico-cerebellar systems to motor skill learning. Neuropsychologia 41, 252–262.
Ernst, M.O., Banks, M.S., 2002. Humans integrate visual and haptic information in a statistically optimal fashion. Nature 415, 429–433. doi:10.1038/415429a
Farshchiansadegh, A., Ranganathan, R., Casadio, M., Mussa-Ivaldi, F.A., 2015. Adaptation to visual feedback delay in a redundant motor task. J. Neurophysiol. 113, 426–433. doi:10.1152/jn.00249.2014
Fine, M.S., Thoroughman, K.A., 2006. Motor adaptation to single force pulses: sensitive to direction but insensitive to within-movement pulse placement and magnitude. J. Neurophysiol. 96, 710–720. doi:10.1152/jn.00215.2006
Fine, M.S., Thoroughman, K.A., 2007. Trial-by-trial transformation of error into sensorimotor adaptation changes with environmental dynamics. J. Neurophysiol. 98, 1392–1404. doi:10.1152/jn.00196.2007
Fiorillo, C.D., Newsome, W.T., Schultz, W., 2008. The temporal precision of reward prediction in dopamine neurons. Nat. Neurosci. doi:10.1038/nn.2159
Fitts, P.M., 1954. The information capacity of the human motor system in controlling the amplitude of movement. J Exp Psychol 47, 381–391.
Foulkes, A.J., Miall, R.C., 2000. Adaptation to visual feedback delays in a human manual tracking task. Exp Brain Res 131, 101–110.
Friston, K.J., Fletcher, P., Josephs, O., Holmes, A., Rugg, M.D., Turner, R., 1998. Event-related fMRI: characterizing differential responses. Neuroimage 7, 30–40. doi:10.1006/nimg.1997.0306
Friston, K.J., Frith, C.D., Turner, R., Frackowiak, R.S., 1995. Characterizing evoked hemodynamics with fMRI. Neuroimage 2, 157–165.

Friston, K.J., Holmes, A.P., Worsley, K.J., Poline, J.-P., Frith, C.D., Frackowiak, R.S.J., 1994. Statistical parametric maps in functional imaging: A general linear approach. Human Brain Mapping 2, 189–210. doi:10.1002/hbm.460020402

Gabrieli, J.D., Stebbins, G.T., Singh, J., Willingham, D.B., Goetz, C.G., 1997. Intact mirror-tracing and impaired rotary-pursuit skill learning in patients with Huntington's disease: evidence for dissociable memory systems in skill learning. Neuropsychology 11, 272–281.

Gibo, T.L., Criscimagna-Hemminger, S.E., Okamura, A.M., Bastian, A.J., 2013. Cerebellar motor learning: are environment dynamics more important than error size? J. Neurophysiol. 110, 322–333. doi:10.1152/jn.00745.2012

Gläscher, J., Daw, N., Dayan, P., O'Doherty, J.P., 2010. States versus rewards: dissociable neural prediction error signals underlying model-based and model-free reinforcement learning. Neuron 66, 585–595. doi:10.1016/j.neuron.2010.04.016

Glover, G.H., Li, T.Q., Ress, D., 2000. Image-based method for retrospective correction of physiological motion effects in fMRI: RETROICOR. Magn Reson Med 44, 162–167.

Gonzalez Castro, L.N., Hadjiosif, A.M., Hemphill, M.A., Smith, M.A., 2014. Environmental consistency determines the rate of motor adaptation. Curr. Biol. 24, 1050–1061. doi:10.1016/j.cub.2014.03.049

Grafton, S.T., Schmitt, P., Van Horn, J., Diedrichsen, J., 2008. Neural substrates of visuomotor learning based on improved feedback control and prediction. Neuroimage 39, 1383–1395. doi:10.1016/j.neuroimage.2007.09.062

Haber, S.N., 2011. Neuroanatomy of Reward: A View from the Ventral Striatum, in: Gottfried, J.A. (Ed.), Neurobiology of Sensation and Reward, Frontiers in Neuroscience. CRC Press, Boca Raton (FL).

Hallett, M., Khoshbin, S., 1980. A physiological mechanism of bradykinesia. Brain 103, 301–314.

Handwerker, D.A., Gonzalez-Castillo, J., D'Esposito, M., Bandettini, P.A., 2012. The continuing challenge of understanding and modeling hemodynamic variation in fMRI. Neuroimage 62, 1017–1023. doi:10.1016/j.neuroimage.2012.02.015

Handwerker, D.A., Ollinger, J.M., D'Esposito, M., 2004. Variation of BOLD hemodynamic responses across subjects and brain regions and their effects on statistical analyses. Neuroimage 21, 1639–1651. doi:10.1016/j.neuroimage.2003.11.029

Hatada, Y., Miall, R.C., Rossetti, Y., 2006. Long lasting aftereffect of a single prism adaptation: Directionally biased shift in proprioception and late onset shift of internal egocentric reference frame. Exp Brain Res 174, 189–198. doi:10.1007/s00221-006-0437-3

Hernandez, L., Badre, D., Noll, D., Jonides, J., 2002. Temporal sensitivity of event-related fMRI. Neuroimage 17, 1018–1026.

Herzfeld, D.J., Vaswani, P.A., Marko, M.K., Shadmehr, R., 2014. A memory of errors in sensorimotor learning. Science 345, 1349–1353. doi:10.1126/science.1253138

Honda, T., Hirashima, M., Nozaki, D., 2012a. Adaptation to visual feedback delay influences visuomotor learning. PLoS ONE 7, e37900. doi:10.1371/journal.pone.0037900

Honda, T., Hirashima, M., Nozaki, D., 2012b. Habituation to feedback delay restores degraded visuomotor adaptation by altering both sensory prediction error and the sensitivity of adaptation to the error. Front Psychol 3, 540. doi:10.3389/fpsyg.2012.00540

Houk, J.C., Wise, S.P., 1995. Distributed modular architectures linking basal ganglia, cerebellum,

and cerebral cortex: their role in planning and controlling action. Cereb. Cortex 5, 95–110.
Howard, I.S., Ingram, J.N., Franklin, D.W., Wolpert, D.M., 2012. Gone in 0.6 seconds: the encoding of motor memories depends on recent sensorimotor states. J. Neurosci. 32, 12756–12768. doi:10.1523/JNEUROSCI.5909-11.2012
Howard, I.S., Wolpert, D.M., Franklin, D.W., 2013. The effect of contextual cues on the encoding of motor memories. J. Neurophysiol. 109, 2632–2644. doi:10.1152/jn.00773.2012
Hu, X., Le, T.H., Parrish, T., Erhard, P., 1995. Retrospective estimation and correction of physiological fluctuation in functional MRI. Magn Reson Med 34, 201–212.
Huang, V.S., Shadmehr, R., 2009. Persistence of motor memories reflects statistics of the learning event. J. Neurophysiol. 102, 931–940. doi:10.1152/jn.00237.2009
Imamizu, H., Miyauchi, S., Tamada, T., Sasaki, Y., Takino, R., Pütz, B., Yoshioka, T., Kawato, M., 2000. Human cerebellar activity reflecting an acquired internal model of a new tool. Nature 403, 192–195. doi:10.1038/35003194
Inoue, M., Uchimura, M., Karibe, A., O'Shea, J., Rossetti, Y., Kitazawa, S., 2015. Three timescales in prism adaptation. Journal of Neurophysiology 113, 328–338. doi:10.1152/jn.00803.2013
Ito, M., 1984. The modifiable neuronal network of the cerebellum. Jpn. J. Physiol. 34, 781–792.
Ito, M., 1998. Cerebellar learning in the vestibulo-ocular reflex. Trends Cogn. Sci. (Regul. Ed.) 2, 313–321.
Ito, M., 2002. The molecular organization of cerebellar long-term depression. Nat. Rev. Neurosci. 3, 896–902. doi:10.1038/nrn962
Ivry, R.B., Keele, S.W., 1989. Timing functions of the cerebellum. J Cogn Neurosci 1, 136–152. doi:10.1162/jocn.1989.1.2.136
Ivry, R.B., Richardson, T.C., 2002. Temporal control and coordination: the multiple timer model. Brain Cogn 48, 117–132. doi:10.1006/brcg.2001.1308
Ivry, R.B., Spencer, R.M.C., 2004. The neural representation of time. Curr. Opin. Neurobiol. 14, 225–232. doi:10.1016/j.conb.2004.03.013
Iwamoto, Y., Kaku, Y., 2010. Saccade adaptation as a model of learning in voluntary movements. Exp Brain Res 204, 145–162. doi:10.1007/s00221-010-2314-3
Izawa, J., Shadmehr, R., 2011. Learning from sensory and reward prediction errors during motor adaptation. PLoS Comput. Biol. 7, e1002012. doi:10.1371/journal.pcbi.1002012
Jennings, J.R., van der Molen, M.W., 2002. Cardiac timing and the central regulation of action. Psychol Res 66, 337–349. doi:10.1007/s00426-002-0106-5
Jennings, J.R., van der Molen, M.W., Brock, K., Somsen, R.J., 1991. Response inhibition initiates cardiac deceleration: evidence from a sensory-motor compatibility paradigm. Psychophysiology 28, 72–85.
Jennings, J.R., van der Molen, M.W., Brock, K., Somsen, R.J., 1992. On the synchrony of stopping motor responses and delaying heartbeats. J Exp Psychol Hum Percept Perform 18, 422–436.
Kao, M.H., Doupe, A.J., Brainard, M.S., 2005. Contributions of an avian basal ganglia-forebrain circuit to real-time modulation of song. Nature 433, 638–643. doi:10.1038/nature03127
Karni, A., Meyer, G., Rey-Hipolito, C., Jezzard, P., Adams, M.M., Turner, R., Ungerleider, L.G., 1998. The acquisition of skilled motor performance: fast and slow experience-driven

changes in primary motor cortex. Proc. Natl. Acad. Sci. U.S.A. 95, 861–868.
Kawato, M., Gomi, H., 1992. The cerebellum and VOR/OKR learning models. Trends Neurosci. 15, 445–453.
Kelly, R.M., Strick, P.L., 2003. Cerebellar loops with motor cortex and prefrontal cortex of a nonhuman primate. J. Neurosci. 23, 8432–8444.
Kheradmand, A., Zee, D.S., 2011. Cerebellum and ocular motor control. Front Neurol 2, 53. doi:10.3389/fneur.2011.00053
Kitazawa, S., Kohno, T., Uka, T., 1995. Effects of delayed visual information on the rate and amount of prism adaptation in the human. J. Neurosci. 15, 7644–7652.
Kluzik, J., Diedrichsen, J., Shadmehr, R., Bastian, A.J., 2008. Reach adaptation: what determines whether we learn an internal model of the tool or adapt the model of our arm? J. Neurophysiol. 100, 1455–1464. doi:10.1152/jn.90334.2008
Koekkoek, S.K.E., Hulscher, H.C., Dortland, B.R., Hensbroek, R.A., Elgersma, Y., Ruigrok, T.J.H., De Zeeuw, C.I., 2003. Cerebellar LTD and learning-dependent timing of conditioned eyelid responses. Science 301, 1736–1739. doi:10.1126/science.1088383
Krakauer, J.W., Ghilardi, M.-F., Mentis, M., Barnes, A., Veytsman, M., Eidelberg, D., Ghez, C., 2004. Differential cortical and subcortical activations in learning rotations and gains for reaching: a PET study. J. Neurophysiol. 91, 924–933. doi:10.1152/jn.00675.2003
Krakauer, J.W., Ghilardi, M.F., Ghez, C., 1999. Independent learning of internal models for kinematic and dynamic control of reaching. Nat. Neurosci. 2, 1026–1031. doi:10.1038/14826
Krakauer, J.W., Mazzoni, P., 2011. Human sensorimotor learning: adaptation, skill, and beyond. Curr. Opin. Neurobiol. 21, 636–644. doi:10.1016/j.conb.2011.06.012
Krakauer, J.W., Pine, Z.M., Ghilardi, M.F., Ghez, C., 2000. Learning of visuomotor transformations for vectorial planning of reaching trajectories. J. Neurosci. 20, 8916–8924.
Krienen, F.M., Buckner, R.L., 2009. Segregated fronto-cerebellar circuits revealed by intrinsic functional connectivity. Cereb. Cortex 19, 2485–2497. doi:10.1093/cercor/bhp135
Large, E.W., & Jones, M.R., 1999. The dynamics of attending: How people track time-varying events. Psych. Rev., 106(1): 119-159.
Logothetis, N.K., 2003. MR imaging in the non-human primate: studies of function and of dynamic connectivity. Curr. Opin. Neurobiol. 13, 630–642.
Logothetis, N.K., Wandell, B.A., 2004. Interpreting the BOLD signal. Annu. Rev. Physiol. 66, 735–769. doi:10.1146/annurev.physiol.66.082602.092845
Malfait, N., Ostry, D.J., 2004. Is interlimb transfer of force-field adaptation a cognitive response to the sudden introduction of load? J. Neurosci. 24, 8084–8089. doi:10.1523/JNEUROSCI.1742-04.2004
Marko, M.K., Haith, A.M., Harran, M.D., Shadmehr, R., 2012. Sensitivity to prediction error in reach adaptation. J. Neurophysiol. 108, 1752–1763. doi:10.1152/jn.00177.2012
Marr, D., 1969. A theory of cerebellar cortex. J. Physiol. (Lond.) 202, 437–470.
Martin, T.A., Keating, J.G., Goodkin, H.P., Bastian, A.J., Thach, W.T., 1996. Throwing while looking through prisms. I. Focal olivocerebellar lesions impair adaptation. Brain 119 (Pt 4), 1183–1198.
Maschke, M., Gomez, C.M., Ebner, T.J., Konczak, J., 2004. Hereditary cerebellar ataxia progressively impairs force adaptation during goal-directed arm movements. J.

Neurophysiol. 91, 230–238. doi:10.1152/jn.00557.2003
Mauk, M.D., Buonomano, D.V., 2004. The neural basis of temporal processing. Annu. Rev. Neurosci. 27, 307–340. doi:10.1146/annurev.neuro.27.070203.144247
Mazzoni, P., Hristova, A., Krakauer, J.W., 2007. Why don't we move faster? Parkinson's disease, movement vigor, and implicit motivation. J. Neurosci. 27, 7105–7116. doi:10.1523/JNEUROSCI.0264-07.2007
Mazzoni, P., Krakauer, J.W., 2006. An implicit plan overrides an explicit strategy during visuomotor adaptation. J. Neurosci. 26, 3642–3645. doi:10.1523/JNEUROSCI.5317-05.2006
McCormick, D.A., Thompson, R.F., 1984. Neuronal responses of the rabbit cerebellum during acquisition and performance of a classically conditioned nictitating membrane-eyelid response. J. Neurosci. 4, 2811–2822.
Medina, J.F., Mauk, M.D., 2000. Computer simulation of cerebellar information processing. Nat. Neurosci. 3 Suppl, 1205–1211. doi:10.1038/81486
Miall, R.C., Jackson, J.K., 2006. Adaptation to visual feedback delays in manual tracking: evidence against the Smith Predictor model of human visually guided action. Exp Brain Res 172, 77–84. doi:10.1007/s00221-005-0306-5
Miall, R.C., Reckess, G.Z., 2002. The cerebellum and the timing of coordinated eye and hand tracking. Brain Cogn 48, 212–226. doi:10.1006/brcg.2001.1314
Miall, R.C., Weir, D.J., Wolpert, D.M., Stein, J.F., 1993. Is the cerebellum a smith predictor? J Mot Behav 25, 203–216. doi:10.1080/00222895.1993.9942050
Middleton, F.A., Strick, P.L., 2000. Basal ganglia and cerebellar loops: motor and cognitive circuits. Brain Res. Brain Res. Rev. 31, 236–250.
Millenson, J.R., Kehoe, E.J., & Gormezano, I., 1977. Classical conditioning of the rabbit's nictitating membrane response under fixed and mized CS-US intervals. Learning & Motivation 8: 351-366.
Monti, M.M., 2011. Statistical Analysis of fMRI Time-Series: A Critical Review of the GLM Approach. Front Hum Neurosci 5, 28. doi:10.3389/fnhum.2011.00028
O'Doherty, J., Dayan, P., Schultz, J., Deichmann, R., Friston, K., Dolan, R.J., 2004. Dissociable roles of ventral and dorsal striatum in instrumental conditioning. Science 304, 452–454. doi:10.1126/science.1094285
O'Doherty, J., Kringelbach, M.L., Rolls, E.T., Hornak, J., Andrews, C., 2001. Abstract reward and punishment representations in the human orbitofrontal cortex. Nat. Neurosci. 4, 95–102. doi:10.1038/82959
O'Doherty, J.P., 2004. Reward representations and reward-related learning in the human brain: insights from neuroimaging. Curr. Opin. Neurobiol. 14, 769–776. doi:10.1016/j.conb.2004.10.016
Ogawa, S., Lee, T.M., 1990. Magnetic resonance imaging of blood vessels at high fields: in vivo and in vitro measurements and image simulation. Magn Reson Med 16, 9–18.
Ohyama, T., Nores, W.L., Murphy, M., Mauk, M.D., 2003. What the cerebellum computes. Trends Neurosci. 26, 222–227. doi:10.1016/S0166-2236(03)00054-7
Orban de Xivry, J.-J., Lefèvre, P., 2015. Formation of model-free motor memories during motor adaptation depends on perturbation schedule. J. Neurophysiol. 113, 2733–2741. doi:10.1152/jn.00673.2014
Pascual-Leone, A., Grafman, J., Clark, K., Stewart, M., Massaquoi, S., Lou, J.S., Hallett, M.,

1993. Procedural learning in Parkinson’s disease and cerebellar degeneration. Ann. Neurol. 34, 594–602. doi:10.1002/ana.410340414
Pekny, S.E., Izawa, J., Shadmehr, R., 2015. Reward-dependent modulation of movement variability. J. Neurosci. 35, 4015–4024. doi:10.1523/JNEUROSCI.3244-14.2015
Perrett, S.P., Ruiz, B.P., Mauk, M.D., 1993. Cerebellar cortex lesions disrupt learning-dependent timing of conditioned eyelid responses. J. Neurosci. 13, 1708–1718.
Pfann, K.D., Buchman, A.S., Comella, C.L., Corcos, D.M., 2001. Control of movement distance in Parkinson’s disease. Mov. Disord. 16, 1048–1065.
Pine, Z.M., Krakauer, J.W., Gordon, J., Ghez, C., 1996. Learning of scaling factors and reference axes for reaching movements. Neuroreport 7, 2357–2361.
Poline, J.-B., Brett, M., 2012. The general linear model and fMRI: does love last forever? Neuroimage 62, 871–880. doi:10.1016/j.neuroimage.2012.01.133
Raj, D., Anderson, A.W., Gore, J.C., 2001. Respiratory effects in human functional magnetic resonance imaging due to bulk susceptibility changes. Phys Med Biol 46, 3331–3340.
Raymond, J.L., Lisberger, S.G., 1998. Neural learning rules for the vestibulo-ocular reflex. J. Neurosci. 18, 9112–9129.
Redding, G.M., Wallace, B., 1988. Adaptive mechanisms in perceptual-motor coordination: components of prism adaptation. J Mot Behav 20, 242–254.
Rohde, M., van Dam, L.C.J., Ernst, M.O., 2014. Predictability is necessary for closed-loop visual feedback delay adaptation. J Vis 14, 4. doi:10.1167/14.3.4
Schlerf, J., Ivry, R.B., Diedrichsen, J., 2012. Encoding of sensory prediction errors in the human cerebellum. J. Neurosci. 32, 4913–4922. doi:10.1523/JNEUROSCI.4504-11.2012
Schlerf, J.E., Verstynen, T.D., Ivry, R.B., Spencer, R.M.C., 2010. Evidence of a novel somatopic map in the human neocerebellum during complex actions. J. Neurophysiol. 103, 3330–3336. doi:10.1152/jn.01117.2009
Schlerf, J.E., Xu, J., Klemfuss, N.M., Griffiths, T.L., Ivry, R.B., 2013. Individuals with cerebellar degeneration show similar adaptation deficits with large and small visuomotor errors. J. Neurophysiol. 109, 1164–1173. doi:10.1152/jn.00654.2011
Schmidt, R.A., 1969. Movement time as a determiner of timing accuracy. J Exp Psychol 79, 43–55.
Schmidt, R.A., Christina, R.W., 1969. Proprioception as a mediator in the timing of motor responses. J Exp Psychol 81, 303–307.
Schmidt, R.A., Zelaznik, H., Hawkins, B., Frank, J.S., Quinn, J.T., 1979. Motor-output variability: a theory for the accuracy of rapid motor acts. Psychol Rev 47, 415–451.
Schneiderman, N., Gormezano, I., 1964. Conditioning of the nictitating membrane of the rabbit as a function of CS-US interval. J Comp Physiol Psychol 57, 188–195.
Schultz, W., 1998. Predictive reward signal of dopamine neurons. J. Neurophysiol. 80, 1–27.
Schultz, W., Dayan, P., Montague, P.R., 1997. A neural substrate of prediction and reward. Science 275, 1593–1599.
Seidler, R.D., 2010. Neural correlates of motor learning, transfer of learning, and learning to learn. Exerc Sport Sci Rev 38, 3–9. doi:10.1097/JES.0b013e3181c5cce7
Seidler, R.D., Noll, D.C., Chintalapati, P., 2006. Bilateral basal ganglia activation associated with sensorimotor adaptation. Exp Brain Res 175, 544–555. doi:10.1007/s00221-006-0571-y
Seidler, R.D., Noll, D.C., Thiers, G., 2004. Feedforward and feedback processes in motor control. Neuroimage 22, 1775–1783. doi:10.1016/j.neuroimage.2004.05.003

Sereno, M.I., Dale, A.M., Reppas, J.B., Kwong, K.K., Belliveau, J.W., Brady, T.J., Rosen, B.R., Tootell, R.B., 1995. Borders of multiple visual areas in humans revealed by functional magnetic resonance imaging. Science 268, 889–893.

Shadmehr, R., Krakauer, J.W., 2008. A computational neuroanatomy for motor control. Exp Brain Res 185, 359–381. doi:10.1007/s00221-008-1280-5

Shadmehr, R., Mussa-Ivaldi, F.A., 1994. Adaptive representation of dynamics during learning of a motor task. J. Neurosci. 14, 3208–3224.

Shadmehr, R., Smith, M.A., Krakauer, J.W., 2010. Error correction, sensory prediction, and adaptation in motor control. Annu. Rev. Neurosci. 33, 89–108. doi:10.1146/annurev-neuro-060909-153135

Shmueli, K., van Gelderen, P., de Zwart, J.A., Horovitz, S.G., Fukunaga, M., Jansma, J.M., Duyn, J.H., 2007. Low-frequency fluctuations in the cardiac rate as a source of variance in the resting-state fMRI BOLD signal. Neuroimage 38, 306–320. doi:10.1016/j.neuroimage.2007.07.037

Smith, M.A., Ghazizadeh, A., Shadmehr, R., 2006. Interacting adaptive processes with different timescales underlie short-term motor learning. PLoS Biol. 4, e179. doi:10.1371/journal.pbio.0040179

Smith, M.A., Shadmehr, R., 2005. Intact ability to learn internal models of arm dynamics in Huntington's disease but not cerebellar degeneration. J. Neurophysiol. 93, 2809–2821. doi:10.1152/jn.00943.2004

Smith, M.C., 1968. CS-US interval and US intensity in classical conditioning of the rabbit's nictitating membrane response. J Comp Physiol Psychol 66, 679–687.

Spraker, M.B., Prodoehl, J., Corcos, D.M., Comella, C.L., Vaillancourt, D.E., 2010. Basal ganglia hypoactivity during grip force in drug naïve Parkinson's disease. Hum Brain Mapp 31, 1928–1941. doi:10.1002/hbm.20987

Stanley, J., Krakauer, J.W., 2013. Motor skill depends on knowledge of facts. Front Hum Neurosci 7, 503. doi:10.3389/fnhum.2013.00503

Sutton R.S. & Barto A.G., 1998. Reinforcement learning: an introduction. MIT Press, Cambridge.

Tanaka, H., Sejnowski, T.J., Krakauer, J.W., 2009. Adaptation to visuomotor rotation through interaction between posterior parietal and motor cortical areas. J. Neurophysiol. 102, 2921–2932. doi:10.1152/jn.90834.2008

Taylor, J.A., Klemfuss, N.M., Ivry, R.B., 2010. An explicit strategy prevails when the cerebellum fails to compute movement errors. Cerebellum 9, 580–586. doi:10.1007/s12311-010-0201-x

Taylor, J.A., Krakauer, J.W., Ivry, R.B., 2014. Explicit and implicit contributions to learning in a sensorimotor adaptation task. J. Neurosci. 34, 3023–3032. doi:10.1523/JNEUROSCI.3619-13.2014

Thoroughman, K.A., Fine, M.S., Taylor, J.A., 2007. Trial-by-trial motor adaptation: a window into elemental neural computation. Prog. Brain Res. 165, 373–382. doi:10.1016/S0079-6123(06)65023-1

Thoroughman, K.A., Shadmehr, R., 2000. Learning of action through adaptive combination of motor primitives. Nature 407, 742–747. doi:10.1038/35037588

Torres-Oviedo, G., Bastian, A.J., 2012. Natural error patterns enable transfer of motor learning to novel contexts. J. Neurophysiol. 107, 346–356. doi:10.1152/jn.00570.2011

Torres-Oviedo, G., Vasudevan, E., Malone, L., Bastian, A.J., 2011. Locomotor adaptation. Prog. Brain Res. 191, 65–74. doi:10.1016/B978-0-444-53752-2.00013-8
Tseng, Y.-W., Diedrichsen, J., Krakauer, J.W., Shadmehr, R., Bastian, A.J., 2007. Sensory prediction errors drive cerebellum-dependent adaptation of reaching. J. Neurophysiol. 98, 54–62. doi:10.1152/jn.00266.2007
Tunik, E., Houk, J.C., Grafton, S.T., 2009. Basal ganglia contribution to the initiation of corrective submovements. Neuroimage 47, 1757–1766. doi:10.1016/j.neuroimage.2009.04.077
Turner, R.S., Anderson, M.E., 2005. Context-dependent modulation of movement-related discharge in the primate globus pallidus. J. Neurosci. 25, 2965–2976. doi:10.1523/JNEUROSCI.4036-04.2005
Turner, R.S., Desmurget, M., 2010. Basal ganglia contributions to motor control: a vigorous tutor. Curr. Opin. Neurobiol. 20, 704–716. doi:10.1016/j.conb.2010.08.022
Turner, R.S., Desmurget, M., Grethe, J., Crutcher, M.D., Grafton, S.T., 2003. Motor subcircuits mediating the control of movement extent and speed. J. Neurophysiol. 90, 3958–3966. doi:10.1152/jn.00323.2003
Turner, R.S., Grafton, S.T., McIntosh, A.R., DeLong, M.R., Hoffman, J.M., 2003b. The functional anatomy of parkinsonian bradykinesia. Neuroimage 19, 163–179.
Tursky, B., Shapiro, D., Crider, A., Kahneman, D., 1969. Pupillary, heart rate, and skin resistance changes during a mental task. J Exp Psychol 79, 164–167.
Verstynen, T.D., Deshpande, V., 2011. Using pulse oximetry to account for high and low frequency physiological artifacts in the BOLD signal. Neuroimage 55, 1633–1644. doi:10.1016/j.neuroimage.2010.11.090
Vindras, P., Desmurget, M., Viviani, P., 2005. Error parsing in visuomotor pointing reveals independent processing of amplitude and direction. J. Neurophysiol. 94, 1212–1224. doi:10.1152/jn.01295.2004
Vindras, P., Viviani, P., 2002. Altering the visuomotor gain. Evidence that motor plans deal with vector quantities. Exp Brain Res 147, 280–295. doi:10.1007/s00221-002-1211-9
Viviani, P., Burkhard, P.R., Chiuvé, S.C., Corradi-Dell'Acqua, C., Vindras, P., 2009. Velocity control in Parkinson's disease: a quantitative analysis of isochrony in scribbling movements. Exp Brain Res 194, 259–283. doi:10.1007/s00221-008-1695-z
Wei, K., Körding, K., 2009. Relevance of error: what drives motor adaptation? J. Neurophysiol. 101, 655–664. doi:10.1152/jn.90545.2008
Wong, A.L., Shelhamer, M., 2011. Saccade adaptation improves in response to a gradually introduced stimulus perturbation. Neurosci. Lett. 500, 207–211. doi:10.1016/j.neulet.2011.06.039
Xu-Wilson, M., Zee, D.S., Shadmehr, R., 2009. The intrinsic value of visual information affects saccade velocities. Exp Brain Res 196, 475–481. doi:10.1007/s00221-009-1879-1
Yamazaki, T., Nagao, S., 2012. A computational mechanism for unified gain and timing control in the cerebellum. PLoS ONE 7, e33319. doi:10.1371/journal.pone.0033319
Yin, H.H., 2014. Action, time and the basal ganglia. Philos. Trans. R. Soc. Lond., B, Biol. Sci. 369, 20120473. doi:10.1098/rstb.2012.0473
Zelaznik, H., Spring, J., 1976. Feedback in response recognition and production. J Mot Behav 8, 309–312. doi:10.1080/00222895.1976.10735087
Zelaznik, H.N., Shapiro, D.C., Newell, K.M., 1978. On the structure of motor recognition

memory. J Mot Behav 10, 313–323.

Appendix: Supplementary material for Chapter 4

Supplementary Figure 1: Movement variables not used as parametric modulators of imaging data

All variables are plotted as a function of target distance, trial success (hits vs. misses), and feedback condition (feedback vs. no feedback).

A. Time to line, defined as the difference between the participant's reaction time and time at which the participant's hand crossed the release time.

B. Movement duration, defined as the difference between the participant's reaction time and time at which the participant's hand reversed trajectory after crossing the release line.

C. Movement amplitude, defined as the distance covered by the hand prior to reversing trajectory.

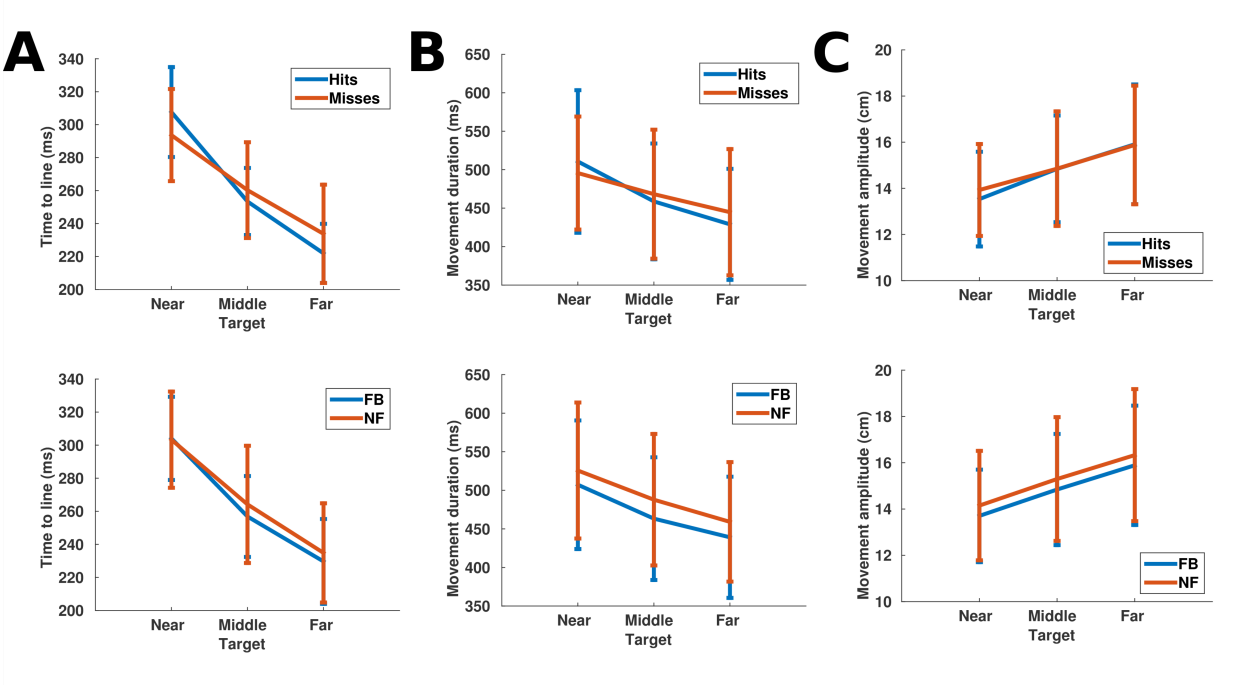

Supplementary Figure 2: Correlation matrix comparing movement parameters and behavioral effects of interest

From top to bottom, RT = reaction time (the interval between presentation of the target and puck and the initiation of movement in each trial), time to line (the difference between the participant's reaction time and time at which the participant's hand crossed the release time), Mov Dur = movement duration (the difference between the participant's reaction time and time at which the participant's hand reversed trajectory after crossing the release line), Speed = release speed (the time taken to traverse a small window immediately preceding the release line), FB Dist = feedback distance (speed plus perturbation), movement amplitude (the distance, in centimeters, covered by the hand prior to reversing trajectory), Mot Err = motor error (the unperturbed difference between the puck's landing, as determined by hand speed alone, and the target distance), Abs Mot Err = the absolute value of motor error, Vis Err = visual error (the difference beteween the perturbed puck location seen by participants and the target distance), Abs Vis Err = absolute value of visual error. For all matrices, colorbar is as in Panel D.

A. Near target only.

B. Middle target only.

C. Far target only.

D. All targets.